Finger Knuckle Print and Palmprint for efficient person recognition

Wafa El-Tarhouni

Ph.D

2017

Finger Knuckle Print and Palmprint for efficient person recognition

Wafa El-Tarhouni

A thesis submitted in partial fulfilment

of the requirements of the

University of Northumbria at Newcastle

for the degree of

Doctor of Philosophy

Research undertaken in the Faculty of Engineering and

Environment

Department of Computer and Information

Sciences

January 2017

الْحَمْدُ لِلَّهِ رَبِّ الْعَالَمِينَ

[All] praise is [due] to Allah, Lord of the worlds

Dedication

This thesis is dedicated to the most precious treasures in my life: my mother, sisters and brothers. Their supplication (Duaa) is the light that illuminates my path towards achieving my dreams, and their support helps me to endure the hardships in my life.

I am sorry to make you always worry about me, but I believe that all I have achieved is because of your prayers and Duaa. You are the constant motivation which supports me in my life and drives me to reach my goals.

I am forever indebted to you. No words are enough to describe how much I love you.

Acknowledgments

Accomplishing this thesis has been part of my obligation of lifelong learning, and studying for a PhD has been challenging but the rewards are immeasurable. I have broadened my horizons and I have gained a great deal of knowledge which will help me on a personal and professional level. First and foremost, my deepest gratitude and thanks go to God for providing me with this chance and helping me to fulfil this mission. Without His generosity, none of this or any other achievement would have been possible. AL HAMDU LELLAH.

My special thanks go to my principal supervisor Prof. Ahmed Bouridane for providing me with his continuous support, inspiration, guidance and encouragement; and for giving me the opportunity to undertake the study under his supervision.

There have also been many others along the way who have kept encouraging me and have cheered me in my journey, in particular my friends Mohammad, Safa and Aham. I also thank all those others who have lent their hands to this study.

I would like to sincerely acknowledge the financial support of the General Peoples Committee for Higher Education, Libya, which gave me the opportunity to study in the UK.

Many thanks go to all staff members of the School of Computer and Information Science for their support with all study resources.

Declaration

I declare that the work contained in this thesis has not been submitted for any other award and that it is all my own work. I also confirm that this work fully acknowledges opinions, ideas and contributions from the work of others.

I declare that the Word Count of this Thesis is approximately 36,506 words.

Name: Wafa El-Tahouni

Signature: wafa

Date: 31-01-2017

Abstract

Biometric person recognition systems are increasingly being used to enhance the security of physical and logical security systems. Palmprint and finger knuckle print recognition have gained attention in research and practical domains, providing a means of identification for security system access and personal recognition and presenting an interesting and challenging research problem. The overall aim of this work is to investigate biometric systems able to recognise people using their palmprints and finger knuckle prints. The work investigates the theoretical concepts behind palmprint and finger knuckle print recognition and proposes new algorithms to extract features for recognition systems able to identify a person from a test sample with a strong degree of confidence. The research has led to five contributions.

The first contribution is concerned with the development of an ensemble learning framework using a variant of local binary patterns constructed from Pascal's coefficients of order n, termed Pascal's coefficient multiscale local binary pattern. In addition, a feature extraction technique which combines pyramid histograms of oriented gradients and Pascal's coefficient local binary patterns by concatenating the features for use in classification is also proposed. Secondly, a fusion approach is proposed by combining local binary pattern histograms of Fourier features with Gabor filter technique to generate a single feature extraction to improve palmprint recognition. The third contribution is related to a novel feature extraction method applied for use in palmprint and Finger Knuckle Print recognition. The multi-shift local binary pattern approach extends the original shift local binary pattern concept to a multi-scale dimension to obtain more robust and discriminating feature representations by extracting histograms and concatenating them into a single feature vector. The fifth contribution proposes a novel Fibonacci sequence local binary pattern descriptor and multi-scale Fibonacci sequence local binary pattern descriptor by carefully modifying the operator thresholding scheme at the pixel values. To achieve this Fibonacci numbers have been used to generate a distribution of binary codes at every pixel position in order to create descriptors that are more robust against lighting variations of images. Finally, a new feature set is developed for finger knuckle print recognition. This is inspired by using the completed local binary pattern, termed the dynamic threshold CLBP, which employs only the sign and magnitude components. The novelty proposes to encode the magnitude features using a dynamic thresholding technique to concatenate the sign and magnitude features.

Publications

IEEE Conference Papers: (Published)

- El-Tarhouni, Wafa, Muhammad K. Shaikh, Larbi Boubchir, and Ahmed Bouridane. "Multi-scale shift local binary pattern based-descriptor for finger-knuckle-print recognition." In *Microelectronics* (ICM), 2014 26th International Conference on, pp. 184-187. IEEE, 2014.

- El-Tarhouni, Wafa, Larbi Boubchir, and Ahmed Bouridane. "Finger-Knuckle-print recognition using dynamic thresholds completed local binary pattern descriptor." In Telecommunications and Signal Processing (TSP), 2016 39th International Conference on, pp. 669-672. IEEE, 2016.

- El-Tarhouni, Wafa, Larbi Boubchir, Noor Al-Maadeed, Mosa Elbendak, and Ahmed Bouridane. "Multispectral palmprint recognition based on local binary pattern histogram fourier features and gabor filter." In Visual Information Processing (EUVIP), 2016 6th European Workshop on, pp. 1-6. IEEE, 2016.

Journal Papers: (Published)

- El-Tarhouni Wafa , Boubchir Larbi, Elbendak Mosa and Bouridane Ahmed. Multispectral palmprint recognition using Pascal coefficients-based LBP and PHOG descriptors with random sampling. Neural Computing and Applications, pp.1-11, 2017.

Journal Papers: (Submitted)

- El-Tarhouni wafa, Ahmed Bouridane, and Larbi Boubchir. Dynamic Thresholds Completed Local Binary Pattern Based-Descriptor for Finger-Knuckle-Print Recognition. International Journal of Advances in elecommunications, Electrotechnics, Signals and Systems (IJATES), (Under Review).

- El-Tarhouni, and Ahmed Bouridane. Finger knuckle print recognition using a Fibonacci sequence local binary pattern descriptor. Springer Journal of Multimedia Tools and Applications, (Under Review).

Contents

List of Figures

Acronyms

Acronym	Description
FKP	**F**inger **K**nuckle **P**rint
PHOG	**P**yramid **H**istogram of **O**riented **G**radient
PCA	**P**rincipal **C**omponent **A**nalysis
LDA	**L**inear **D**iscriminate **A**nalysis
RLDA	**R**andom **L**inear **D**iscriminate **A**nalysis
LBP	**L**ocal **B**inary **P**attern
SLBP	**S**hift **L**ocal **B**inary **P**attern
MSLBP	**M**ulti-scale **S**hift **L**ocal **B**inary **P**attern
FSLBP	**F**ibonacci **S**equence **L**ocal **B**inary **P**attern
FMSLBP	**M**ulti-scale **F**ibonacci **S**equence **L**ocal **B**inary **P**attern
dTCLBP	**d**ynamic **T**hreshold **C**ompleted **L**ocal **B**inary **P**attern
PCLBP	**P**ascal **C**oefficients **L**ocal **B**inary **P**attern
PCMLBP	**M**ulti-scale **P**ascal **C**oefficients **L**ocal **B**inary **P**attern
RSM	**R**andom **S**ampling **M**ethod
LBP-HF	**L**ocal **B**inary **P**attern **H**istogram **F**ourier features
SR-KDA	**K**ernel linear **D**iscriminant **A**nalysis using **S**pectral **R**egression
KNN	**K** **N**earest **N**eighbour **C**lassifier
NIR	**N**ear **In**fra **R**ed
ROC	**R**eceiver **O**perating **C**haracteristic
PolyU	Hong Kong **Poly**technic **U**niversity
LIF	**L**eft **I**ndex **F**inger
LMF	**L**eft **M**iddle **F**inger
RIF	**R**ight **I**ndex **F**inger
RMF	**R**ight **M**iddle **F**inger

Chapter 1

Introduction

1.1 Background

The term biometrics is derived from the combination of two Greek words, metrics and bio, which mean measure and life [89, 13]. It has been employed since the early 20th century to refer to developments in the fields of statistical and mathematical methods appropriate for data analysis problems in the biological sciences. Biometrics, also called biometric recognition, concerns the use of anatomical features (such as the iris or fingerprint) or behavioural attributes (for examples, signature, gait) of a person for recognition by automated means.

To date, a wide range of applications have employed passwords or ID cards for security purposes in order to identify individuals and control access. Such applications include border and airport security, controlling entry to restricted areas and online banking. With the enhanced integration of machines and the Internet in people's everyday activities, it is crucial to ensure the security of sensitive and personal information. Biometric methods can either replace the use of Personal Identification Numbers (PINs) or provide an additional layer of security, potentially blocking unauthorised access to Automated Teller Machines (ATMs), mobile telephones, computer networks and personal computers. The main problem associated with traditional password-based techniques is that it is possible to steal or breach passwords and obtain illegal entry, whereas biometric traits are hard to copy, steal or forge.

Many biometric traits are now used for real-time recognition. Of these, perhaps the most successful are scans of the fingerprint, iris or face (see Figure 1.1). In addition, biometric methods employing hand geometry, retinal scans, voice patterns and signatures are also available. Thus, biometrics comprises a variety of techniques for the unique identification of humans using one or more physical or behavioural modalities. Since the features used are unique to each individual, such methods are able to guarantee a person's identity in situations requiring secure, controlled access. Perhaps the best known and most widely used biometric attribute is the fingerprint [1]. In theory, it is impossible for two individuals to have identical fingerprints [1]. A fundamental property of biometrics is that the attribute examined is unique to the individual. In addition, such an attribute must be universal, meaning that it is common to all, and permanent, remaining stable throughout the person's lifetime. Furthermore, extraction should be straightforward.

There is currently ongoing research activity concerning a broad range of both physical and behavioural biometric properties (see Figure 1.2). In terms of the former, many biometric traits such as fingerprints, irises, retinal capillary structures, faces and hands can be

used for recognition. Behavioural biometric traits include handwriting and the voice. With ever-increasing incidences of security breaches and fraud, there is also increasing demand for more sophisticated means of identification and individualized verification, and the topic is thus highly salient.

A biometric recognition system extracts features from a person's biometric traits and recognizes him/her by matching those features with already enrolled, stored templates usually available in a biometric database. This is fundamentally a pattern-matching approach and the components of biometric systems include modules for data acquisition, feature extraction, matching extracted features with stored template features and finally making a decision concerning authorization. Based on the requirements of the application, a person's identity can be subject to verification or identification, for either of which purposes biometric methods can be used. In either case, the biometric features of the individuals concerned should be stored in a database. For verification, the person submits proof of identity and this is then accepted or rejected, depending on whether or not there is a match to the individual's information in the database. In other words, the algorithm establishes whether or not the person is in fact who he or she claims. In the case of identification, the system is designed to recognize the presence of the individual, verifying whether or not there is a match, by comparing the source of the input with all entries in the database.

The success of any biometric recognition system depends on the following attributes of a feature: a) uniqueness, where each individual should have a unique biometric attribute; b) universality, in that most people have the same features; c) stability, so that there are no changes over a period of time; and d) measurability, allowing them to be computed with ease [9].

Studies have previously examined various intra-modalities for biometric recognition approaches, including hand geometry, palmprints, vein patterns and finger knuckle prints (FKPs) [123]. Among the different types of biometric identifiers, hand-based biometric methods have come to play a significant role in modern security systems due to the various advantages of the hand's biometric features. Among these is the fact that commercial, low-resolution cameras make data acquisition comparatively straightforward and economical. Moreover, hand-based access systems work both indoors and outdoors and can operate in extreme weather and lighting conditions. Also, among adults, the features of the hand are more stable over time than other biometric traits. Finally, individual biometric data for the hand are highly reliable and are able to discriminate individuals successfully among different populations [72].

1.2 Overview of biometrics

There are advantages and disadvantages to many of the human characteristics proposed as biometric traits. Indeed, there is no "optimal" biometric trait. Which attributes are selected depends on the specific requirements of applications. This section presents a brief summary of various biometric traits.

1. In many forensic applications, deoxyribonucleic acid (DNA) is used for investigations in cases such as murder or the identification of a corpse. DNA presents unique patterns, except in the case of identical twins. A DNA can be extracted from blood, hair and skin, inter alia. DNA collection often comprises samples collected from crime scenes or when an individual requests a sample. However the collection of DNA brings with it many concerns, one of which concerns privacy. The collection of DNA

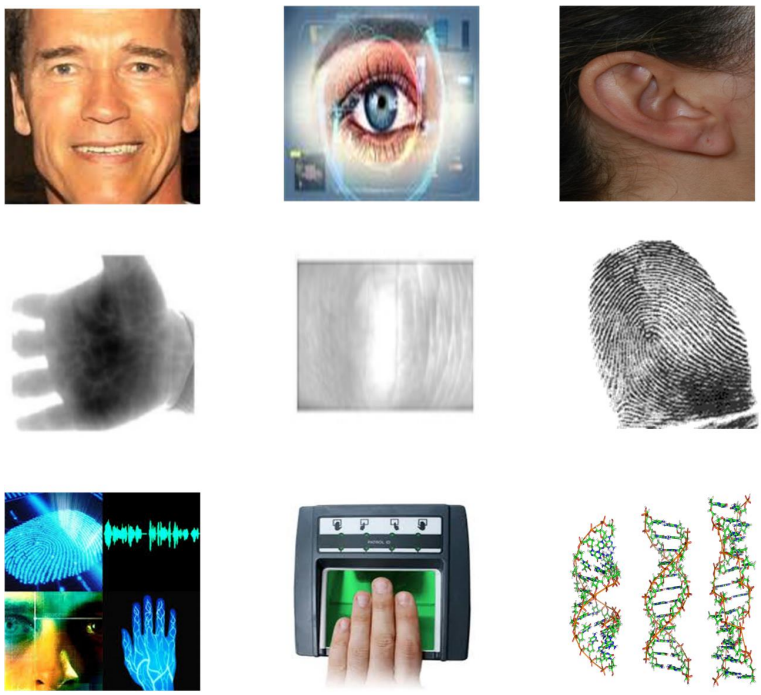

Figure 1.1: Biometric Modalities e.g. face, palmprint, FKP etc.

can be undertaken unintentionally and the DNA bears data concerning, genetics and genetic disorders.

2. Faces can be extracted without the approval of the individuals concerned, but a face has a limited number of features to capture for precise identification. However, identical twins bear some very similar traits. It is accepted that there exist some issues when recognising people, since the features of an individual face can dramatically change due to external or internal effects such as ageing, displaying emotion or the state of the environment surrounding the capture of the image. This has resulted in face recognition not being preferred for high-security applications. Nevertheless, face recognition plays a significant part in surveillance systems.

3. Fingerprint recognition has been the most widely used mode of biometric technology. Fingerprint recognition systems have been used for personal recognition for over a hundred years. Fingerprint recognition technology has seen immense developments with impressive outcomes, especially with automated systems. Fingerprint patterns bear various features in terms of orientation, minutiae points and pores, and these features are unique for all individuals. The reasonable accessibility of fingerprint scanners adds to the positive aspects of using the techniques of fingerprint recognition systems. Such techniques could be embedded in portals such as Laptops, mobile phones or personal digital assistants. However, such technologies may still have weaknesses because there exist a number of individuals in society who cannot give faultless images of their prints due to them being too old or having certain genetic issues.

4. A finger knuckle is situated on the back surface of a finger, also known as the dorsum of the hand. The basic skin patterns of the outer surface around the phalangeal joint of an individual finger bear characteristics with the capability to differentiate

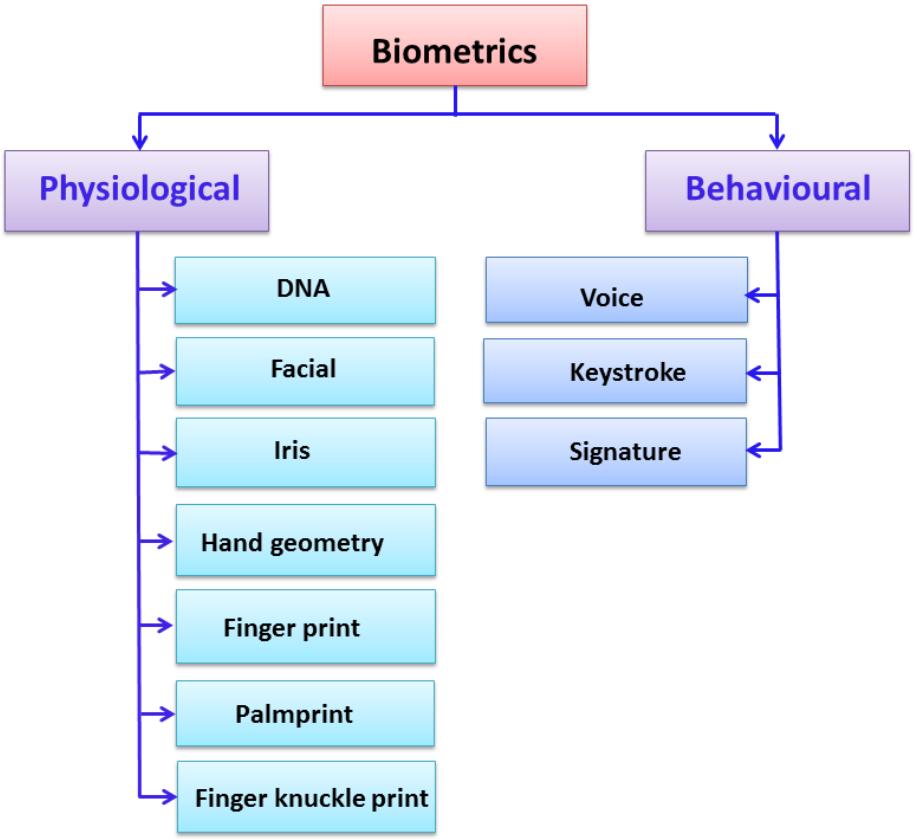

Figure 1.2: Biometric classification [46].

individuals. The surface skin patterns of the finger knuckle contain highly rich and unique features that provide a new but promising way to accomplish the biometric identification of a person.

5. The iris is another biometric modality. The texture of an individual's iris is unique and does not change during an individuals lifetime and bears a great deal of information which could be used for recognition purposes. A large amount of textural data can be supported by current iris recognition techniques. Iris images can even be captured from a distance and most commercial iris recognition apparatus are based on IrisCode, a technique developed by Daugman [20].

6. Hand geometry recognition systems are able to identify a person by simply using data from the size of their hands, where the individual width and length of fingers and the size of palms are taken to consideration for identification. Hand geometry recognition technology is also used in access control applications. Due to the limited amount of data, its use is also suitable for verification applications.

7. Palmprints have an abundance of rich characteristics such as wrinkles, major lines, singular points, minutiae points and texture. These features can be used to identify an individual using either high resolution data identification or low resolution data for verification problems. This technology is explained in more detail in Chapter 2.

8. Person recognition can also be carried out by combining behavioural and physiological biometrics. For example, speaker recognition is widely used in phone-based applications with no requirement of the extra input of a sensor. Speaker recognition techniques face multiple issues, since speech cannot be precisely stable, and identical twins cannot be separated by means of voice recognition techniques. Speech can also be affected by medical conditions, emotionality and age.

9. A behavioural biometric such as the signature is commonly used in legal, commercial and governmental transactions. People can have a variety of signatures. A signature would often not be the sole factor used to identify an individual; however, several effects due to one's emotional state or physical condition can affect the consistency of signatures used for recognition. Forgeries may also occur in order to reproduce identical signatures to impede the recognition process.

10. A plethora of biometric traits have also been proposed, such as gait, lip prints, brain signals, ears, teeth, retinas, odour, keystrokes, height, weight and gender. However, it is beyond the scope of this thesis to discuss them all.

1.3 Biometric recognition

A typical biometric recognition system, which can be divided into four main steps: image acquisition, pre-processing, feature extraction and classification. In the image acquisition stage, the images captured are obtained from various types of sensore/scanner devices, such as CCD-based scanners, digital scanners, video cameras and tripods. This is followed by an image pre-processing stage which aims to enhance the visual quality of the image and eliminate variations caused by the rotation and translation of the original image. The captured image contains significant and discriminative information which can be used to recognize persons. Feature extraction is the step that is responsible for extracting the discriminating characteristics of the captured image. Then, these extracted features are stored as standard templates in a database. It should be noted that the main contributions to the development of the FKP and palmprint recognition systems proposed in this study are related to the feature extraction stage. Finally, the classification task aims to recognize the correct person by comparing the recognition template to existing standard templates using various metrics. Figure 1.3 shows a general diagram of a biometric recognition system.

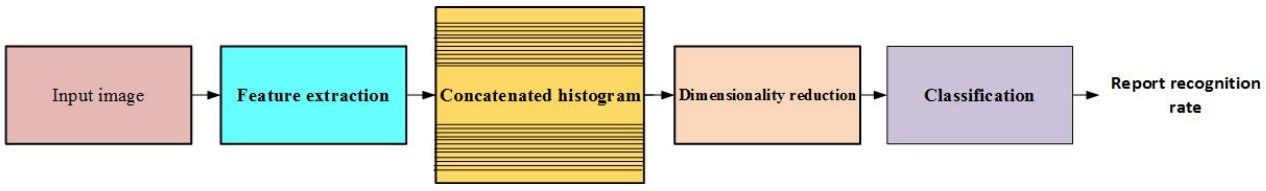

Figure 1.3: The architecture of a biometric recognition system showing extraction feature and recognition modules

1.4 Research motivation

Biometric recognition technology has been incorporated intensively in many applications, including mobile devices, surveillance, human-machine interaction, mobile telephones and security. The purpose of this work is motivated by the desire to reduce the intensive computation necessary in such recognition systems and also to provide improved recognition performance. Palmprint and FKP biometric modalities have the potential to be used for personal identification and authentication applications. It is worth noting that observing images of FKP and palmprint patterns is often affected by problems such as noisy sensor data and variations in illumination. Therefore the recognition of a specific person with high confidence is a critical issue. Thus, one of the key challenges related to improving FKP and palmprint recognition performance is to devise a robust coding scheme for such patterns. Recent studies in the area of biometric recognition attempt to solve this problem by establishing models that can be used to identify a person more accurately. The development of new subspace methods and feature descriptors are significant and broadens the categories that have attracted the attention of researchers. The overall purpose of and motivation for this research concern the introduction of vision-based techniques able to recognize palmprint and FKP patterns.

1.5 Research aims and objectives

This study contributes to the area of biometric recognition. It investigates novel techniques in the field of palmprint and FKP approaches to feature extraction. The main objective of this thesis is to investigate approaches for extracting features from palmprint and FKP images and thus to contribute to the development of new techniques for palmprint and FKP person recognition.

In this research, the main objectives are as follows:

O1: To develop novel algorithms for feature extraction that are efficient for FKP and palmprint recognition.

O2: To investigate the concepts of single-scale and multi-scale and their combination to extract robust features.

O3: To investigate the concept of random sampling for the reduction of feature vector dimensionality to give high performance biometric recognition using palmprint and FKP modalities

O4: To investigate ensemble classifiers to improve recognition.

O5: To develop a recognition framework and to evaluate the performance of the proposed approaches when compared with some existing approaches.

1.6 Thesis organization

This thesis consists of 8 chapters, including the introduction (Chapter 1), as shown in Figure 1.4. It is structured in two parts. The first part sets out the palmprint recognition system in Chapters 2, 3 and 4. The rest of the chapters comprise the second part, addressing the

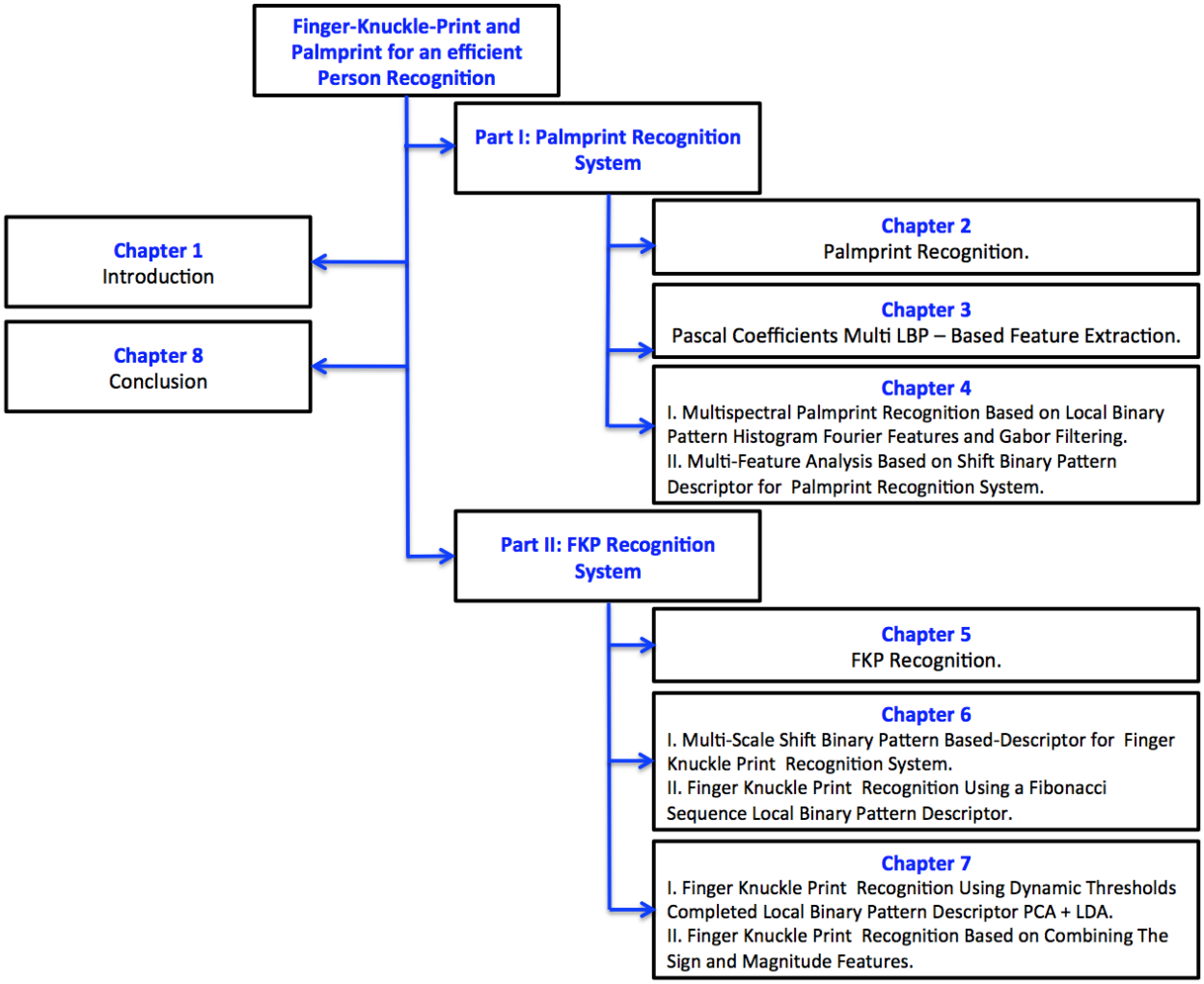

Figure 1.4: Thesis Organization

finger knuckle print (FKP) recognition system. An overview of the thesis is presented below.

Part I: Palmprint recognition system

Chapter 2 provides a brief overview of essential techniques and concepts drawing on previous studies of palmprint recognition systems, including statistical techniques, subspace-based techniques and coding-based approaches. It also covers important issues related to palmprint biometrics. This chapter has presented a background the of techniques used in this research to reduce length dimensionality of the feature vectors including some classification methods.

Chapter 3 introduces novel feature extraction techniques based on Pascal coefficients and Local Binary Pattern (LBP) descriptors. The features extracted are processed by computing palmprint feature vectors through the fusion of Pascal coefficients based on LBP and Pyramid Histograms of Oriented Gradient (PHOG) descriptors. The chapter also discusses the experimental results of the proposed method on plamprint images.

Chapter 4 presents fusion approach that generates a new set of features. It is composed of two parts. The first part covers the first proposed combination of LBP histograms (LBP-HF) and the Gabor filter technique and discusses the results obtained. The second part describes the modified Shift Local Binary Patter (SLBP) designed to extract palm features, which is termed the multi-scale SLBP (MSLBP). It also discusses the experimental results and their analysis.

Part II: FKP recognition system

Chapter 5 presents a brief overview of different approaches to FKP recognition. The rich features of the FKP are the key challenge for personal recognition systems. Thus far, researchers have proposed several methods for feature extraction and matching in FKP recognition. FKP algorithms can be placed into several different categories in the literature, including subspace-based and code-based approaches.

Chapter 6 introduces efficient methods to provide robust and discriminative representations of FKP features. It consists of two parts. The first part of this chapter covers the first proposed method which is based on SLBP, originally constructed using the LBP histogram. It uses the MSLBP descriptor, which extends the original SLBP to a multiple scale perspective to obtain more robust and discriminatory representations of FKP features. The second part of the chapter discusses the second proposed method, which consists of a new algorithm for extracting textural features from FKP images, namely the Fibonacci Sequence LBP (FSLBP). It also includes another proposed method which is an extension to the FSLBP approach, namely a multi-scale FSLBP descriptor. For the proposed descriptors, the threshold is adjusted using sequence (Fibonacci) values to compute the image descriptor, enabling optimal performance in terms of classification.

Chapter 7 is concerned with a modification to the Completed Local Binary Pattern (CLBP) descriptor aimed at analysing the performance of the FKP recognition system. The first part of the chapter describes the modified method, which is termed the dynamic Threshold CLBP (dTCLBP) descriptor, as a basic feature in the initial recognition phase. The dTCLBP feature is the combination of two components, sign and magnitude, where the sign component is the same as in the original LBP while the magnitude feature is encoded by the dynamic threshold. The second part of this chapter focuses on improving the performance of the dTCLBP descriptor by dividing FKP images into three blocks. The two different histograms for the sign and magnitude components of dTCLBP are concatenated to form the feature vector for pattern classification.

Chapter 8 reviews the material presented in the previous chapters and provides the conclusions and summarizes the key points raised in the research. It also offers recommendations for possible future work.

Part I: Palmprint recognition system

Chapter 2

Palmprint Biometric Recognition

2.1 Introduction

Over the past decade, palmprint recognition has attracted considerable interest among researchers, and research in this area is becoming increasingly active. The success of a palmprint biometric recognition system depends on the attribute of palmprints, namely their uniqueness, universality and stability. The problems associated with palmprint recognition relate to the quality of the images acquired, which are often affected by variations in illumination, orientation and noisy sensors, making the task of recognition more complicated. Researchers have designed very powerful approaches with the aim of addressing the problems associated with palmprint image recognition. They have also addressed the even more challenging problem of real-time palmprint recognition using large databases. Different algorithms have been proposed to overcome these challenging problems. So far, the algorithms developed mainly include various methods for feature extraction and matching. This chapter presents and illustrative background, including a comprehensive literature review of the essential techniques and concepts, drawing on previous studies on palmprint recognition. It also reviews various techniques used for dimensionality and classification processes in this research. This chapter is organized as follows : Section 2.2 provides a background of palmprint biometric recognition. Section 2.3 is dedicated to presenting an overview of the application and methods of image extraction process for palmprint biometric. Section 2.4 addresses the techniques that have been applied in this research for dimensionality reduction, while section 2.5 provides the methods that have been used for the recognition stage. Section 2.6 describes the palmprint database used, followed by concludes this work in section 2.6.

2.2 The palmprint as a biometric trait

Palmprint carries unique information about a person and it can be used to discriminate between individuals on the basis of their physiological characteristics. The inner area located between the wrist and fingers is known as the palmprint. The inner area of a hand contains powerful features which are the key to personal recognition. The inner surface of the palmprint has three flexion creases, secondary creases and ridges. It is known that, flexion creases and the main creases develop between the third and fifth months after birth; however, the exterior lines develop soon after birth [11]. The flexion lines are known as principal lines and the secondary lines as wrinkles. Figure 2.1 shows five major kinds of features

observable on a palmprint. These different features can be used to recognize a person uniquely. Palmprints contain similar geometric features called delta points, principal lines, minutiae, ridges and creases. The principal lines are the heart line, the head line and the life line [95]. The ridge features of the palmprint can be extracted from principal lines and minutiae for recognition purposes. From the point of view of image acquisition, systems of palmprint recognition are classified as offline and online.

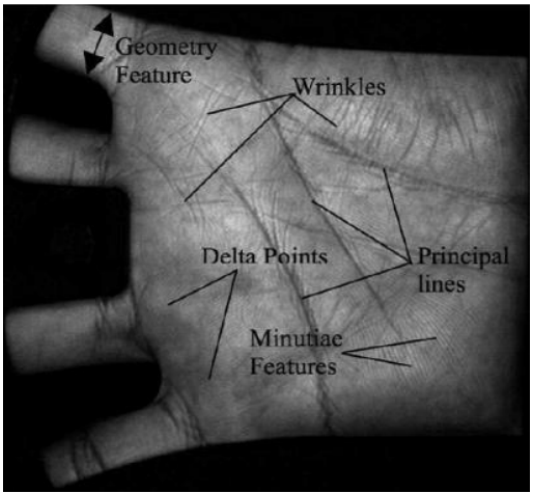

Figure 2.1: Typical palmprint features

2.2.1 Offline palmprint recognition

Images previously captured of palmprints are processed by covering the palmprint region with ink, which is then set on a piece of paper. Then a scanner is used to digitalise the paper covered by the inked image, which is stored in a computer in order to further process it. Examples of these images are shown in Figure 2.2. This method is not suitable for use in real-time applications, and the identification of images may vary due to the amount of ink used. Both excessively large and small quantities of ink may produce unacceptable results. In addition, acquiring the results take longer, and so this type of application is suitable and appropriate for forensic application, but is not good for civil or financial usage.

Figure 2.2: Offline palmprint images.

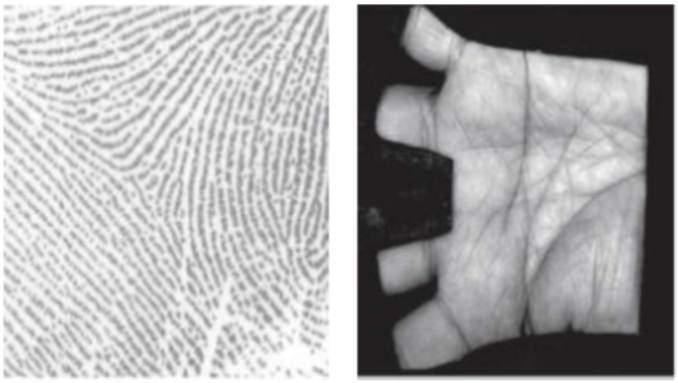

Figure 2.3: Palmprint image in: (a) high resolution; and (b) low resolution.

2.2.2 Online palmprint recognition

Here, a sensor connected to a computer is employed to capture palmprint images for real-time processing using techniques such as CCD-based palmprint scanners and digital scanners, as shown in Figure 2.4. There are two kinds of palmprint images, with high or low resolution (see Figure 2.3). Using high resolution of 500 dpi or more, it is possible to represent the minutiae of palmprint images in their entirety and these images are appropriate for use in forensic applications and criminal detection [42]. The cost of using high-resolution techniques is higher, and the reason for that is the wide area covered. Such palmprint recognition techniques thus do not satisfy the requirements of civil and commercial applications. In contrast, low-resolution imaging, for example of 75 or 150 dpi, is appropriate for civil and commercial applications such as access control, as it can still represent most of the palm lines and textural information. However, it is worth mentioning that low-resolution images can extract only the principal lines and wrinkles, while high-resolution images also capture more discriminating features including ridges, singular points and minutiae, all of which can be extracted for recognition.

Figure 2.4: Image acquisition systems using: (a) CCD-based scanner; (b) digital camera hand .

2.3 Image extraction process

The palmprint scanner is used to capture images of palmprints. There are two areas of pre-processing: image alignment and region of interest (ROI) extraction. ROI extraction is known as the cropping of the palmprint image from the image of a hand. Matching two palmprints require the extraction of valuable features that are ideally independent of acquisition conditions such as variations in illumination, orientation and noisy sensors which make the task of recognition more complicated. This process is termed feature extraction, which is a core part of palmprint recognition. Then, to assess an individual's identity, these features will be compared in a process named feature matching. Most of this study is devoted to these two stages of biometric identification given this focus, the scope of this thesis does not encompass acquisition devices or pre-processing stages in the palmprint recognition system.

This section describes previous approaches to feature extraction and feature matching, and shows how these approaches overcome the difficulties associated with palmprint recognition, enabling robust recognition and fast computation. Various techniques have been developed for palmprint recognition, as proposed by many researchers. The techniques developed involve various techniques to extract features and for distance matching. Palmprint recognition in the literature is represented using different feature extraction and matching approaches, which can be classified in four categories, namely: line-based, statistical, subspace-based and coding methods. Several algorithms based on these four approaches have been suggested in the literature. Some studies on fusion have been proposed to assist in the accurate classification of palmprint images. In addition, some techniques exist that are complicated to be classified within any particular category [53].

2.3.1 Line-based approaches

The improvement of edge detection can be achieved by the use of line-based approaches by employing the existing edge detection algorithms to extract palmprint creases. Palmprint lines are the most obvious features in the images and they are very important in detection and recognition. This has led researchers to focus their attention on the extraction of principal lines. The lines are either matched directly or represented as different types for matching.

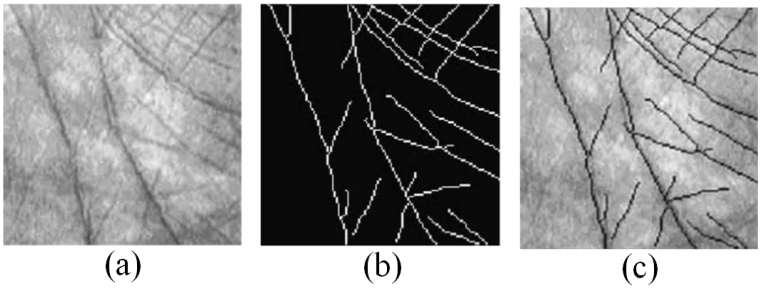

Figure 2.5: An example of line detection [109]: (a) an original palmprint image; (b) detected lines; and (c) original palmprint image overlapped with the extracted lines.

Shu et al. [95] extracted offline palmprint line features using directional line detectors that extract lines in different directions. The proposed algorithm aims to generate 20 directional patterns, detecting line features in each direction, with the line features roughly

considered as straight line segments by eradicating shorter or overlapping segments. This method is powerful and mitigates the problems associated with palm line extraction. It is not susceptible to noise, but misses many palmprint line details and can not be used in online palmprint recognition.

Han et al. [38] suggested palmprint recognition through the structural extraction of information based on Sobel edge detection and morphological operations to enhance line features. For the representation of the features, the ROI is segmented to form three different block sizes and straight line segments or feature points are primarily used instead of ridges. Palmprint identification is performed by training a neural network classifier. In another approach, Wu et al. [106] employed the Sobel mask method, computing the magnitudes of palm lines and then projecting them along the x and y axes to create histograms. The histograms are considered as inputs of hidden Markov models (HMMs).

Boles et al. [6] used Sobel masks and thresholds to create binary edge images. Then the palmprint features are extracted, and the Hough transform is applied to the six lines with the highest densities in the palmprint array. Leung et al. [65] also used Sobel masks for the extraction of palm lines. A palm feature vector was constructed using the numbers of lines present on the palmprint after calculating the thresholding, which was based on the percentage of the image area. Line segment Hausdorff distances were used to compute the differences between the sets of line segments extracted from different palmprint images. Further, Sobel masks and morphological operations were used by Diaz et al. [22] where two separated feature extractors were employed to attain the gradient of the palmprints. A neural network was applied to determine the measure of similarity for palmprint classification. However, methods using Sobel or canny operators are only able to detect single pixel-wide edges of the palmprint lines.

Zhu et al. [135] proposed an algorithm based on hierarchical recognition, and the features used are major lines. The gradient images of four different orientations are computed for the principal lines. Then, the resulting four gradient images are overlapped and de-noised and the overlapping image filtered and then used in combination with the edges detected by employing a canny edge operator with the AND operation. For matching purposes, the bidirectional method is used.

Wu et al. [105] suggested a canny operator to detect palmprint lines, and to represent the palm lines a line feature vector was created. The algorithm can distinguish lines with a similar structure but with different intensity distributions. The magnitude and angle of the direction of each edge point is determined and the fuzzy energy of each orientation derivative computed to create the feature vector. The Euclidean distance is used to find the measure of similarity for palmprint matching.

To concurrently detect the location and worth information from a palmprint, Liu et al. [70] suggested a line detector method explicitly designed to extract structural and strength features. However, the palmline detector inspects the intensity of the nucleus of the mask and counts pixels with the same brightness as the nucleus within a univalue segment assimilating nucleus (USAN), but these operations consume a great deal of time.

Wang et al. [103] employed steerable filters to extract palmprint lines. Steerable filters are also known as a set of orientation filters. Their method was split into a two-stage filter with global and then local filtering to detect palm lines. Kung et al. employed a low resolution edge map to generate a feature vector and used a decision-based neural network (DBNN) classifier for face recognition and palmprint verification [61]. The authors pointed out that the preliminary investigation verified that the DBNN recognizer is effective for the recognition task.

Huang et al. [40] employed a Modified Finite Radon Transform (MFRAT) to detect principal lines and major wrinkles and to extract orientation features. This method is based on a pixel-to-area algorithm that compares two binary edge maps to calculate the match scores between two palmprint images. The researchers asserted that it exhibited good performance against small translations and rotations. However, the pixel-to-area comparison increased the time required.

In a continuation of studies of palmprint recognition, Shit et al. [94] suggested a modification of the radon transform, incorporating a fuzzy function to extract features. Bicubic interpolation was used to reduce the feature matrix. For classification purposes, the authors used collaborative representation-based classification (CRC). Tunkpien et al. [84] proposed a compact method using a simple and quick algorithm to detect principle lines in palmprint images using three consecutive filtering operations related to gradient and morphological operators. Figure 2.5 presents a sample of the detection of the presence of lines. However, some features of palmprints can be missed by the line detection process and this is still an open issue in image processing [109].

2.3.2 Statistical-based approaches

Statistical tools such as entropy, energy, mean and variance are employed in statistical-based approaches for feature extraction task. Statistical techniques are classified as local or global methods. A local statistical method transforms images into a different domain. Then the images that have been transformed are divided into small blocks and the means and variances of each small block are stored as feature vectors. Researchers in local statistics also use global statistical methods, which are techniques that calculate global features such as moments and centres of gravity and density from entire transformed images. Correction coefficients, norms and Euclidean distance have been adopted in palmprint matching.

Figure 2.6: Sample of representations of statistical palmprint features [69]: (a) an original palmprint image; (b) Fourier transform partition by radius and (c) Fourier transform partition by angle.

In study by Zhang et al. [125], an over-complete wavelet expansion (OWE) was used and the directional context modeling of each wavelet subband was determined and computed in order to accumulate the predominant coefficients of the wrinkles and principal lines. A set of statistical components comprising the gravity centre, density, spatial dispersivity and energy were found to determine and characterize the palmprint, including the chosen directional context values. Therefore a classification and recognition system based on these statistical components was subsequently developed and satisfactory results were achieved.

Another study proposed a multi-resolution feature extraction system for palmprint recognition based on the multi-scale wavelet transform [28]. The original image is aligned

and segmented into many blocks. A palmprint is split into multi-scale wavelet sub-images and the mean and variance of each block are computed to create a normalized vector. Euclidean distance and nearest neighbour distance are used to match the query image into its relevant class.

Global statistical approaches calculate global statistical features (moments, centres of gravity and density) directly from the entire palm image. Pang et al. [86] used invariant Zernike moments, including Zernike moments, pseudo-Zernike moments and Legendre moments, as feature extraction techniques to represent palmprints. An invariant moment has advantages such as being invariant to orthogonality, rotation, translation and scale properties, and stability in the presence of noise and deformations. The authors matched palmprint vectors with moments of different orders employing Euclidean and Norm 1 distances. The higher order moments exhibit greater information with regard to palmprint recognition because they correlate with finer features.

Soo proposed an algorithm for palmprint recognition employing Hu invariant moments and Otsu binarization [82]. The equalization of the histogram and a normalized histogram were calculated and then the remapping of the sequence was performed using a regulated histogram. Then, a smoothing filter was used to eliminate the small wrinkles and retain large principal lines. Otsu binarization was used to maximize the variance between the split regions, and Hu invariant moments were extracted and used for palmprint identification. The researcher calculated the moments at three levels and compared the results for each level with Euclidean distance.

Badrinath et al. [4] proposed a palmprint verification system using low-order Zernike features from small partitions (sub-images) of palmprints. The palmprint was extracted from the captured hand image employing a low-cost flat bed scanner. In this system, the matching scores of sub-images are combined employing a weighted sum rule for the final decision. The proposed approach is robust to hand translation and rotation on the scanner and is also robust to occlusion.

A quaternion model has been proposed based on local and global features for multispectral biometrics [111]. The model was based on the extraction of global red, green, blue and near-infrared (NIR) features of multispectral palmprint images using quaternion principal components analysis (PCA) and the quaternion Discrete Wavelet Transform (DWT) to extract local features. Matching was performed using Euclidean distance to measure the dissimilarity between different features. Figure 2.6 gives an example of the extraction of statistical palmprint features.

2.3.3 Subspace-based approaches

Subspace-based methods, also known as appearance-based approaches, have been suggested to consider a palmprint image as a high-dimensional vector and hence mapping it into a lower dimensional vector. Principal Component Analysis (PCA), Fisher Discriminant Analysis (FDA), independent component analysis (ICA) and linear discriminant analysis (LDA) were initially used in face recognition. The coefficients acquired in the subspace are employed as features and a distance metric and some other classifiers are implemented for matching purposes. Rather than subsequently employing the subspace algorithms, researchers can employ DCT, Gabor filters and wavelets. Subspace feature extraction techniques provide a powerful representation, low computational cost, ease of implementation and reliable splitting, and are extensively used in various areas such as face and palmprint recognition. PCA is one of the most commonly used techniques applied to extract feature vectors.

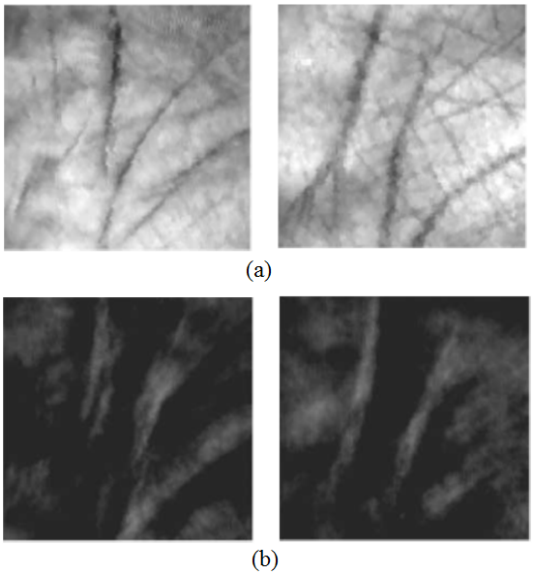

Figure 2.7: Sample of palmprint features [71]: (a) subpalmprint samples in the training set; (b) eigenpalms derived from the above samples.

Lu et al. [71] were among the first to propose the use of PCA in palmprint recognition. In their approach, the original palm images are transformed into a small feature space set, named "eigenpalms", which are the eigenvectors of the training set and can describe the principal components of the palm images. Notwithstanding the success of PCA, some challenges still remain which require further research.

Two-dimensional PCA (2DPCA) have been introduced effectively in palmprint recognition [90]. This particular process is reliant on a 2D image matrix rather than a 1D vector, and an image covariance matrix is created by employing the original palm image matrices. Unlike the palm covariance matrix related to PCA, the size of the palm covariance matrix applied in 2DPCA is significantly smaller. Thus, the advantages of 2DPCA include a precise assessment of the covariance matrix which is much more straightforward to determine the corresponding eigenvectors takes less time.

Zuo et al., [136] presented a new projection which relies on a bilateral directional PCA (BD-PCA) provided with an Assembled Matrix Distance (AMD) metric for image recognition. BD-PCA is employed to extract features by decreasing dimensionality in both the column and row directions in order to avoid the problem of overfitting. Finally, an AMD metric is presented to determine how far apart the two feature matrices are; subsequently, nearest neighbour and nearest feature line classifiers are applied to improve recognition performance.

Pan et al., [85] suggested an approach using a Gabor feature-based (2D)2PCA for palmprint recognition. Gabor features of five levels and six orientations are extracted through the convolution of the Gabor filter bank and the original image. Then (2D)2PCA is used to reduce the dimensions of the feature space in two directions, which results in fewer coefficients being needed to represent an image. Finally, Euclidean distance is employed together with the nearest neighbour classifier for classification. The outcomes from experiments have revealed the usefulness of the suggested GB(2D)2PCA regarding both speed and accuracy.

PCA focuses on how the images are represented rather than discrimination, whereas LDA is used to find the optimal projection matrix and then its ratio of scatter between-

class and within-class can be maximized in a feature subspace with a lower dimensionality (Fisher criterion). This is more suitable than PCA for classifying palmprints. Wu et al. [108] suggested a new Fisher palm recognition technique dependent on PCA-LDA. The PCA is employed to decrease the size of the dimensions of the initial palmprint, and then LDA is applied to carry out the projection of the image. For classification, Euclidean distance is used as a matching function.

Wang at al. [102] suggested a Kernel Linear Discriminant Analysis (KFDA) algorithm to extract features of palmprints for the recognition task. A tool with no fixed peg is conceived to capture the palm images. However, it has been observed that the features taken from these palmprints bear some nonlinearity because of the uncontrollability of the rotation and the stretching of hands. KFDA is employed to detect higher order relations among images of palmprints in order to accomplish the recognition task. The outcomes acquired from Wang et al.'s experiments indicated that KFDA performs better than eigenpalms and Fisher palms, principally with regard to using only a few training samples.

Du et al. [23] used both horizontal 2DLDA and vertical 2DLDA to extract the Gabor features of palmprints, and moreover applied a distance-based adaptive strategy to fuse these two features together. In order to perform palmprint recognition, the nearest neighbour classifier is used and this technique reduces the time required for the process.

Locality Preserving Projection (LPP) is a linear subspace technique for manifold learning, with various characteristics that are nonlinear. The aim of LPP is to preserve the local structure of the palmprint image space by taking account of different structures with much detail, and this can effectively address a generalized eigenvalue issue. The technique seems to be less affected by noise than PCA and LDA [110].

Hu et al. [39] developed a two-dimensional LPP (2DLPP) which extracts the appropriate features from the palm image according to a locality preserving criterion. The principal advantage of 2DLPP over LPP is that it offers a more accurate approximation of the original palmprints and therefore can directly solve the singularity problem. Thus, this can help to avoid losses of important information in recognition. Although it is argued that 2DLPP is more powerful than LPP, it does suffer from the limitation that it de-emphasizes discriminant information, which is essential in connection with the recognition problem. Figure 2.7 presents an example of finding useful palmprint representations in the subspace.

2.3.4 Texture and transform domain feature-based approaches

The palmprint image can be regarded as a textural image, comprising of the principal lines, wrinkles, ridges and other information. Palmprint recognition based on texture coding usually involves small feature size, fast matching speed and high accuracy in identification. The Fourier, wavelet, Gabor and Gabor wavelet transforms are all techniques that rely on the texture of the palm to extract features.

Li et al. [69] introduced a novel method to extract the features by transforming a palm image from a spatial domain to a frequency domain by employing the two-dimensional Fourier transform, following which the feature extraction. The researchers pointed out that the proposed approach shows high performance in terms of recognition rate and efficiency related to the palmprint database, as well as low time consumption.

Chen et al. [15, 16] proposed the contourlet transform, which is a novel two-dimensional extension of the wavelet transform, to be used to extract invariant palm features employing multiscale and directional filter data. The similarity between palmprint feature vectors can be measured using the AdaBoost classifier.

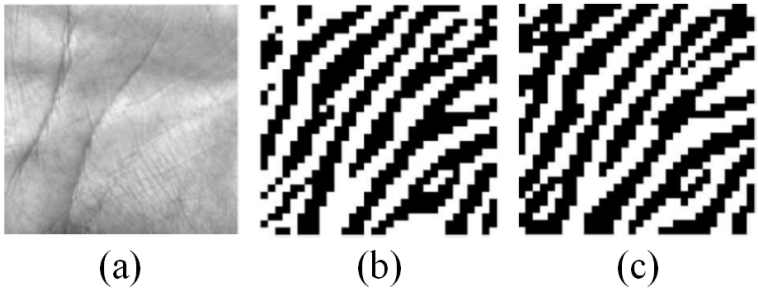

Figure 2.8: Example of the palmprint features extracted by 2D Gabor filtering [71]: (a) preprocessed palmprint image; (b) real part of texture palmprint image; (c) imaginary part of texture palmprint features.

Choge et al. used 2D-DCT to extract features from palmprints derived from the small blocks of the segmented part at the centre of the palm image [51]. The standard deviations of the 2D-DCT coefficients of each small patch are used as its features. This approach can minimize palmprint feature size in an effective way, but is suitable only for a small-scale database. Badrinath et al. [5] proposed another version with 1D-DCT coefficients of adjacent rectangular regions of variable size and orientation to represent palmprint images. The matching of the binary features of two palmprints is then conducted employing the Hamming distance, while the nearest neighbour approach is applied for classification.

Among the palm texture extraction methods, Gabor filter is more often employed to extract local direction features. Zhang et al. [122] suggested an online palmprint recognition system. In the pre-processing of a palmprint image, a low-pass filter and boundary tracking technique are adopted. The authors employed a 2D Gabor filter to convolve the palmprint image and the phase information of the filter responses is encoded as bitwise palm features. The normalized Hamming distance was employed as a similarity metric with regard to two 2048-dimensional texture feature vectors. Subsequently, this approach can represent the feature well, but as a result of using only a Gabor filter of 45° and disregarding other directions, it provides highly correlated features from different palmprint images.

Kong [55] proposed a new method for palmprint identification that employs low-resolution images and texture-based feature extraction. A palmprint is dealt with as a textural image and an adjusted Gabor filter is used to obtain information which is relevant to the texture. In addition, the Hamming distance is employed to assess the effectiveness of this particular process.

To improve performance, Kong et al. [52] proposed another approach termed the fusion code method, which convolves pre-processed palmprint images to encode the phase of the filter responses from a bank of Gabor filters in four orientations with the purpose of calculating four palm codes. It should be noted that, regarding the fusion rule, the four palm codes are combined to create the fusion code. Therefore, it is established that in this case the fusion code is independent of the brightness and contrast that is apparent in palmprint images. The similarity of two fusion codes is computed employing their normalized Hamming distance. Figure 2.8 represents an instance of the information extracted from a palmprint image using a 2D Gabor filter.

LBP is a widely used method in various application and a number of papers on LBP have been published. For example, Michael has proposed an innovative touchless palmprint identification system [75]. Hand tracking and palmprint ROI extraction technique are

employed to track and capture a user's palmprint in a real-time video stream. Here, the LBP algorithm is employed for palmprint feature extraction. Classification is accomplished by applying a modified Probabilistic Neural Network (PNN). In [134], it is the first time that the LBP and LTP descriptors are applied to the energy or direction representations of palmprint extracted by the modified finite radon transformation (MFRAT), which to reduce the noise interference.

Recently a great progress has been made in LBP research. In [36] the hierarchical multiscale LBP is a presented. It is an approach that improves the performance by extracting the information from the non-uniform bins. First, the LBP descriptor is extracted with a larg radius, and then, the counterpart LBP of those non-uniform patterns is extracted by a smaller radius. Compared with multi-scale LBP, their proposed technique enables more than 1% improvement. In another approach, Guo [32] proposed a novel collaborative representation model with a hierarchical multiscale local binary pattern (HM-LBP). The discriminative information from non-uniform palmprint patterned is extracted, and its dimension is reduced by PCA. This method has achieved excellent performance in both effective recognition accuracy and speed, which is able to fit for the real-time palmprint recognition system.

One of the successful extensions to the basic LBP operator is called Uniform LBP (ULBP) where the [98], ROI palmprint is decomposed into sub-bands with complex directional wavelet coefficients up to 3-levels; each sub-band is divided into sub-blocks; and ULBP histogram of each sub-block is calculated. Then ,fisher linear discrimination is used reduce the size of the dimensionality.

2.3.5 Coding-based approaches

Coding-based approaches are some of the most promising palmprint recognition techniques because of their small feature dimensions, fast classification speed and high accuracy. Such coding-based methods aim to filter the palmprint and then encode the filtered palm image using certain rules. Researchers are continually improving these algorithms in relation to three aspects: filter design, the coding scheme and matching. Several palmprint coding methods have been suggested in the literature. Gabor filters are commonly applied at the first stage. The encoding process aims to build a bitwise representation for high-speed matching. High-speed matching is carried out using bitwise Hamming distance or bitwise angular distance. This approach has very low memory requirements and a fast matching speed, and thus has been very prominent in palmprint representation and matching.

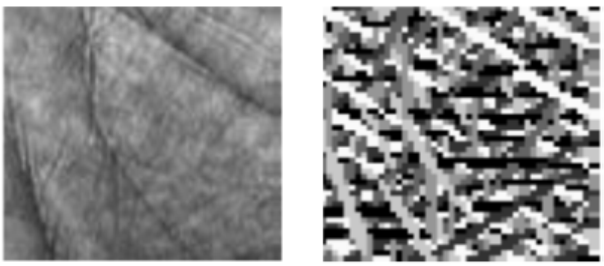

Figure 2.9: Example of competitive coding for palmprint recognition [54]: (a) ROI palmprint image; (b) competitive coding palmprint features.

Kong, et al. [54] suggested a novel feature extraction method for palmprint identification that is known as the competitive coding scheme. The competitive coding method applies multiple 2D Gabor filters to extract local orientation data from the palmprint lines and stores this information in the competitive code as palm features. An angular match is calculated through an exclusive OR operation between the two sampling points. This approach yields more accurate matches than others and performs best regarding accuracy. The execution time for the verification procedure, incorporating pre-processing, feature extraction and final matching, is 1s, which is sufficient for real-life applications.

Jia et al. [44] suggested a robust line orientation code (RLOC) for palmprint verification as an improved model of the competitive code. RLOC employs modified finite Radon transformation (MFRAT) to extract the palmprint orientation features more accurately, and it also solves the sub-sampling problem in a more optimal manner. The advantage of this approach is that the usage of an enlongated training set can overcome the considerable rotation problem caused by imperfect preprocessing. A winner-takes-all rule is suggested for coding, as is employed in competitive coding, to estimate the orientation of the palmprint image. To improve robustness, the researchers designed a matching model named pixel-to-area comparison which has better a fault tolerance ability for slight translations, rotations and distortions. The approach has some advantages, although that the matching speed is slower than with other coding methods. However, it employs the bitwise Hamming distance and bitwise angular distance and its speed is three times faster than competitive code in estimating the orientation features of each local region.

Yue et al. [120] examined the problem of determining the orientation of each Gabor filter in competitive coding-based palmprint identification. Taking into account statistical orientation distribution and orientation separation characteristics, a modified fuzzy C-means (FCM) algorithm was proposed with the aim of finding the orientation feature of each Gabor filter. The experimental results indicated that the approach attains high efficiency in contrast to that of the original competitive coding method and several state-of-the-art techniques such as Robust Line Orientation Code (RLOC) and ordinal measures. Furthermore, regarding verification accuracy and computational complexity, a competitive code with six orientations is the most suitable choice in support of palmprint identification.

Guo et al. [33] suggested a new approach, namely the binary orientation co-occurrence vector (BOCV), to be used for multiple orientation features for a local region. This multiple orientation is extracted from the filtering responses and preservation is implemented by combining the responses as a vector. Thresholding is undertaken to binarize the responses as a vector. The BOCV can represent the local orientation features in an improved manner and it is more robust to small palmprint image rotations. The Hamming distance is used for recognition purposes.

Based on the ordinal code, Zhao et al. [96] suggested phase coding using 2D orthogonal Gabor filtering, in a method termed orthogonal coding which is robust to variations in illumination. The researchers proposed a phase coding scheme using 2D orthogonal Gabor filters. These filters with multiple orientations are used to extract textural data and a phase coding method is applied to describe the palmprint image. A normalized Hamming distance is employed to calculate the similarity metric for palmprint matching. The execution time of the proposed approach is longer than that of ordinal coding, but it is adequate as a real-time application.

Zhang et al. [124] proposed a fractal coding method to describe texture. A sub-image is extracted from a training set of palmprints and stored as a template. The fractal code of the template of the palmprint images is matched with that of a sample of the person's current

palmprint image, which can reduce the overall response time. The results of experimental evaluations from two databases clearly show the effectiveness of the suggested approach. The researchers claimed that the approach was also appropriate for noisy palmprint images.

Wu et al. [107] suggested a Derivative of Gaussian Code (DoGCode) technique which first convolves the palm image employing a 2D Gaussian filter and then encodes the zero-crossing data of the horizontal and vertical slope values. The Hamming distance is used to compute how similar the two DoGCodes of the palmprint are. This approach has many advantages, such as the very low memory requirements and fast matching speed, and it achieves a much greater accuracy than fusion coding, which is one of the most powerful palmprint recognition methods.

Tamrakar et al. [99] suggested the XOR-SUM code, based on the concatenation of real and imaginary palmprint code images with four orientations, to enhance the performance of the palmprint recognition system. The researchers applied DWT decomposition up to two stages on the ROI, which offers a small-sized AROI, increasing accuracy and affording faster matching. Then the real and imaginary parts of each corresponding orientation Gabor filter are convolved with the AROI image. Each of the real and imaginary parts of the palm code are binarized with a threshold and combined with an XOR operation for each orientation. Then, the combined images of all orientations are concatenated together to obtain the feature vector of the palmprint. Compared to palm coding, competitive coding and contourlet transform-based techniques, the XOR-SUM Code technique employs not only part of the actual parts of the Gabor filter but also the imaginary parts of the Gabor filter, which also contains significant data. Figure 2.8 represents a sample of extracted codes. Since the coding scheme can employ all of the features of the palmprints image and compare many features in a small amount of time, it is appropriate to identify palmprint in a huge database.

2.3.6 Fusion approaches

The fusion of different biometric sources as a means of implementing classification, termed multibiometrics, is a trend that aims to capture more information from the human being in order to combine the multimodal biometrics acquired from the user. Information fusion in multibiometrics can be employed at various levels in a biometric identification process, such as at the levels of the sensor, feature extraction, matching score and decision. When two biometric traits such as face and palm are obtained from the same imaging set up, combination can be done at the pixel level.

Chin et al. [18] proposed a multimodal biometric recognition system that fuses palmprint and fingerprint images. The characteristics of palmprint and fingerprint images are first enhanced employing a series of preprocessing methods. Then a bank of 2D Gabor filters is applied to extract palmprint and fingerprint features independently, which are then concatenated into a single feature vector.

A method called non-subsampled contour transform has been proposed [119]. This is a full shift invariant, multiple direction expansion that has better direction frequency localization and faster implementation than other methods and can extract directional features for multispectral images. The scores are generated individually for each set of palmprint images under the red, green, blue and NIR spectral. In this study, the maximum and sum of the score fusion methods were used for recognition and it was demonstrated that fusion affords better results than single spectrum analysis. Moreover, the sum of the score level fusion provides better results than the maximum of score level fusion.

A novel multispectral palmprint recognition method has also been proposed based on single spectrum palmprint images and the 1D log-Gabor [72]. The 1D log-Gabor is deemed to exhibit the best performance in palmprint recognition because it is Gaussian on a logarithmic scale and can be used to produce zero DC components for any bandwidth. The phase features are generated by combining the results of real and imaginary parts of each spectrum palmprint image to process the inherent unique characteristics of the palmprint. A normalized Hamming distance is then applied for matching palmprint features. However, fusion at the matching score level and fusion at the image level are used to enhance the performance of palmprint recognition. In other work, an efficient online personal identification system based on the Multi-Spectral Palmprint (MSP) using the Radial Basis Function (RBF) has been proposed [74], with the processing undertaken by segmenting the MSP into non-overlapping and equally sized blocks and subsequently applying a two-dimensional block-based discrete cosine transform (DCT) over each block. Zigzag scanning is used on each transform block and a reordering of the coefficients is performed to produce the feature vector. All resulting vectors are then concatenated to produce an observation vector or matrix. Finally, an RBF network is used for modelling and classification purposes.

Several fusion matching score levels can be used for the fusion of multi-spectral palmprint images. Recently, proposed the Multi-class Projection Extreme Learning Machine (MPELM) has been proposed [112], inspired by the extreme learning machine (ELM), for which pre-processing was conducted by applying David Zhang's method which extracts a central area from a palm image for feature extraction [122]. A image combination method based on a fast digital Shearlet transform was used, which gives optimal approximation performance compared to the classical wavelet transform and curvelet transform. Ultimately, the MPELM dominant pattern for an image is obtained by applying an MPELM classifier to the sets of pattern vectors to find the final multi-spectral palmprint classification. The MPELM based-method is fast in terms of computation and can also achieve better results than the ELM.

Wang et al. [116] proposed a hierarchical multi-feature scheme which is applied to facilitate coarse to fine matching of palmprint feature images. Two levels of features are determined: geometrical features based on distance and texture features based on Zernike moments. Classification is performed using two different neural networks for two different palmprint feature vectors and the output is fused into a recognition system.

2.3.7 Other approaches

Some methods are difficult to classify because the researchers have combined numerous image-processing methods to extract palmprint features and standard classifiers are used as neural networks to generate the final decision.

Chen et al. [14] proposed a dual-tree complex wavelet transform to resolve the weakness of the traditional wavelet transform in a process in which the approximate shift-invariant attribute of the dual-tree complex wavelet and its directional selectivity make it a very attractive prospect for invariant palmprint pattern recognition. The researchers used the Fourier transform on each subband and regarded the spectrum magnitudes as features. Support vector machines (SVMs) were used as a means of classification in pattern recognition.

In another study, Chen et al. [17] suggested a new model for palmprint recognition, applying a time series technology known as symbolic aggregate approximation (SAX) to represent palmprint features. The researchers extracted a series of local features (such as average intensity) along a spiral and minimum distance to compare two palmprint feature

vectors. This approach has many advantages, including that it is easy to implement, flexible and computationally effective. The proposed approach was tested on a small-sized palmprint database.

Doi et al. [115] proposed an efficient system using a reliable and real-time process. To find the feature points, the researchers used the intersection points of the palmar flexion creases and the extended skeletal line of the fingers. To obtain valuable data, the angles between the principal lines and the extended skeletal lines are also represented as significant features. Root mean square deviation is employed to compute the differences between the two feature vectors.

The Two-Phase Test Sample Representation (TPTSR) technique has been introduced and used for palmprint identification for the first time [67]. In the first phase, TPTSR represents the test sample as a linear combination of all the training samples and determines the M nearest neighbours of sample used in the test. In the second stage, the test sample is linearly represented with new coefficients, weighting the M nearest neighbours in a linear combination to classify the test sample.

Koichi et al. introduced a palmprint identification method employing phase-based image matching [41]. The amplitude spectrum of two segmented palmprint images is employed to determine rotation and scale differences. One of the palm images is rotated and scaled and the process continues the removal of the amplitude information in the frequency band. Then, Band-Limited Phase-Only Correlation (BLPOC) is adopted to calculate how identical the two extracted palm images are. BLPOC only concerns low to medium frequency data.

A method known as the Coarse-to-Fine K-Nearest Neighbour Classifier (CFKNNC) has been suggested [113] as an improvement on the performance of the coarse k-nearest neighbour classifier (CKNNC). To simplify the interpretation of representation-based distance, the CFKNNC is capable of taking into consideration the dependent relationship between various training samples. The CFKNNC exploits representation-based distance to select the closest neighbours of the test sample from the set of training samples.

2.4 Techniques used for dimensionality reduction

In image recognition applications there is an issue of gathering, processing and storing large amounts of data. Dimensionality reduction has become a necessity for to determine the more discriminative features for use at the classification stage. Data reduction is used to address this problem. The idea is how to efficiently and determine a low-dimensional subspace in a high-dimensional image space. In virtually every type of data one can think of, use a statistical dimensionality feature reduction process to determine which features are relevant for the classification problem. This section reviewes some common techniques that used in this research to reduce the size of feature vectors.

2.4.1 Principal components analysis

PCA, also called Karhunen-Love transformation, is a linear transformation that obtains the variance of the input data. PCA is a powerful unsupervised method for transforming a number of possibly correlated attributes into a number of uncorrelated attributes named principal components. This technique computes the eigenvectors of the covariance matrix and approximate the original data set by a linear combination of the leading eigenvectors. The idea of using the PCA approach is to reduce the size of a data set without much loss of features, where the eigenvectors help to find the optimal feature subspace in the lower

dimensionality needed for the recognition of a test image. Suppose the training data set of the image is $Z_1, Z_2, \ldots, Z_N$, where N is the number of image in the training data set. The images are mean centered at the training set by subtracting the matrix Z from the mean image, as defined as follows [71]:

$$\phi_i = Z_i - \mu, \quad \text{where} \quad \mu = \frac{1}{N}\sum_{i=1}^{N} Z_i \tag{2.1}$$

The data matrix Z is multiplied by transpose Z^T to obtain the covariance matrix Ω [71]:

$$\Omega = ZZ^T \tag{2.2}$$

The covariance matrix Ω has eigenvectors and corresponding non-zero eigenvalues. The eigenvectors are sorted in ascending order of the eigenvalues. To reduce the dimensionality, it is necessary to select the eigenvectors with the largest eigenvalues to be components of the eigenvectors which represent the variance space of the training image set. The mathematical representation of this transformation matrix can be expressed as follows:

Step 1: Centralize all training images by subtracting the mean image as in Equation 2.1.

Step 2: Compute the covariance matrix as in Equation 2.2.

Step 3: Compute the eigenvectors of the covariance matrix.

Step 4: Sort the eigenvectors by decreasing eigenvalues.

Step 5: Choose k eigenvectors with the largest eigenvalues.

Step 6: Transform the samples onto the new subspace.

2.4.2 Kernel linear discriminant analysis using spectral regression

A nonlinear extension of LDA known as kernel discriminant analysis maps the original measurements into a higher dimensional space using the "kernel trick" [49]. Let $x_i \in R^d$, $1, \ldots, m$ be training vectors represented as an $m \times m$ kernel matrix K such that $K(x_i, x_j) = (\Phi(x_i)\Phi(x_j))$, where $\Phi(x_i)\Phi(x_j)$ denotes the embedding of data items x_i and x_j. If ν defines a projective function into the kernel feature space, then KDA can be expressed as follows [10]:

$$\underset{\nu}{max} D(\nu) = \frac{\nu^T S_b \nu}{\nu^T S_t \nu} \tag{2.3}$$

where S_b and S_t define the between-class and total scatter matrices in the feature space, which respectively have the following form [10]:

$$S_b = \sum_{k=1}^{c} m_k(\mu_\phi^{(k)} - \mu_\phi)(\mu_\phi^{(k)} - \mu_\phi)^T \tag{2.4}$$

$$S_t = \sum_{k=1}^{c} (\phi(x_i) - \mu_\phi)(\phi(x_i) - \mu_\phi)^T \tag{2.5}$$

where $\mu_{\phi}^{(k)}$ and μ_{ϕ} denote the centroids of the k^{th} class and the global centroid in the feature space, and the number of samples is represented by m_k in the k^{th} class. Equation 2.3 can be solved by the eigenproblem $S_b = \lambda S_t$:

$$\underset{\alpha}{max} D(\alpha) = \frac{\alpha^T K W K_\alpha}{\alpha^T K K_\alpha} \tag{2.6}$$

Here $\alpha = [\alpha_1, \alpha_2, \ldots, \alpha]^T$ is the eigenvector satisfying $KWK_\alpha = \lambda KK_\alpha$, and $W = (W_l)_{l=1,\ldots,n}$ is an $m \times m$ block diagonal of positive examples, with the lower part assigned to the negative class. Each eigenvector α produces a projection function ν into the feature space. The KDA projections are computed as [10]:

$$\begin{aligned} W\phi &= \lambda\phi, \\ (k + \delta I)\alpha &= \phi \end{aligned} \tag{2.7}$$

An eigenvector of W is represented by ϕ with eigenvectors ϕ computed directly using the Gram-Schmidt method. I is the identity matrix and the regularization parameter is $(\delta > 0)$. However, $(k + \delta I)$ is positive definite and Cholesky decomposition is used to solve the linear equations in Equation 2.7. Thus, the linear system is written as follows [10]:

$$K * \alpha = \phi \Leftrightarrow \begin{cases} U^T\theta = \phi \\ U\alpha = \theta \end{cases} \tag{2.8}$$

For example, first the system is solved to find vector θ and then vector α. U is an upper triangular such that $U^T \times U = K\star$. SR-KDA will solve a set of regularized regression problems with no eigenvector calculation involved. The outcome is a great improvement in terms of computational cost and provides better handling of large kernel matrices. After obtaining α, the decision function for new data items is calculated as follows [10]:

$$f(x) = \sum_{i=1}^{m} \alpha_i K(x, x_i) \text{ where } K(x, x_i) = (\phi(x), \phi(x_i))$$

2.5 Techniques used for classification

This section discusses the techniques used in recognition taskes. Once feature extraction is done, a matching method is applied to classify the features and to make a final decision whether two features belonged to the same person or not. The following reviews some useful techniques.

2.5.1 LDA-based classification

LDA classification is a generative probabilistic method and is one of the most popular approaches used for biometric recognition. The basic concept of LDA is to separate classes by finding a suitable border between them, and the classification is then executed in the transformed space depending on some metric such as Euclidean distance. Mathematically, the LDA criteria can be met by maximizing the ratio of the determinant of the within-class variance to the determinant of the between-class variance. The classification procedure can

be divided into two steps: (1) computing the posterior (confidence) values for each class; and (2) determining the index of the class to which the test sample belongs in relation to the class with the maximum scores by solving $\arg\max_k g_k$ [26, 100]. Thus:

$$g_l(x_i) = x^T \Sigma_l^{-1} \mu_l - \frac{1}{2} \mu_l \Sigma_l^{-1} \mu_l + log\pi_l, \tag{2.9}$$

where Σ_l is the class covariance matrix of the class l, μ_l is the mean vector of the class l and π_l is the prior probability of the class l.

These are calculated as follows [26, 100]:

$$\hat{\mu_l} = \frac{1}{n_l} \sum_{i=1}^{n_l} x_i, \tag{2.10}$$

$$\hat{\Sigma_l} = \frac{1}{n_l} \sum_{i=1}^{n_l} (x_i - \mu_l)(x_i - \mu_l)^T, \tag{2.11}$$

$$\hat{\pi_l} = \frac{n_l}{n}, \tag{2.12}$$

where
n_l: is the number of images in class l;
n : is the total number of objects in the training set.

The classifier ia construction as follows:

Step 1: Compute the mean vector $\hat{\mu_l}$ and prior probability of class $\hat{\pi_l}$, as in equations 2.10 and 2.12.

Step 2: Calculate $\hat{\Sigma_l}$, which is the pooled covariance matrix, as in equation 2.11, which must be positive definite.

Step 3: Estimate the linear discriminant [1] as in equation 2.9.

Step 4: Choose the maximum of $\arg\max_l g_l$[26, 100].

2.5.2 K nearest neighbour classifier

A KNN classifier a useful classification technique based on the closest trained palmprint datasets created from SR-KDA. It is one of the simplest algorithms in the category of machine learning algorithms [93]. The KNN will search through the image training dataset for the k-most similar instances. In this classifier, the majority vote of the neighbours is taken into account for the classification of the image. To determine the distance matrix, the Euclidean distance is calculated between the training and testing image features in the KNN classifier. The Euclidean distance is described as follows:

[1] Matlab can to find discriminant functions with the classify command.

$$D(A,B) = \sqrt{\sum_{i=1}^{m}(A_i - B_i)^2} \tag{2.13}$$

where A is the feature vector for each class in the testing sample, B is the feature vector for each class in the training sample and m is the number of feature vectors.

The distance matrix summation value is calculated and sorted in increasing order. The classification is found by the minimum distance between the palmprint test image and training sets. Consequently, to classify the image accurately, the first k elements are selected, from which their class labels are searched for and majority voting determines the class index of the test image. The construction of the KNN classifier can be summarized as follows:

Step 1: Compute the distance between the testing set and each instance in the training sets.

Step 2: Sort the distances in increasing numerical order and pick the first k elements.

Step 3: Compute and return the most common class in the k nearest neighbours.

In our experiments, k=3 is selected for the algorithm to find the majority class for the unknown vector.

2.6 Palmprint database

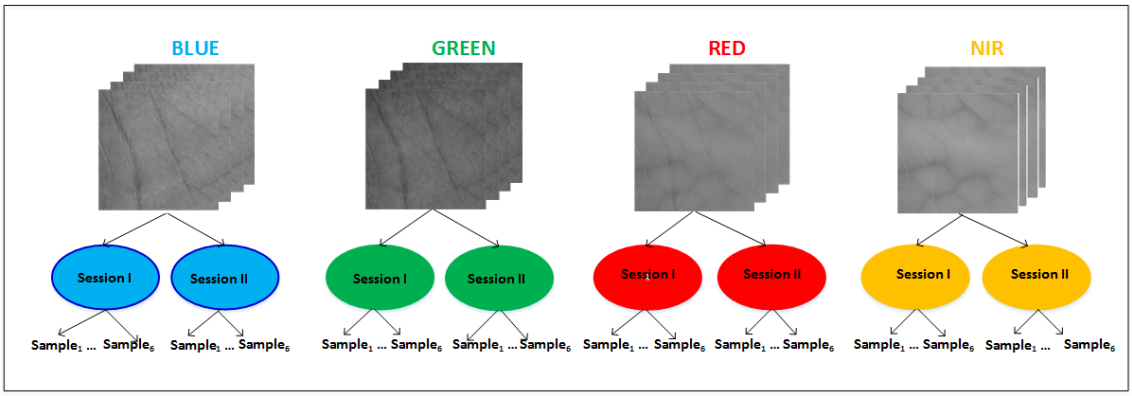

Figure 2.10: Structure of the Hong Kong Polytechnic University palmprint database [121].

The Hong kong Polytechnic University multispectral palmprint database was employed in the experimentation process. The multispectral palmprint images used in the study were gathered from 250 volunteers (195 males and 55 females), aged between 20 and 60 years. The database contains four types of palmprint images captured with visible and infrared light under red, green, blue and NIR illumination. These images were gathered in two separate stages. In each session, six images were provided of each of the subject's left and right palms for each of the red, green, blue and NIR spectral, as shown in Figure 2.10. Overall, for each illumination type, the database contains 6000 (500x12) images obtained from 500 different palms. Therefore, the database contains 6000x4=24000 palmprint images in total. The average interval between consecutive sessions was approximately nine days.

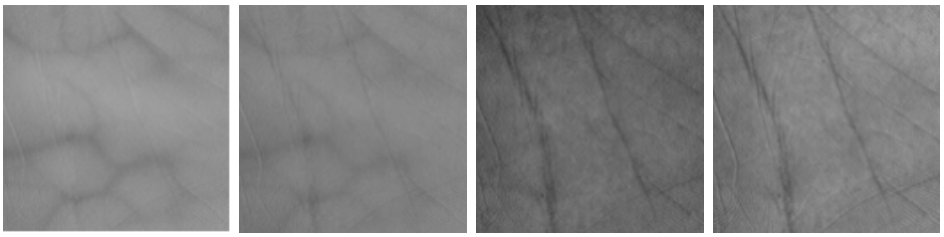

(a) (b) (c) (d)

Figure 2.11: Sample ROI images extracted from multispectral palmprint images from PolyU database: (a) NIR, (b) red, (c) green, and (d) blue.

Figure 2.11 presents sample palmprint images of different spectral (red, green, blue and NIR).

2.7 Summary

This chapter has focused on the most common types of palmprint recognition identified in the literature. The palmprint is presented as a biometric identifier. It affords a rich source of information in terms of its features, such as principal lines, ridges, texture, minutiae points and delta points whose characterize are unique to a human. Over the years, a number of approaches have been reported for use in palmprint recognition systems. This literature review provides a summary of information derived from existing related work. In terms of feature extraction, a number of approaches in palmprint recognition have been classified in several different categories in the literature, including structure-based, statistics-based, subspace-based and code-based approaches. However, there some approaches that cannot be grouped into any one category. Moreover, some fusion methods have been implemented to build palmprint recognition systems with a view to improving the accuracy of the identification process. This chapter has presented a background the of techniques used in this research to reduce length dimensionality of the feature vectors including some classification methods.

The next chapter presents a novel feature extraction technique based on a combination of the PHOG descriptor and PCLBP descriptor.

Chapter 3

Multispectral Palmprint Recognition using Pascal Coefficients-based LBP and PHOG Descriptors with Random Sampling

3.1 Introduction

Histograms derived from LBP representation have been proven to be highly discriminative descriptors. Due to its texture discriminative properties, simplicity and low computational complexity, the LBP method is becoming widely adopted in various pattern recognition problems. Many studies have considered LBP descriptors. The original version of the LBP descriptor only considers the eight neighbours of the pixel, labelling the pixels of an image by thresholding the neighbourhood of each and considering the result as a binary number, as originally proposed by Ojala et al. [83] who showed the high discriminative power of this operator for texture classification.

The extensive study on Local features led to the development of various methods and techniques focusing on improving the robustness to noise and illumination by using different encoding or thresholding schemes. With this large number of methods based texture features, a number of survey papers on LBP-based texture descriptors haven been published. For example, Median Binary Pattern (MBP), Fuzzy LBP (FLBP), Local Quantized Pattern (LQP) and Shift LBP (SLBP) [62]. However, only few studies use LBP texture feature in palmprint recognition systems. For example, Goa [36] presented a hierarchical multiscale LBP which improves the performance by extracting information from the non-uniform bins. Another recent work [32] where useful information from non-uniform palmprint patterned is extracted to generate histogram bins called Hierarchical Multiscale Local Binary Patterns (HM-LBP). This approach focusses on LBP-based descriptors where the thresholding and encoding schemes are modified to analyse the local texture features of digital images with great success.

The main contributions of this chapter are three-fold. First, it introduces a new descriptor called the Pascal coefficient LBP which is a modified Shift LBP (SLBP) descriptor

[62, 24], however, there does not exist any report on the use of SLBP-based descriptor so far. This approach has various advantages, such as its simplicity and robustness against changing image conditions. The main idea is to use a variable number of intervals to generate a distribution of binary codes for every pixel position, to investigate the advantages of using the pixels response from the visible light to the infrared. In the proposed technique, the main difference from SLBP is that the threshold value is tuned using Pascal coefficients of order n with an alternating sign (section 3.2). Furthermore, this variant is also extended to MLBP in this chapter, referred to as the PCMLBP descriptor, for which the features of the different scales are first extracted and their histograms subsequently concatenated into a long feature (section 3.3). To achieve higher recognition rates, a fusion feature scheme is proposed to form a new set of palm features. Finally, the concept is based on a combination of the PHOG descriptor with the PCLBP descriptor, so that the histogram bins have a more powerful discriminatory power (section 3.4). Nevertheless, having a large number of features can become an issue and can hamper classification. To solve this problem, PCA is used to reduce the size of the dimensionality of the vector of palm features (section 2.4.1 of chapter 2). Random sampling is used to generate multiple feature subsets. In addition, a multiple LDA classifier is constructed from many individual classifiers and a powerful decision rule is used for the purpose of combination and this is known as ensemble learning (section 3.5). Section 3.6 gives a description of the experimental set-up and results, followed discussion in section 3.7 and Computational complexity in section 3.8. The chapter ends with a summary in section 3.9.

3.2 Pascal coefficients-based LBP-based feature extraction

As mentioned previously, only eight neighbours of the central pixel are considered in the original LBP. Ojala et al. [83] were among the first to propose the use of LBP in pattern recognition by demonstrating the superior discrimination of this descriptor for texture classification. In this approach, the adoption of a different pixel threshold is suggested. Modifying the labels of the pixels of the palmprint by means of binary coding is a simple and effective technique. First, the value of the current pixel, g_c, is used as a threshold for each of its neighbouring g_p $\{0, 1, \ldots, Q-1\}$, taking the result as a binary number. PCLBP code is created for each pixel location. By changing the expression $(g_p - g_c)$ in $LBP_{Q,r}(w,z) = \sum_{p=0}^{Q-1} S\left(g_p - g_c\right)^{2^p}$ to $(g_p - g_c - l)$.

The PCLBP is represented in Equation 3.1 for a location (w, z) and a value l. Here, l takes the different coefficients of Pascal values with an alternating sign, as shown in Equation 3.3; for each change in l, a new binary number is formed and included in the histogram pattern.

$$\mathrm{PCLBP_{Q,r}}(w,z,l) = \sum_{p=0}^{Q-1} S\left(g_p - g_c - l\right)^{2^p} \tag{3.1}$$

where Q is a set of sample points regularly spaced on a circle of radius r, whereas S can be described as follows:

$$S(w) = \begin{cases} 1 & \text{if } w \geq 0 \\ 0 & \text{otherwise} \end{cases} \tag{3.2}$$

In our case, l is the coefficient in a Pascal triangle of order n, which represents a threshold value; l is defined as follows [63]:

$$l_{n,j} = (-1)^j \binom{n}{j}, \quad j = 0, 1, .., n \tag{3.3}$$

where

$$\binom{n}{j} = \frac{n!}{j!(n-j)!} \tag{3.4}$$

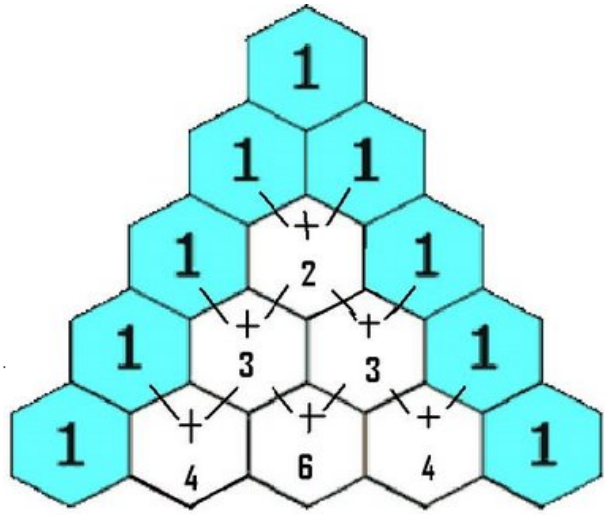

Figure 3.1: Construction of Pascal coefficients.

If n is set equal to 3, for example, the Pascal coefficients (l) from equation 3.3 will be ($(-1)^0\binom{3}{0}$=1, $(-1)^1\binom{3}{1}$= -3, $(-1)^2\binom{3}{2}$=3 and $(-1)^3\binom{3}{3} = 1$), which correspond to the fourth row of the Pascal triangle as shown in Figure 3.1. Therefore, for each pixel location, l will generate four binary codes which will contribute to the histogram. Thus, similarly to other LBP techniques, the final histogram is divided by $n+1$, resulting in a histogram sum equal to the number of pixel positions considered [62].

3.3 Pascal coefficients multi LBP-based feature extraction

The proposed PCMLBP method is predicted to be an efficient and effective descriptor for palmprint recognition. In the proposed method, the idea behind the multi-scale version of the PCLBP is to improve the performance of the classification. In a multi-scale version, the principle is based on changing the radius of the PCLBP and then concatenating all the resulting features. However, there is an issue in multi-scale of high dimensionality of combinations; this problem can be overcome by means of effective feature selection to reduce unnecessary or redundant features. Figure 3.2 provides examples of different values of Q and R for circular neighbourhoods.

Changes in the dimensions of radii depend on the distance of the neighbouring pixel from the centre of the window used, making it possible to generate a multi-scale representation

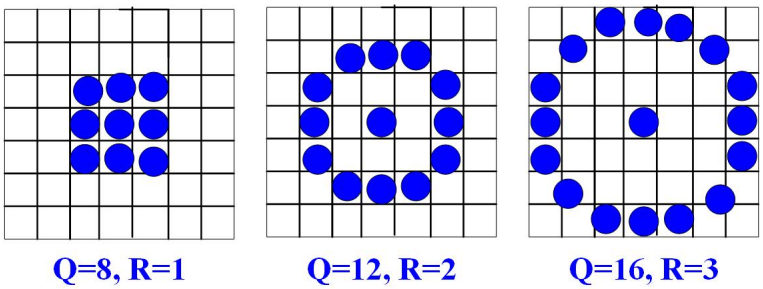

Figure 3.2: Multi-scale LBP.

by concatenating PCLBP histograms that determine the size of the radius [83] (e.g., 2^8 yields 1280 bins for 5 scales ($R = 1, 3, 5, 7, 9$)). The information contained in the histogram relates to how the multi-scale features are distributed over the whole palmprint image. The multi-scale approach would yield higher accuracy compared to the single-scale description of PCLBP. The histogram of PCLBP for each scale of image size $A \times B$ is calculated as follows:

$$H_{Q,r}(p) = \sum_{i=0}^{A-1} \sum_{j=0}^{B-1} k\left(\text{PCLBP}_{Q,r}(i,j), p\right), \tag{3.5}$$

$$p \in [0, n-1], \text{ and } r \in [0, R]$$

where
n : is the maximum bin value of the PCLBP;
R : is the maximum radius used to the multi-scale.

$$k(x,y) = \begin{cases} 1 & \text{if } x = y \\ 0 & \text{otherwise} \end{cases} \tag{3.6}$$

The PCLBP histograms calculated at various radii provide local information on the observation vector. The resultant multi-scale palmprint histogram is as follows:

$$F_{Q,r} = [H_{Q,1}, H_{Q,2}, \ldots, H_{Q,R}] \tag{3.7}$$

In the proposed technique, PCA is used to reduce the high dimensionality and avoid overfitting of the resulting palmprint feature vectors (see section 2.4.1).

3.4 Pyramid histogram orientation gradient (PHOG)-based feature extraction

A PHOG descriptor represents a spatial structural layout of a local image shape in a flexible manner. First, the PHOG extracts the edge contour of given known stimuli using, for example, a canny edge detector. The image is then split into spatial grids by means of an iterative technique which will double the number of splits in every dimension; for example level k would have 2^k cells in each dimension. Then, the histograms of oriented gradients (HOGs) are computed using the 3×3 Sobel mask, followed by the weighted contribution of each edge in accordance with its magnitude. Every single cell's histogram is given a particular quantity described as M bins. The bins relate to number of edge directions in an

angular range. Figure 3.3 presents the structure of the HOG descriptor. The final PHOG descriptor is then obtained where the HOGs are found one after the other at the same level, as shown in Figure 3.4. Therefore, the final PHOG descriptor of an image is obtained from the HOGs computed at various pyramid levels. The PHOG descriptor for the event region is a vector of the dimension $t = M \sum_{k=0}^{K} 4^k$. A pyramid K=3 is used with a bin size M=8 and a range of orientation of [0,360]. This results in a descriptor of the dimension 680 [7, 50].

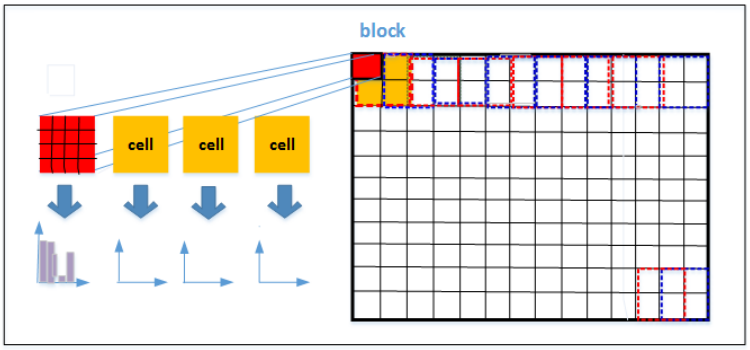

Figure 3.3: Structure of HOG descriptor.

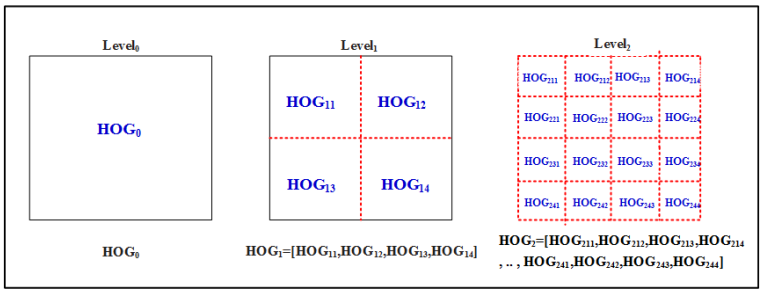

Figure 3.4: Structure of PHOG descriptor.

3.5 Feature sampling

As mentioned in section 2.5.1, LDA outperforms common subspace methods. However, there is still plenty of room to improve its performance further. One likely avenue for improvement has been proposed which enhances performance by employing numerous LDAs trained on various parts of the data which are then combined in an ensemble [101].

An ensemble is a method used to merge a number of weak classifiers to build up a strong classifier, as shown in Figure 3.5. Such multiple classifier ensembles are variously called mixtures of experts or combinations of multiple classifiers [59]. The idea is to use a set of weak classifiers and assemble them to build an ensemble classifier with a powerful decision rule. It should be noted that weak classifiers do not always make the same error [68]. The overall error of the combined classifiers together provides an outcome that improves considerably on what any individual classifier could achieve on its own. One main condition for the success of combining different weak classifiers is that the outcomes of single classifiers for the same

inputs must vary [60]. The diverse individual classifiers are obtained by employing various training datasets, various feature datasets, different types of single classification methods and a fusion rule. A multiple LDA classifier is constructed in this study by combining many individual weak classifiers, aiming to build a more robust LDA classifier that includes the overall palm feature space without loss of discriminant information [101].

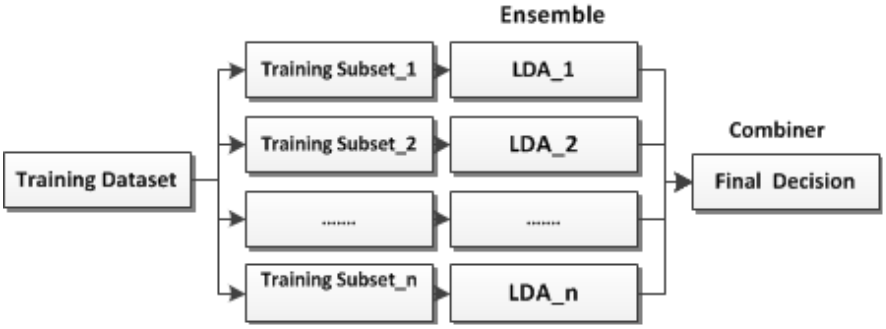

Figure 3.5: Diagram of proposed ensemble learning for palmprint recognition

3.5.1 Random sampling-based LDA for palmprint recognition

The random sampling method (RSM) is a common ensemble building method used to improve the precision of weak classifiers. The classifiers are constructed using the concept of random sampling of the palmprint feature to develop an ensemble from the individual classifiers trained using different feature subsets. This section proposes the application of the random sampling procedure to build many weak LDA classifiers. Different palmprint feature subsets are first randomly selected. Then, a LDA classifier is built on each of those palm subsets, and a fusion rule is used at the end for prediction with the palm testing set. The proposed random sampling LDA classification methodology includes the following steps:

Step 1: Generate K random training data set.

Step 2: Use PCA on the palm training sets. Then remove all the eigenvectors with null eigenvalues.

Step 3: The K LDA classifiers are the constructs from the K random sampling.

Step 4: In the palm recognition step, the outcomes of the K LDA classifiers are fused using a fusion rule to generate with a final decision.

3.5.2 Fusion process

A fusion strategy can be performed at three levels of either the sensor data, feature and matching-scores. Data fusion is used to combine numerous sources of raw information to create new raw data that are estimated to be more useful than the inputs. Feature level fusion combines different features in feature spaces. Decision fusion is used to combine results coming from many classifiers. Fusion rules are used to combine the individual classifiers, and types include majority voting and logical AND/OR fusion rules. In the

proposed approach, fusion can be undertaken at two levels of features level and matching-scores.

1. Feature level fusion: A fusion technique is desired in the field of biometric recognition because it can provide sufficient informational content. Moreover, it should be simple to access and concatenate into one feature vector. In the proposed approach, a palmprint image sample has two different types of feature, PCLBP and PHOG. PCLBP and PHOG features are concatenated for the purpose of classification, as shown in Figure 3.6.

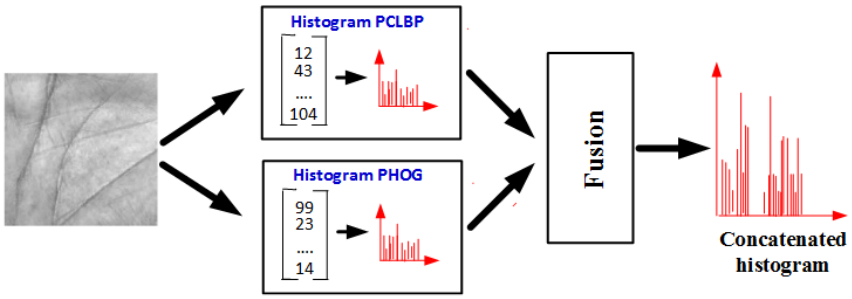

Figure 3.6: Schematic illustration of fusion PCLBP and PHOG descriptors.

2. Decision level fusion: The objective of using fusion is to improve performance by constructing an ensemble of several LDA classifiers which are trained on different subsets. In the proposed method, several classifiers are combined by applying the *sum score* rule to reduce overall error. The overall accuracy of palmprint recognition appears to be improved using this ensemble approach. Figure 3.5 provides the general scheme of the proposed classification approach.

3.6 Experiments and results

3.6.1 Protocol I

In our experiments, an evaluation protocol similar to DWT [111], NFS [113], CFKNNC [113] and TPTSR [67] was used. NFS is the nearest feature space classifier, which uses the distance between the test sample and space spanned by the training samples from a class. The discrete wavelet transform (DWT) method was designed to extract local features from palmprints. Jing at al. [67] introduced the two-phase test sample representation (TPTSR) method. In the first phase, TPTSR represents the test sample as a linear combination of all the training samples and determines the M nearest neighbours of the test sample. In the second phase, the test sample is linearly represented with new coefficients, weighting the M nearest neighbours in a linear combination to classify the test sample. The coarse-to-fine-k-nearest neighbour classifier CFKNNC method is used to improve on the performance of the CKNNC.

In this protocol, training was carried out using 6 palmprint samples of the first session while in testing 6 palmprint images from second session (six training sets and six test sets) were used. Therefore, for each spectrum (green, red, blue and NIR) there are 3000 (500x6)

training samples and 3000 (500x6) test samples. For palmprint features, a PCMLBP descriptor was generated with different radii for five scales (R=1,3,5,7,9) and eight neighbours, resulting in a PCMLBP having a scale of 1280 (5x256) for the five scales. Furthermore, when using a combined PCLBP-PHOG, the PCLBP descriptor was generated with a radius, which is equal to six and eight neighbours. For the PHOG descriptor, we used L=3 pyramids, a bin size of N=8 and a range of orientations [0,360]. This results in a descriptor with a dimension of 680. It should be noted that the experimentation process was repeated 10 times to obtain the different training datasets. The results obtained from the experiments are listed in Table 3.1 showing the recognition rates obtained for 250 random subsets of the feature dataset.

Methods	Recognition Rate (%)			
	Blue	Green	Red	NIR
DWT [111]	93.83	93.50	95.20	94.60
NFS [113]	97.30	96.37	97.97	98.17
CFKNNC [113]	98.83	98.77	98.00	96.40
TPTSR [67]	78.13	98.02	98.58	98.34
Proposed PCMLBP	**98.90**	97.27	**98.74**	97.54
Proposed PCLBP+PHOG	**99.40**	**99.07**	**99.60**	**99.27**

Table 3.1: Comparison of recognition rates calculated for Protocol I of the proposed approach and state-of-the-art techniques for different spectral bands (blue, green, red and Nir), computed using six training sets and six testing sets

In the case of the blue spectrum, the PCLBP-PHOG approach yields the highest recognition rate of 99.4%, while the PCMLBP has the second highest rate of 98.90%. Moreover, it can be seen that, in the case of the green spectrum, the PCLBP-PHOG method achieves the best result with a rate of 99.07%. Furthermore, compared to other existing approaches, the ensemble method results in increased performance of 2.7%, 0.3%, 5.57% and 1.05% over NFS, CFKNNC, DWT and the TPTSR respectively. The PCMLBP method offers the best result of 97.27%, higher than for NFS and the DWT, but 1.5% and 0.75% lower than CFKNNC and the TPTSR, respectively. In relation to the red spectrum, the PCLBP-PHOG yields better results than the NFS, CFKNNC, DWT and TPTSR. Furthermore, the results indicate that PCLBP-PHOG obtains good result, with a performance accuracy of 99.6% followed by the PCMLBP with a rate of 98.74%. The table also confirms that the accuracy of performance of the PCLBP-PHOG is greater than that of the the NFS, DWT and TPTSR methods. In addition, the experiments reveal that the PCMLBP technique achieves an accuracy of 97.54%, outperforming the DWT and CFKNNC methods, although 0.63% and 0.8% lower than the NFS and TPTSR methods respectively for the NIR spectrum.

Furthermore, using an ensemble of several LDA classifiers has an impact on the recognition rates, giving an improvement in recognition accuracy compared to the individual LDA classifier recognition rates. The results of the different features selected (50, 100, 150, 200, 250, 300 and 350) for the training sets in the PCLBP-PHOG approach are shown in Figure 3.9. The X-axis denotes the number of palm features in the training sample, while the Y-axis denotes the accuracy of the test palmprints. The multi-classifier recognition rate of the blue

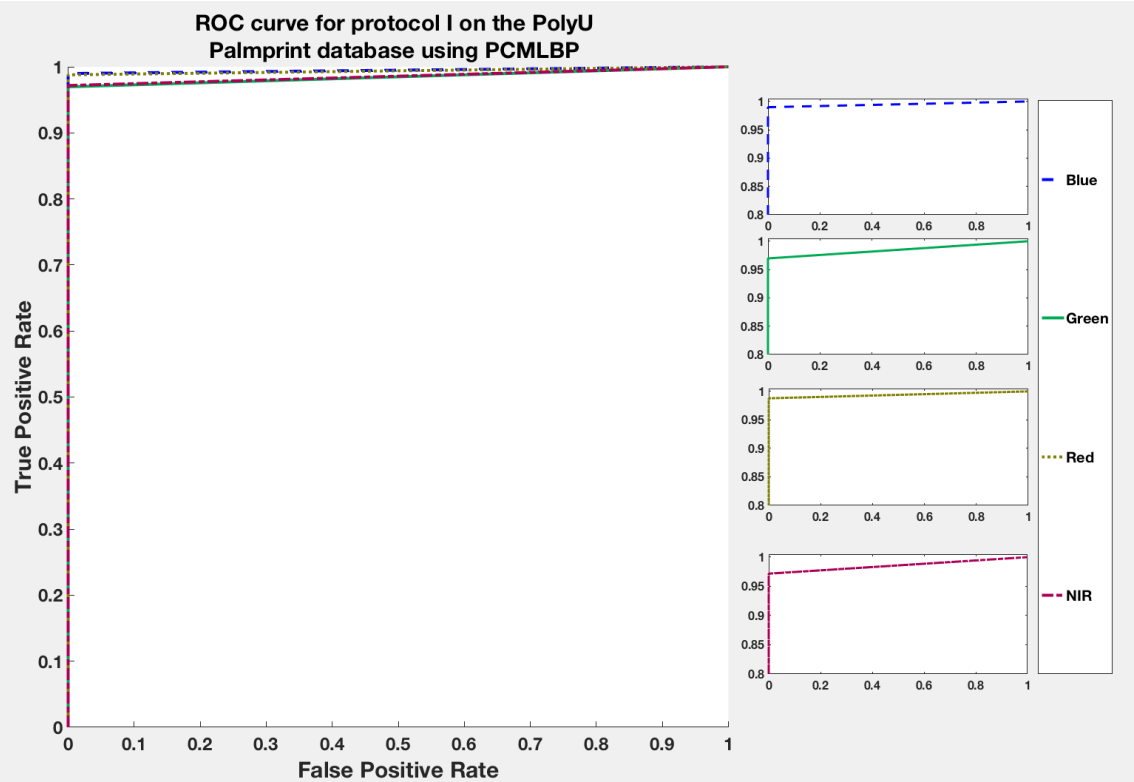

Figure 3.7: LDA ROC curves for the PCMLBP descriptor under the blue, green, red and NIR spectra using six images captured in the first session for the training set and six images captured in the second session for the testing set.

spectrum offers the highest performance, above all other spectra, when using the PCMLBP features. However, red was the best spectrum when the fusion PCLBP-PHOG was applied. Figures 3.7 and 3.8 illustrate the receiver operating characteristic (ROC) curves, plotting the false acceptance rate (FAR) vs the genuine acceptance rate (GAR) for the different multispectral palmprint data sets. These curves represent the red, green, blue and NIR spectra. It is evident from these figures that the recognition rate of the multi-classifiers in the proposed PCLBP-PHOG method is better for the red spectrum than the other spectral bands (blue, green and NIR).

Methods	Recognition Rate (%)			
	Blue	Green	Red	NIR
RBF [132]	96.70	96.50	98.20	98.40
NFS [113]	95.10	92.87	95.40	95.63
Proposed PCMLBP	**97.99**	95.44	97.67	95.84
Proposed PCLBP+PHOG	**99.17**	**98.33**	**99.34**	**98.77**

Table 3.2: Comparison of recognition rates calculated for Protocol II of the proposed approach and state-of-the-art techniques (RBF and NFS) for different spectral bands (blue, green, red and NIR), computed using three training samples and six testing samples.

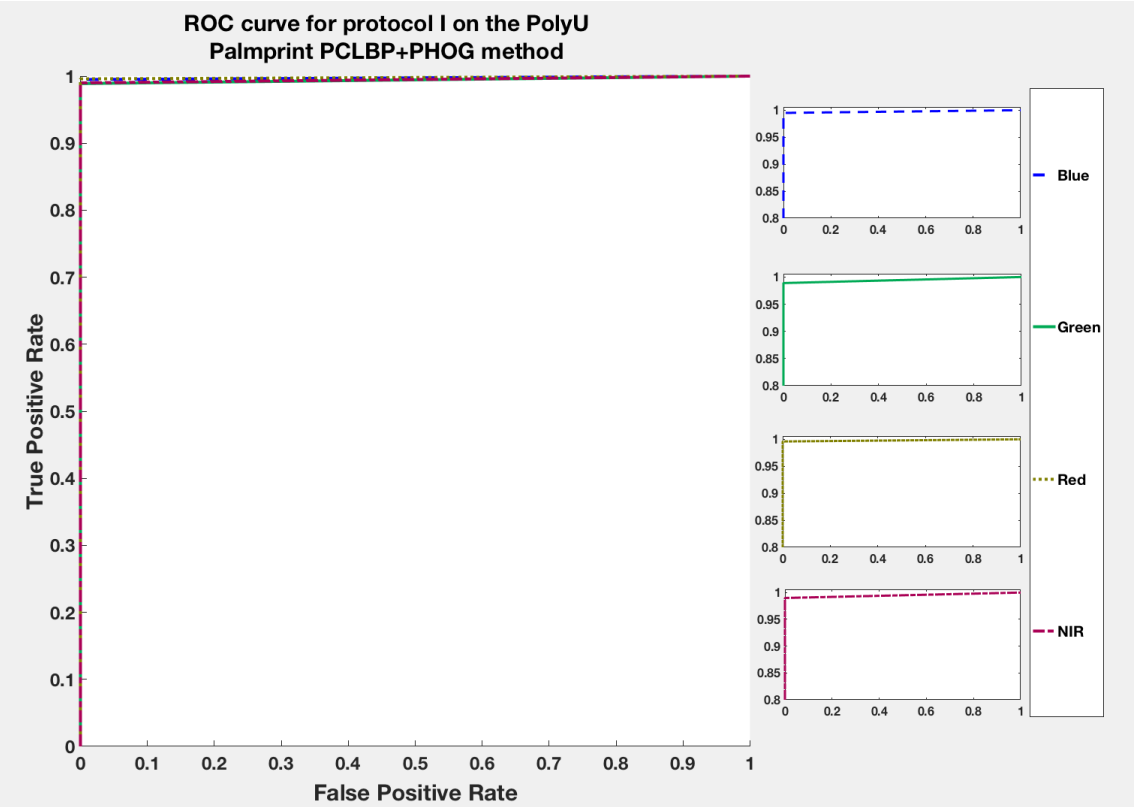

Figure 3.8: LDA ROC curves for the PCLBP and PHOG descriptors under the blue, green, red and NIR spectra using six images captured in the first session for the training set and six images captured in the second session for the testing set.

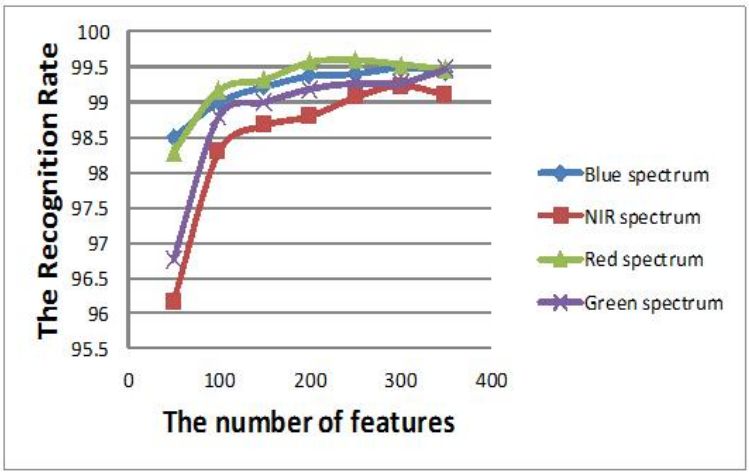

Figure 3.9: Recognition rates for the six training samples and six testing samples from the PolyU multispectral palmprint database. The horizontal axis represents the number of features (50, 100, 150, 200, 250, 300 and 350) and the vertical axis indicates the recognition rates of the PCLBP-PHOG descriptor for the four spectra (blue, green, red and NIR).

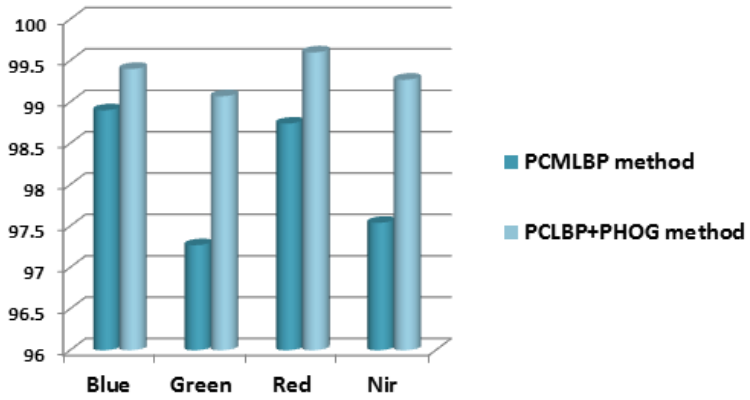

Figure 3.10: Comparison of PCMLBP and PCLBP+PHOG approaches in Protocol I .

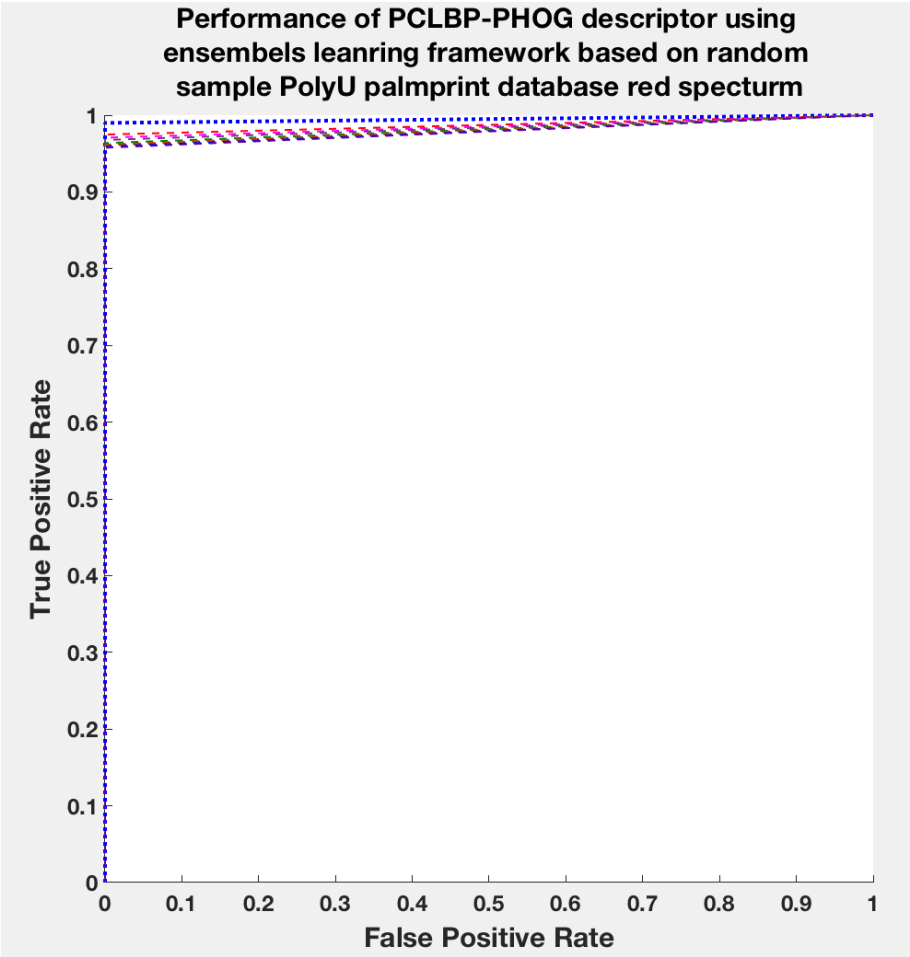

Figure 3.11: LDA ROC curves for the PCLBP and PHOG descriptors under the red spectrum using six palmprint images were gathered in the first session for the training sample and six palmprint images were gathered in the second session for the testing sample. Comparison of the use of single classifiers versus an ensemble approach.

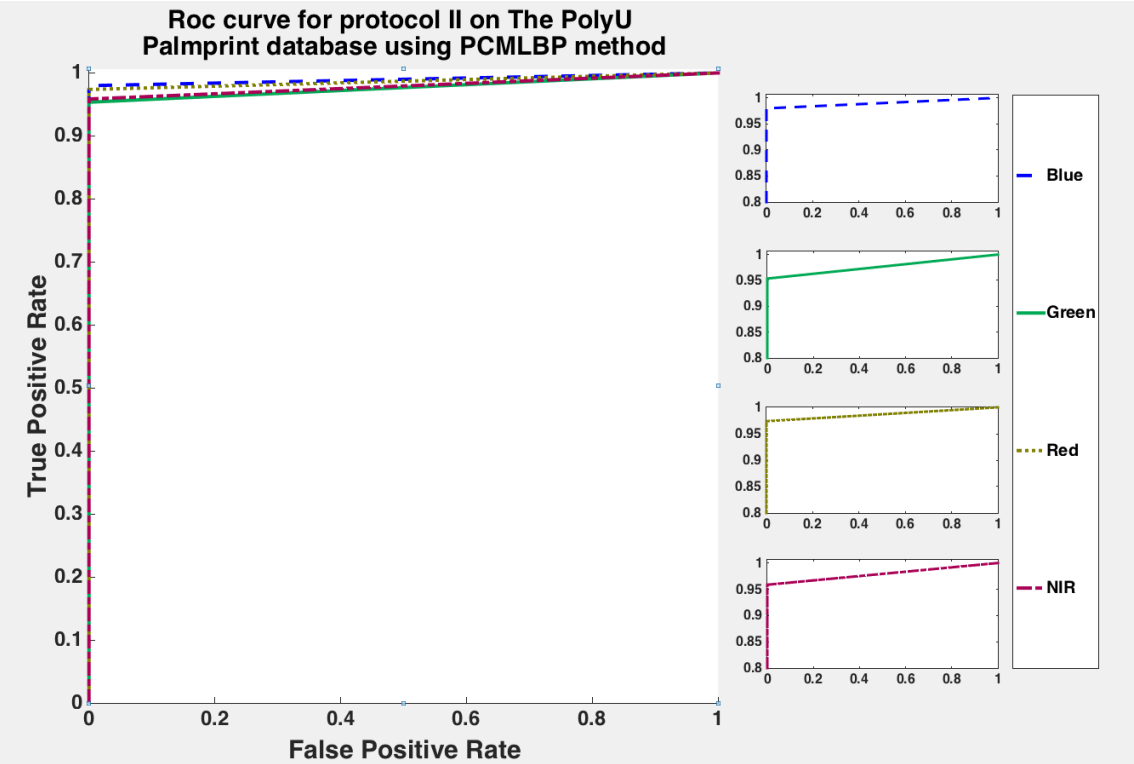

Figure 3.12: LDA ROC curves for the PCMLBP descriptor under the blue, green, red and NIR spectra using three palmprints images gathered in the first session for the training sample and six palmprint images gathered in the second session for the testing sample.

3.6.2 Protocol II

To validate the performance of the proposed methodology, the standard evaluation protocol [132, 113] as followed. The use the first three images under the blue, green, red and NIR spectra were used for the training sample along with six palm images from the second session for the testing sample. Moreover, all parameters of the proposed methods were initialized as described in Protocol I. A detailed comparison of the results using the LDA ensemble trained on a subset of 250 random features is summarized in Table 3.2.

The RBF kernel function is used to optimize the feature space such that the samples from the same class are well clustered while the samples from different classes are pushed far away. The method proposed in a previous study [113] has been introduced in protocol I.

Table 3.2 clearly demonstrates the advantage of the robustness of the PCLBP-PHOG approach in terms of the histogram features, in addition to its effectiveness over other reported methods. The PCLBP-PHOG offers attractive recognition performance rates of 99.17%, 98.33%, 99.34% and 98.77% for the blue, green, red and NIR spectra respectively. Moreover, the results displayed in the table indicate that the PCMLBP approach outperforms the NFS. In the case of the red spectrum, the PCMLBP method achieves an accuracy of 97.67%, which is higher than the NFS but 0.53% lower in comparison with the RBF. The recognition rate of the PCMLBP in relation to the blue spectrum is 97.99% and thus outperforms the RBF method. However, the PCMLBP method still achieves lower results

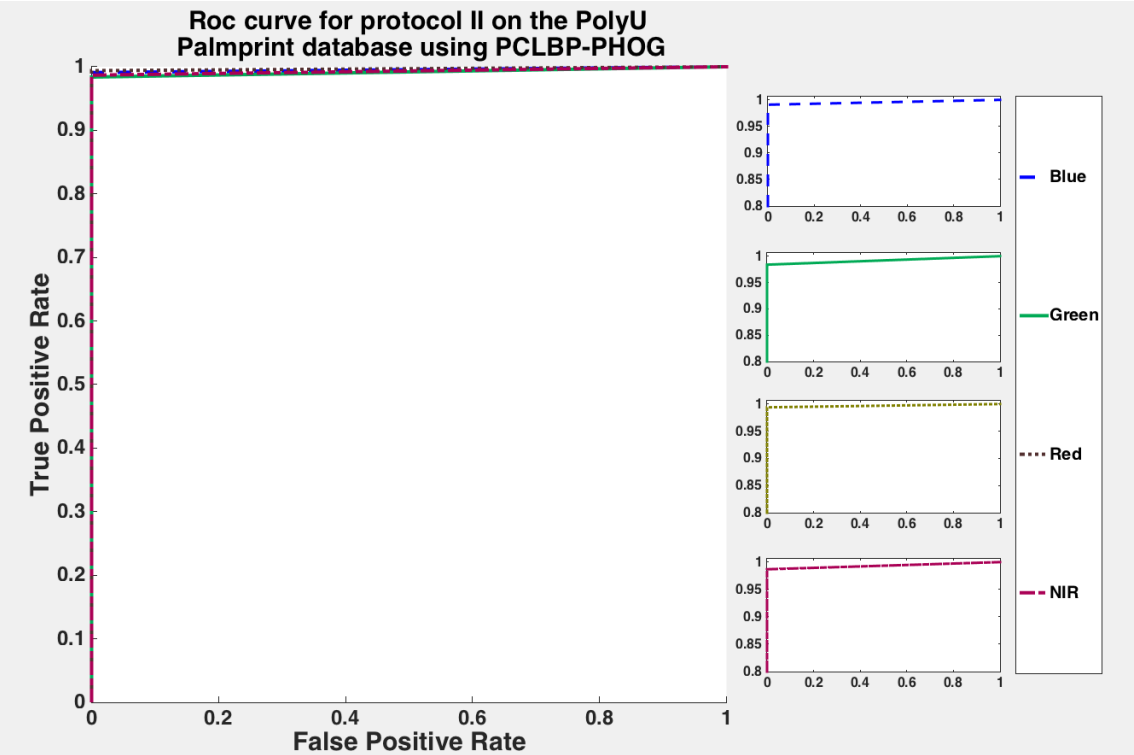

Figure 3.13: LDA ROC curves for the PCLBP and PHOG descriptors under the blue, green, red and NIR spectra using three palmprint images gathered in the first session for the training sample and six palmprint images gathered in the second session for the testing sample.

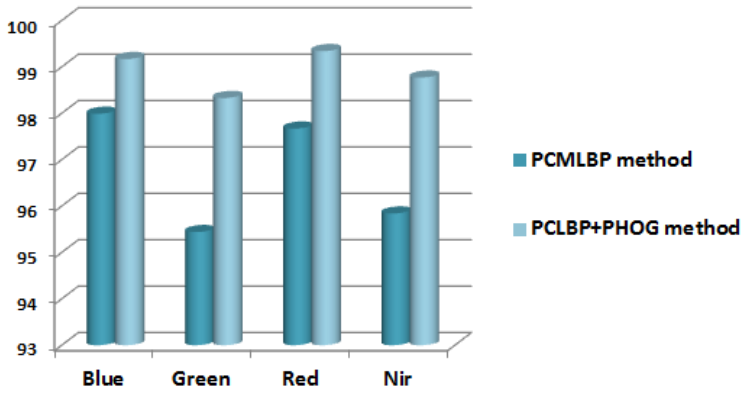

Figure 3.14: Comparison of PCMLBP and PCLBP+PHOG approaches in Protocol II .

than the RBF method for the other spectra (green, red and NIR). The ROC curves for the PCMLBP method are shown in Figure 3.12. The effectiveness of the PCLBP-PHOG approach is presented in Figure 3.13, which reflects the ROC curves showing the best recognition rates for all spectra.

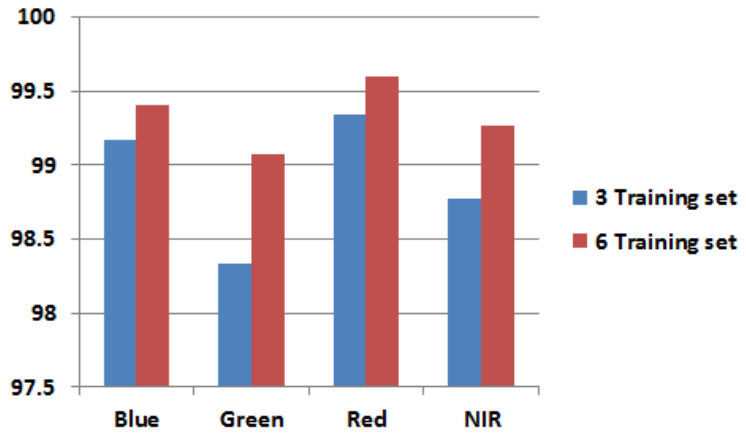

Figure 3.15: Comparison of PCLBP+PHOG approaches for training sampling.

3.7 Discussion

The proposed approach successfully captures discriminating information using the multi-LDA classifier. The method combines several LDA classifiers based on random sampling using the sum score rule. This leads to much improved recognition rates compared to other existing methods. The results are plotted in Figure 3.11 showing that the ensemble of several LDA classifiers has an impact on recognition rates. It has also been proved that the accuracy of recognition is higher than that of individual LDA classifiers.

From the two experiments, it can be noticed that the results of the proposed method for Protocol II are slightly less impressive in comparison to the results obtained in Protocol I. This is because three training and six testing samples were used for the experimentation in Protocol II, which does not seem to provide as much discriminative power as when using six training and six testing samples in Protocol I. Moreover, as different training and testing samples were used in the two experiments, a comparison is provide based on the number of testing and training samples used in existing techniques. The PCLBP-PHOG approach is found to outperform existing methods in all respects. The ROCs in Figures 3.7, 3.8, 3.12 and 3.13 plot the false acceptance rate versus the genuine acceptance rate for the different multispectral palmprint data sets, represented by the red, green, blue and NIR spectra. As shown in these figures, it is possible to achieve greater accuracy using six training and six testing samples compared to three training and six testing samples. Moreover, several results in Tables 3.1 and 3.2 show that the PCLBP-PHOG method performs well and can obtain a higher recognition rate than PCMLBP and other state-of-the-art techniques. It is also observed from the tables and graphs that the use of red spectrum palmprints yields better performance in comparison to other spectra. The red spectrum captures better the palm lines and vein structures and this helps in the comparison and classification of palms with similar palm lines [121]

3.8 Computational complexity

The first method used different radii of the PCLBP operator. It is noticeable that there are too many patterns in the multi-scale PCLBP, with high computational complexity. The

second method is a combination of PHOG and PCLBP, which leads to the dimensionality problem and further increases computational complexity. Thus, the idea was to reduce the dimension size, which has a large number of palmprint features for use in the classification. The dimension of the PCLBP-PHOG feature vector can be reduced by using feature selection or extraction methods. PCA was applied to a randomly selected feature subset in order to reduce both the dimensionality of the palmprint feature vector and the computational complexity involved. The performance of the proposed PCLBP-PHOG method was compared to other methods. The experimental results obtained showed that it gives outstanding results when compared to other existing methods.

3.9 Summary

A novel multi-spectral palmprint recognition methodology has been proposed based on the combination of PCLBP and PHOG descriptors. The study used random sampling to construct many individual LDA classifiers and applied PCA to reduce the dimensions of feature vectors of random length feature vectors. In this work, fusion rules are used to fuse a number of LDA classifiers and thus demonstrate the concept of the proposed framework proposed. The experimentation was performed according to two different protocols, confirming that the proposed methodology achieves higher recognition rates. Furthermore, it can be observed that, in the PCMLBP approach, both with three and six training samples there is better performance for the blue spectrum band than other bands. Moreover, the PCLBP-PHOG approach achieves higher recognition rates and outperforms the PCMLBP and other state-of-the-art techniques, with the red spectrum band performing better compared to other spectra.

It is not possible to know in advance the texture descriptor which gives the best results since the success of a classification process depends on the discriminative power of the extracted features. From the evaluation of the resulting images, it is concluded that the proposed method yields a high discriminative power of Pascal coefficients. Pascal coefficients should produce a distribution of binary codes which will pick up the normal distribution nature of that neighborhood. The advantage of a normal distribution is its simplicity, and in many cases, methods developed based on normal theory work quite well even when the distribution is not exactly normal. This is demonstrated by the fact that the results achieved outstanding recognition rates of 99.60% . An additional aspect is that the computational cost is significantly reduced, as the PCLBP outputs are pooled into a histogram of 256.

The next chapter introduces the proposed fusion technique that generates a new set of palm features based on the combination of multiple features at the feature level in the palmprint biometric system.

Chapter 4

Fusion of Information at Feature Level in Palmprint Biometric System

4.1 Introduction

Fusing multiple features within one biometric modality has attracted increasing attention and interest among researchers during recent decades, because this concept is useful in addressing a wide range of real-world problems. It is understood that every single area that deals with a combination of types of information from different sources, either to generate a single representational type or to reach an outcome, will involve information fusion in pattern recognition. Current studies related to palmprint recognition combining features have achieved better outcomes than those using the previous technique, which used a single source. Additional features may represent various elements of palmprints, so the use of various features does have a meaningful effect on palmprint recognition techniques. As mentioned previously in Chapter 3, the process of information fusion can be broadly classified into three different types: sensor level, feature level and decision level fusion. The effectiveness of the extraction of new informative data is increased by raw data fusion, which combines numerous sources of raw data. For example, images captured with a number of spectral bands can be combined to create a new image with the greater amount of information content available in all spectral bands. Then, this single image can be used by the operator or in image processing instead of using the original images.

In recent years, feature-level fusion has increasingly been studied by many engaged in biometric technology. The idea of feature fusion is how to extract different features using various methods from the same models, and then to fuse them together using optimization algorithms. Effective discriminative information can be extracted while still reducing any redundant information of the features. This can lead to improvements in the effectiveness and efficiency of palmprint recognition. Although, there have been several studies in this area, feature concatenation tends to be the method most commonly used. Some schemes prefer feature concatenation before selection or transformation, whereas approaches to decision fusion comprise, for example, majority voting, ranked list combinations and logical AND/OR fusion rules.

This chapter is has two main objectives: (i) enhance the quality of extracted palmprint image features and (ii) develop new and efficient algorithms for palmprint recognition. The

chapter introduces a novel fusion approach that combines two algorithms: Local Binary Pattern Histogram Fourier Features (LBP-HF) and the Gabor filter technique for feature extraction. A multi-feature extraction using LBP-HF and orientation properties of the Gabor filter is applied to improve the accuracy of palmprint recognition. In addition, the chapter presents a Multi-scale Shift local binary pattern histogram (MSLBP), which is modified by extending the SLBP by using multi-scale, and the aim is to develop a more accurate extraction features of palmprint to enhance the recognition accuracy.

Concatenating multiple feature vectors are attributed to large amount of information which reduces the efficiency of a system. These irrelevant attributes simply add noise to the feature vector which affect the overall accuracy, increasing the complexity, time and system resources needed. Most features in a data set take form of the dimension of the processing space used by the algorithms, the higher the dimensionality of the processing space the higher the computational cost involved in the algorithm processing.

To minimize these problems a dimensionality reduction based on the SR-KDA technique is used to reduce the dimensionality and extract the discriminative information in order to offers better performance and robustness than the single information sources for palmprint recognition in the case of illumination and rotation distortions. Experiments are carried out and the results show that the proposed approaches outperform other state-of-art contenders.

The main body of this chapter is composed of two main sections. Section 4.2 proposes a fusion technique that generates a new set of palm features based on the combination of LBP-HF and the Gabor filter technique. This section is organized as follows. Subsection 4.2.2 provides the description of methodology used, and subsection 4.2.3 addresses the experimental results, while subsection 4.2.4 provides a discussion of the results.

Section 4.3 then describes the different steps constituting the proposed multispectral palmprint recognition process. Subsection 4.3.2 describes the methodology of the palmprint recognition process. The experimental set up is explained in section 4.3.3, and the results are discussed in section 4.3.4. Finally, section 4.4 concludes this chapter.

4.2 Multispectral palmprint recognition based on local binary pattern histogram Fourier features and Gabor filtering

4.2.1 Introduction

The first part of this chapter is concerned with a new framework for feature fusion in palmprint biometric systems which uses a concatenation method to fuse the information extracted from LBP-HF and Gabor filtering techniques. The proposed technique aims to improve the accuracy of the palmprint recognition process. Fusion techniques which combine feature vectors to generate a new fused feature vector tend to be associated with dimensionality problems. The high dimensional fused feature vector is thus reduced to lower dimensionality using the SR-KDA method. This is able to improve the discriminatory power in the new fused feature vector due to the rich information gained from feature fusion. The evaluation of the performance of the proposed approach was conducted using a multispectral palmprint database containing images captured under different spectral wavelengths, with green, red, blue and NIR spectra. The evaluation results show that the proposed approach yields improved performance compared to a number of existing methods, including the specific techniques described elsewhere [67, 111, 113, 132].

4.2.2 The framework of the proposed palmprint recognition system

This section proposes and describes a new methodology that combines two feature extraction algorithms. It can be divided into three processes: feature extraction, dimensionality reduction and classification. The first process in the proposed framework is to extract the palm features of LBP-HF and Gabor filter for use as one vector of feature extraction. Feature extraction is the most important step in improving the recognition process. The resulting high dimensional feature vector increases the computational cost of the proposed approach. The SR-KDA is used to overcome this problem (see section 2.4.2). In designing the proposed recognition system, the KNN classifier is then used for the final decision (see section 2.5.2). The following subsections describe the proposed framework in detail.

4.2.2.1 Gabor filter-based feature extraction methodology

Gabor filter is widely used for image processing, computer vision and pattern recognition. The Gabor filter was originally proposed by Dennis Gabor [27]. It provides effective discriminative features under various image brightness and dissimilarity conditions. A 2D Gabor function $g(x, y)$ and a Fourier transform of Gabor function $G(x, y)$ can be characterised as follows[25]:

$$g(x,y) = (\frac{1}{2\pi\delta_x\delta_y}) \exp(-\frac{1}{2}(\frac{x^2}{\delta_x^2} + \frac{y^2}{\delta_y^2}) + 2\pi j\omega x) \tag{4.1}$$

$$G(x,y) = \exp(-\frac{1}{2}(\frac{(u-W)^2}{\delta_u^2} + \frac{v^2}{\delta_v^2})) \tag{4.2}$$

where $\delta_u = \frac{1}{2}\pi\delta_x$ and $\delta_v = \frac{1}{2}\pi\delta_y$, with the Gabor functions forming a complete but non-orthogonal basis set. Localized frequency descriptors are provided by expanding the signals using this basis. Considering $g(x, y)$ as the mother Gabor wavelet, a self-similar filter dictionary can subsequently be acquired using suitable rotation and dilation of $g(x, y)$ across generating functions [25]:

$$\begin{gathered} g_{mn}(x,y) = a^{-m} g(x',y'), \quad a > 1, \quad m,n = integer \\ x' = a^{-m}(xcos\theta + ysin\theta), \quad y' = a^{-m}(-xsin\theta + ycos\theta) \end{gathered} \tag{4.3}$$

where $\theta = \frac{n\pi}{K}$ and K represents the total number of orientations. The scale a^{-m} in Equation 4.3 aims to guarantee that energy is independent of m. If U_l and U_h indicate the frequencies of the lower and upper centres of interest, let K denote the number of orientations and S represents the number of scales in the multiresolution decomposition. For the projection of filters, a design strategy is used to ensure that the half-peak magnitude of filter responses in the frequency spectrum touch one another.

The non-orthogonality of the Gabor wavelets implies that there is redundant information in the filtered images, and the following strategy is used to reduce this redundancy [25].

$$\begin{gathered} a = (\frac{U_h}{Ul})^{\frac{1}{S-1}}, \ delta_{a_u} = \frac{(a-1)U_h}{(a+1)\sqrt{2\ln 2'}} \\ \delta_v = tan(\frac{\pi}{2k})(U_k - 2ln(\frac{2\delta_u^2}{U_h}))(2\ln 2 - \frac{(2\ln 2)^2\delta_u^2}{U_h^2})^{-\frac{1}{2}} \end{gathered} \tag{4.4}$$

where $W = U_h$ and $m = 0, 1, .., S-1$. For palmprint feature extraction, Gabor filters of different scale and orientation are used to ensure that maximum information with minimum redundancy will be captured. The proposed method employs 4 scales ($m = 0, 1, 2, 3$) and 6 orientations ($n = 0, 1, 2, 3, 4, 5$) of the Gabor wavelet, resulting in a total of 24 Gabor images for each input image. Convolving the palmprint image with the 24 Gabor filters that use 6 different orientations and 4 different scales comprises the Gabor feature set.

4.2.2.2 Local binary pattern histogram Fourier features

G. Zhao et al. [133] proposed a rotation-invariant image descriptor based on uniform patterns and coefficients of the discrete Fourier transform. An LBP histogram was calculated for the whole input image and rotationally invariant features were constructed using a histogram with a Discrete Fourier Transform (DFT). Rotation invariance is globally determined and its features do not vary with rotation of the resulting image. Because of rotation, a shift occurs in the polar representation (P, R), thus providing an array of features which does not vary with the rotation of the input image. The features calculated with the input histogram rows remain invariant to cyclic shifts. DFT is applied to LBP as follows [133]:

$$H(n, u) = \sum_{r=0}^{p-1} h_I(U_p(n, r))e^{-i2ur/p} \tag{4.5}$$

where n the number of 1 bits in the pattern (number of rows) and r the rotation of the pattern (number of columns).

Furthermore, $h_I(U_p(n, r))$ is the pattern for the uniform LBP histogram. DFT maintains a cyclic shift in DFT coefficients. If $h'(U_p(n, r)) = h(U_p(n, r - a))$, then $H'(n, u) = H(n, u)e^{-i2\pi u\alpha/p}$. Therefore, with any $n_1 \geq 1$, $n_2 \leq p - 1$,

$$\begin{aligned} H'(n_1, u)\overline{H(n_2, u} &= H(n_1, u)e^{-\frac{i2\pi u\alpha}{p}}\overline{H(n_2, u)}e^{-\frac{i2\pi u\alpha}{p}}, \\ &= H(n_1, u)\overline{H(n_2, u)} \end{aligned} \tag{4.6}$$

The rotation of the image by the angle between two sampling points is represented by α; i.e. $\alpha = a(360°/p)$, $a = 0, 1, \ldots, p-1$, where $\overline{H(n_2, u)}$ defines the complex conjugate of $H(n_1, u)$. The Fourier magnitude spectrum, which we call the LBP-HF features, is given by [133]:

$$|H(n, u)| = \sqrt{H(n_1, u)\overline{H(n_2, u)}} \tag{4.7}$$

The sign LBP-HF can be calculated through the original LBP and with magnitude LBP-HF. It is computed as follows [133]:

$$\mathrm{LBP_M(X, Y)} = \sum_{\mathrm{r=0}}^{\mathrm{p-1}} \mathrm{S(|f(x, y) - f(x_p, y_p)| - c)2^p} \tag{4.8}$$

where c is a threshold to be determined adaptively. It can be set to the mean value of the whole image, i.e. $|f(x, y) - f(x_p, y_p)|$.

Table 4.1: Comparison of recognition rates of the proposed method with the state-of-the-art methods for different: blue, green, red and NIR spectra bands. The computation of the recognition rate is obtained for a palmprint with 6 samples of training and 6 samples of testing in Protocol I.

Methods	Recognition Rate (%)			
	Blue	Green	Red	NIR
NFS [113]	97.30	96.37	97.97	98.17
DWT [111]	93.83	93.50	95.20	94.60
TPTSR [67]	78.13	98.02	98.58	98.34
Proposed LBP-HF+Gabor	**98.02**	**98.37**	**98.74**	**98.67**

4.2.3 Experiments and Results

4.2.3.1 Protocol I

The aim of this experiment was to evaluate the recognition performance of the proposed technique, with a standard evaluation used protocol similar to those in previous studies [67, 111, 113] is used. The PolyU [121] multispectral palmprint database was used. A total of 500 subjects of each of the blue, green, red and NIR spectra were used in the first protocol. In the training phase, the images obtained in the first session were selected while the remaining images were used in the testing phase (6 training samples and 6 testing samples).

Experiments were conducted to compare the proposed approach with a number of state-of-the-art, including the techniques described elsewhere [113, 111, 67] (see section 3.8.1) where NFS is the nearest feature space classifier which used the distance between the test sample and the space spanned by the training samples from a class. The discrete wavelet transform (DWT) method was designed to extract local features from palmprints. Jing at al. [67] introduced the two-phase test sample representation (TPTSR) method. In the first phase, TPTSR represents the test sample as a linear combination of all the training samples and determines the M nearest neighbours of the test sample. In the second phase, the test sample is linearly represented with new coefficients, weighting the M nearest neighbours in a linear combination to classify the test sample.

As shown in Table 4.1, the LBP-HF+Gabor approach yields the highest classification rate of 98.02% for the blue spectrum. Moreover, it can be seen that, in the case of the green spectrum, the LBP-HF+Gabor method achieves the best result, with a rate of 98.37%. Consequently, there is an improvement of 0.35% compared to TPTSR, a 2.0% improvement compared to NFS and an improvement of 4.87% compared to DWT. In the case of the red spectrum, the results clearly show that the LBP-HF+Gabor approach achieves the best result, with a performance accuracy of 98.74%, representing a gain of 0.16-3.54% in relation to the other reported methods. With regard to the NIR spectrum, the LBP-HF+Gabor approach also obtains the best result, with a performance accuracy of 98.67%, which is also higher than those of the existing TPTSR, DWT and NFS methods. The ROC curve is drawn in Figure 4.1 to provide another biometric performance measure depicting the comparison between multispectral (blue, red, green and NIR) palmprint data sets.

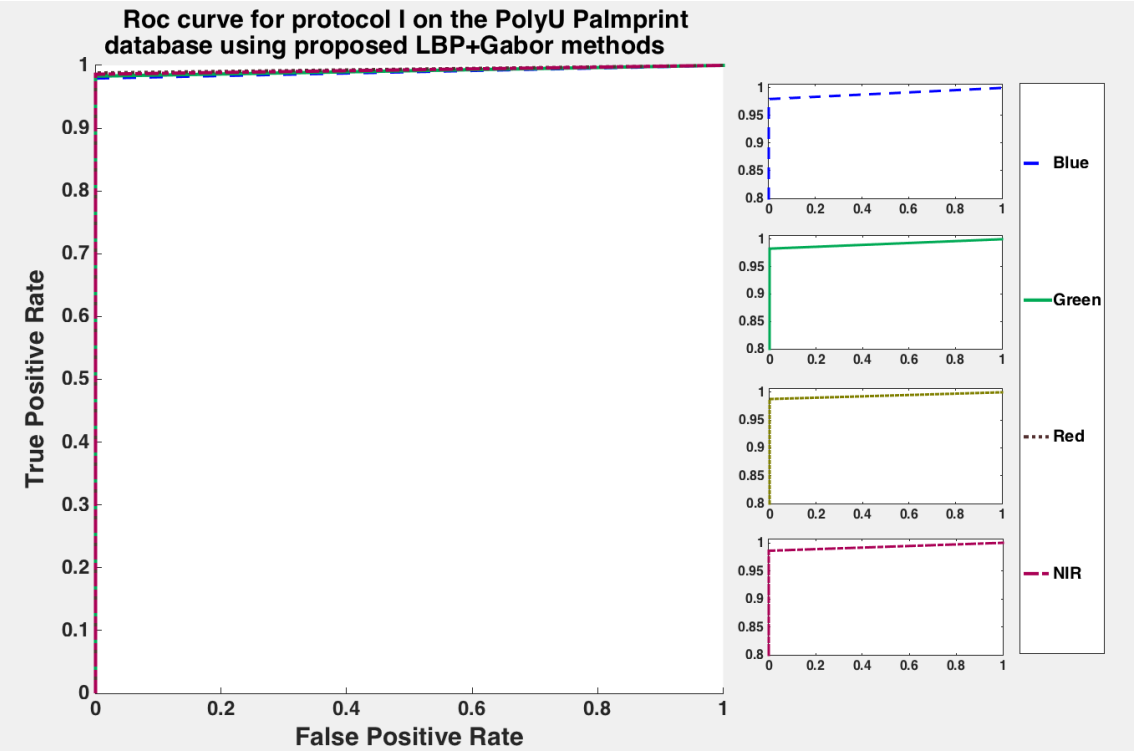

Figure 4.1: ROC curves for the proposed method under the blue, green, red and NIR spectral using six images captured in the first session for the training set and six images captured in the second session for the testing set.

4.2.3.2 Protocol II

The proposed approach was implemented and tested on a similar palmprint database, comparing the proposed LBP-HF+Gabor method to two existing methods, namely NFS [113] and RBF [132]. The proposed approach was evaluated using the multi-spectral palmprint database and followed the same evaluation given in previous studies [113, 132]. The training set consisted of the first three images of each of the red, green, blue and NIR spectra from the first session and the testing dataset consisted of the 6 palmprints of each of the blue, green, red and NIR spectra obtained from the second session.

Table 4.2: Comparison of recognition rates of the proposed method with the state-of-the-art methods for different spectra bands: blue, green, red and NIR. The computation of the recognition rate is obtained for a palmprint with 3 samples for training and 6 samples for testing in Protocol II.

Methods	Recognition Rate (%)			
	Blue	Green	Red	NIR
NFS [113]	95.10	92.87	95.40	95.63
RBF [132]	96.70	96.50	98.20	98.40
Proposed LBP-HF+Gabor	**97.70**	**97.44**	**98.24**	**98.57**

A comparative analysis of the proposed method was performed against two state-of-the-art methods, including the method proposed by Yong et al. [113], and on the radial basis

function (RBF) [132]. The former method has been introduced in protocol I. As previously mentioned in subsection 3.8.2. the RBF kernel function is used to optimize the feature space such that the samples from the same class are well clustered while the samples from different classes are pushed far away.

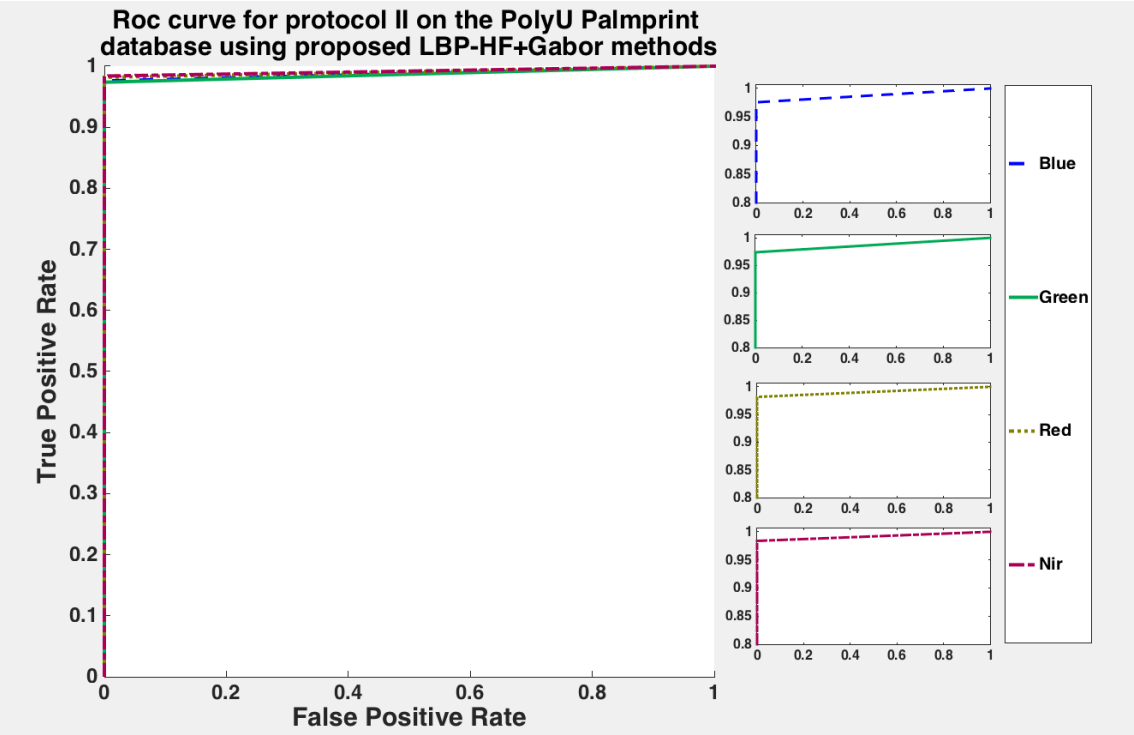

Figure 4.2: ROC curves for the proposed method under the blue, green, red and NIR spectral using three images captured in the first session for the training set and six images captured in the second session for the testing set.

The results shown in Table 4.2 clearly demonstrate the superiority the LBP-HF+Gabor approach in terms of robustness, in addition to its greater effectiveness compared to the other reported methods. The LBP-HF+Gabor approach offers attractive recognition performance rates of 97.44% to 98.57%, which are highlighted in bold in Table 4.2. It should be noted that the recognition rate using the LBP-HF+Gabor approach in relation to the blue spectrum yields an improvement of 1-2.6% compared to the RBF and NFS methods. In the case of the green spectrum, the LBP-HF+Gabor method achieves an accuracy of 97.44%, which is also higher than all other reported methods. Moreover, the LBP-HF+Gabor method also achieves better results of 98.24% and 98.57% respectively for the red and NIR spectra than the RBF and NFS methods. The ROC shown in Figure 4.2 plots the false acceptance rate versus the genuine acceptance rate for the multispectral palmprint data sets, represented by the red, green, blue and NIR spectra.

4.2.4 Discussion

The proposed method successfully captures discriminating information to provide better recognition performance using the KNN classifier. By looking at the results, it can be seen that the proposed methodology achieves outstanding recognition rates compared to other

existing approaches. The experiments conducted were able to achieve recognition rates of 97.44%-98.74% for the blue, green, red and NIR spectra as shown in tables 4.1 and 4.2.

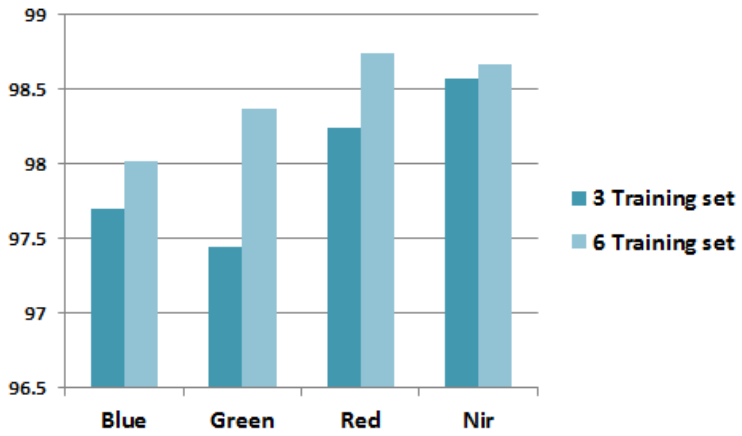

Figure 4.3: Comparison of recognition rates of the proposed method with Protocols I and II for different spectra (blue, green, red and NIR)

It can also be observed from the tables that the recognition rate for the red illumination provides the highest performance compared to the NIR, green and blue spectra for the six training and six test images in Protocol I. The results obtained from the NIR spectrum have shown an improvement compared to the spectra with three training and six testing images in Protocol II. From the experimental results, there seems to be an improvement in the Protocol with six training images and six test images as shown in Figure 4.3. The red and NIR spectral are able to achieve better performance levels than blue and green in both protocols. As mentioned previously in section 3.7, the NIR and red spectral capture the palm lines and vein structures, as shown in Figure 2.11 in chapter 2; this helps in the comparison and classification of palms with similar palm lines [121].

4.3 Multi-feature analysis based on the shift binary pattern descriptor for palmprint recognition system

4.3.1 Introduction

The rich features of the palmprint are the key to personal recognition system. As mentioned earlier, the patterns elicited from palms have excellent discriminatory power as they have more features on the surface, and this plays an important role in the classification stage in terms of displaying discriminative power. Therefore, accurate feature extraction is required to improve the accuracy of the recognition process.

This section presents a multi-scale palmprint recognition approach based on LBP which has resulted in improved performance when compared against a single-scale counterpart. However, it is to be noted that this results in the use of multiple features resulting in high dimensional feature vectors, thus making the method more computationally expensive. The study brings to light interesting facts about the merging of features on an single-scale, resulting in optimal recognition rates. Furthermore, it describes the reduction in the variability of recognition rates among individual scales. This chapter aims to propose a novel multi-shift local binary pattern (MSLBP) approach that extends the single-scale of

the SLBP to a multi-scale dimension to obtain discriminating representations of palmprint information.

4.3.2 Multi-spectral palmprint recognition process: the proposed approach

Palmprint recognition should be determined by using the optimal spectrum type, either red, green, blue or NIR, that results in the highest recognition rate. A typical scheme for such a system comprises the following steps: palmprint image acquisition, feature extraction, dimensionality reduction and classification. The MSLBP descriptor is applied to extract palmprint features in the first phase of recognition. The SR-KDA technique is then used to reduce the dimensionality of the extracted palm feature vector (see section 2.4.2). The correct identification is achieved when the test palmprint label matches the palmprint label of the same subject in the training dataset. The process may result in misclassification when the test palmprint is classified with a palmprint label of a different subject in the training dataset. Then, the new set of proposed palm features is used in the classification process. The success of the classification phase depends on the accuracy of the extracted features.

4.3.2.1 Shift local binary pattern histogram

The technique is considered to be a simple yet effective tool which labels the pixels of an image with a binary number. First, the value of the current pixel, g_c, is applied as a threshold for each of its neighbours g_p $\{0, 1, \ldots, Q-1\}$ taking the result as a binary number. However, in SLBP [62], a local binary code is generated for every pixel position. The SLBP for a position (x, y) and a shift value k, can be represented as shown in Equation 4.9. Here, k is varied within the limits set by l, and for every change in k a new binary code is generated and added to the histogram of patterns.

$$\mathrm{SLBP}_{\mathrm{Q,r}}(x, y, k) = \sum_{p=0}^{Q-1} S\left(g_p - g_c - k\right)^{2^p} \tag{4.9}$$

where Q represents the evenly distributed sample points on a circle with radius r, and S and k can be represented as follows:

$$S(x) = \begin{cases} 1 & \text{if } x \geq 0 \\ 0 & \text{otherwise} \end{cases} \quad \text{and } k\epsilon\left[-l, l\right] \cap Z \tag{4.10}$$

Note that $k = 2.l + 1$ and that, for every different value k assumes within the limits $-l$ and l, a new binary pattern is generated. For example, if $l = 3$, k, which is bounded by the limits, takes the values $\{-3, -2, -1, 0, 1, 2, 3\}$ and then for every pixel position k will contribute seven binary codes to the histogram pattern. Finally, the eventual histogram will be divided by k, which will make the histogram sum equal to the number of pixel positions considered (as is the case for other LBP algorithms). The MSLBP algorithm is summarized in Algorithm 1.

4.3.2.2 Proposed multi-Shift local binary pattern histogram

Shift LBP in its multi-scale version has been used for prediction and has shown improvements in classification performance over the former version of Shift LBP. The principle

Algorithm 1: Shift local binary pattern (LBP) histogram

1. Input: palm image
2. Compute the SLBP feature vector of Equations 4.9 and 4.10
3. Output: palm testing set vectors and palm training set vectors (features vectors)

utilised in a multi-scale is change the radius of the Shift LBP, and then the outcomes will be put together for the capture information. However, an issue pertaining to the high level of dimensionality arises with multi-resolution analysis. This problem can be reduced through the technique of feature selection to reduce the amount of unnecessary information. Figure 4.4 shows the general scheme of the proposed approach.

The variation in the radii, which depends on the neighbouring pixel's distance from the centre, allows the creation of a multi-scale representation by means of concatenating Shift LBP histograms with the determined size of the radius [12]. This histogram contains information about the distribution of the multi-scale features over the whole palmprint image. It has been concluded that the multi-scale version is more precise than the single-scale representation of Shift LBP, with significant noise invariance. Palmprint description for multi-resolution is achieved by the application of Shift LBP operators at r scales to an image. Then, the result of MSLBP histogram for each scale of image size $M \times N$ is calculated by:

$$H_{Q,r}(p) = \sum_{i=0}^{M-1} \sum_{j=0}^{N-1} g\left(\mathrm{SLBP}_{Q,r}(i,j), p\right),\ p \in [1, n+1] \tag{4.11}$$

where k is the maximum bin value of the shift LBP and r is the maximum radius applied to the multi-scale case. The set of histograms computed at different radii provides regional information about the observation vector (for example, 2^8 yields 1024 bins for 4 scales ($R = 1, 3, 5, 7$)). The resulting multi-scale palmprint descriptor is represented by:

$$F_{Q,r} = [H_{Q,1}, H_{Q,2}, \ldots, H_{Q,R}] \tag{4.12}$$

Algorithm 2: Proposed multi-shift local binary pattern (LBP) histogram

Requires: Palm dataset N, Scale-No=4 and radius r=1,3,5,7

1. Input: palm image
2. Read r
3. Compute the MSLBP feature vector of Equations 4.16, 4.17 and 4.18
4. Put MSLBP histogram in concatenated vector.
5. If r less or equal ScaleNo go to step 2.
6. Output: palm testing set vectors and palm training set vectors

In this method, the overfitting of the palm feature vectors due to high dimensionality is addressed by using SR-KDA (see section 2.4.2), which presents an efficient solution to the problem of concatenating all radii of the palmprint features.

4.3.2.3 Palmprint recognition stage

A combination of features brings with it the problem of overfitting due to the high dimensionality of data. Dimensionality reduction is usually performed using methods such as

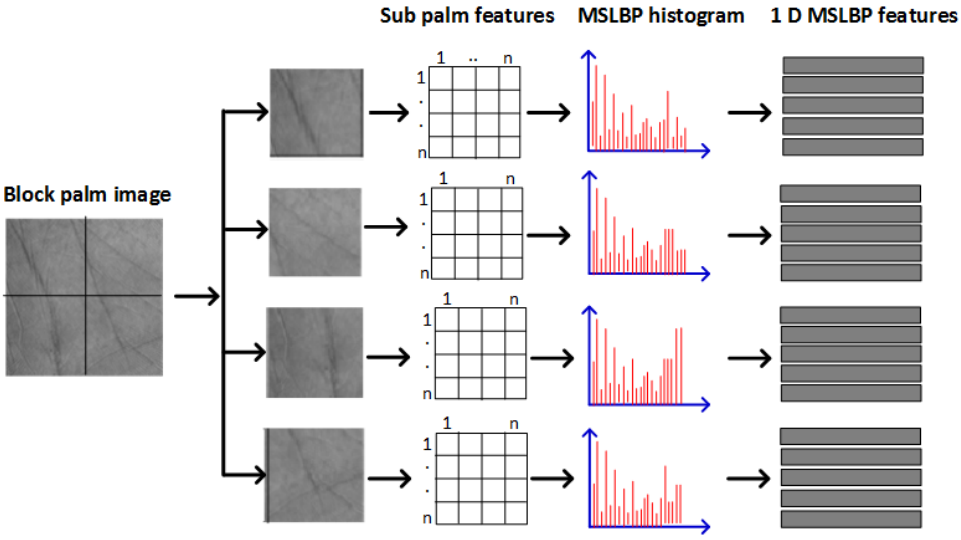

Figure 4.4: The general scheme of the proposed approach

PCA and LDA methods. To avoid this problem and to perform dimensionality reduction in large data problems, kernel discriminant analysis with spectral regression (SR-KDA) is used. SR-KDA was proposed by Cai et al. [10] and is capable of performing spectral graph analysis along with regression in KDA for decomposing a large data matrix. Cai et al. showed that SR-KDA outperforms previous eigen decomposition methods in terms of speed as well as accuracy. In section 2.4.2, SR-KDA was discussed in detail. Most approaches to palmprint recognition rely eventually on a distance comparison, where the distance of palmprints from a set of training images is calculated. Matching is obtained against the closest training palmprints.

In section 2.5.2, it was shown that the recognition stage of the KNN classification algorithm predicts an unlabelled palmprint test vector according to the K training palmprint vectors, which are the nearest neighbours to the test vector. The similarity depends on a precise distance metric, for which similarity is measured according to the Euclidean distance between the palmprint vectors and the palmprint is found which has the highest probability in terms of similarity in relation to the training sets.

4.3.3 Experiments and Results

4.3.3.1 Protocol I

The proposed method was implemented and evaluated employing the PolyU database as described previously [121]. A standard evaluation protocol was employed similar to that used elsewhere [67, 111, 113, 8] where 6 palmprint images of each of the blue, green, red and NIR spectra were selected as the training set and 6 palmprint samples of each of the same spectra were selected as the test set (6 training sets and 6 test sets).

The proposed approach was compared against the NFS [113], DWT [111], CFKNNC [113], TPTSR [67] and Log-Gabor [8] methods which have been described in section 4.2.3.1. Log-Gabor is employed to extract an indexed feature map based on the competitive rule and encoded in Gray binary code. The results of the experiments shown in Table 4.3 present the recognition rates of the feature data set.

Table 4.3: Comparison of recognition rates using proposed approach with state-of-the-art methods using 6 training and 6 testing samples

Method	Recognition Rate (%)			
	Blue	Green	Red	NIR
NFS [113]	97.30	96.37	97.97	98.17
DWT [111]	93.83	93.50	95.20	94.60
CFKNNC [113]	98.83	98.77	98.00	96.40
TPTSR [67]	78.13	98.02	98.58	98.34
Log-Gabor [8]	99.23	99.10	99.30	99.33
Proposed MSLBP	**99.90**	**99.90**	**99.80**	**99.93**

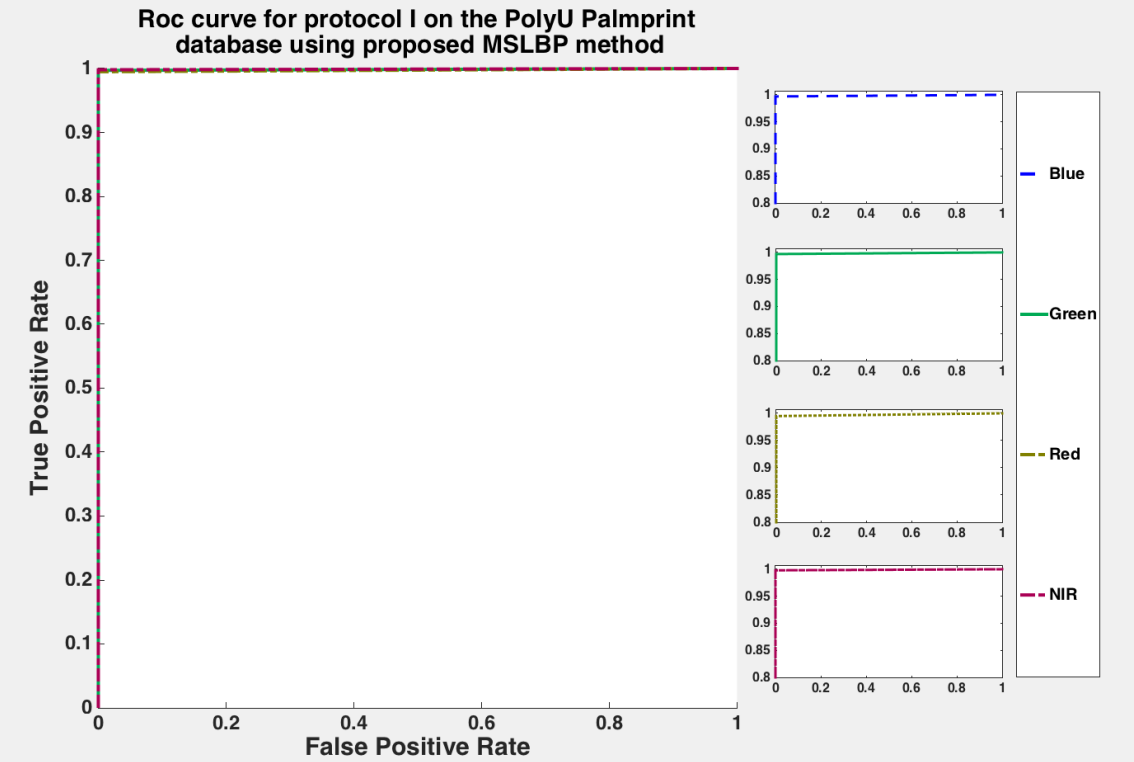

Figure 4.5: ROC curves for the MSLBP descriptor for different spectra (blue, green, red and NIR), computed using six images captured in the first session for the training set and six images captured in the second session for the testing set.

As can be seen in Table 4.3, the proposed approach shows significant improvement compared to the other methods. For the NIR spectrum, the MSLBP approach produces the highest rate of 99.93% (an improvement of approximately 0.60-5.33%). Moreover, it can be seen that, in the case of the blue and green spectra, the recognition performance for the MSLBP is 99.90%, which is also better than the existing TPTSR, NFS, DWT, CFKNNC and Log-Gabor methods. In the case of the red spectrum, the results indicate that the MSLBP again achieves the best result, with a performance accuracy of 99.80%, representing a gain of 0.70-21.63% in relation to all of the other reported methods. It is worth mentioning that the best performance is obtained with the NIR spectrum in comparison to other spectral

palmprints. The ROC curves are also drawn to visualize the performance of proposed MSLBP in protocol I as shown in Figure 4.5.

4.3.3.2 Protocol II

The proposed methodology was tested on 500 subjects of the multi-spectrum palm database. The same protocol set up was adopted as in previous studies [132, 113]. For the purpose of evaluating the performance of the MSLBP descriptor, a training set was built of 1500 images of each of the blue, green, red and NIR spectra, which selected the first three images of the first session. Meanwhile, all the samples of palmprints of each individual from the second session were used for the testing set, which includes 3000 images of each of the blue, green, red and NIR spectra. As mentioned above in section 4.2.3.2, the performance of the proposed method has been compared with the RBF [132] and NFS [113] method.

Table 4.4: Comparison of recognition rates using the proposed approach with the state-of-the-art methods using 3 training and 6 testing samples

Method	Recognition Rate (%)			
	Blue	Green	Red	NIR
NFS [113]	95.10	92.87	95.40	95.63
RBF [132]	96.70	96.50	98.20	98.40
Proposed MSLBP	**99.70**	**99.63**	**99.77**	**99.77**

The results shown in Table 4.4 indicate the advantage of the MSLBP approach in terms of robustness in addition to its superior effectiveness compared to other reported algorithms. The MSLBP approach offers an attractive recognition performance rate of 99.77% in relation to the red and NIR spectral, as highlighted in bold in Table 4.4. In the case of the blue spectrum, the MSLBP method achieves an accuracy of 99.70%, which is also higher in comparison to all the other reported algorithms. In the case of the green spectrum, the results show that there are improvements of approximately 6.76% and 3.13% over the NFS and RBF methods respectively. Figure 4.6 represents the ROC curves for the blue, green red and NIR spectra in protocol II.

4.3.4 Discussion

The results show the effectiveness of the suggested approach for multi-spectral palmprint recognition. The MSLBP successfully captures discriminative information from the palmprint image. This denotes a significant improvement in recognition rates compared to other existing techniques for all spectral bands. By analyzing the results obtained, it can be observed that the results of the proposed methodology for the NIR spectrum outperform those of other spectra, achieving 99.93% and 99.77% respectively for Protocols I and II . In addition, the red spectrum band also shows better results than the blue and green spectra with 3 training and 6 testing samples. As mentioned previously in section 3.9, the NIR and red spectra capture the palm lines and show the vein structures; this helps in the comparison and classification of palms with similar palm lines [121, 112], as shown in Figure 2.11 in section 2.6.

As different training and testing samples were used in our experiments, a comparison is provided based on the number of testing and training datasets used in existing methods.

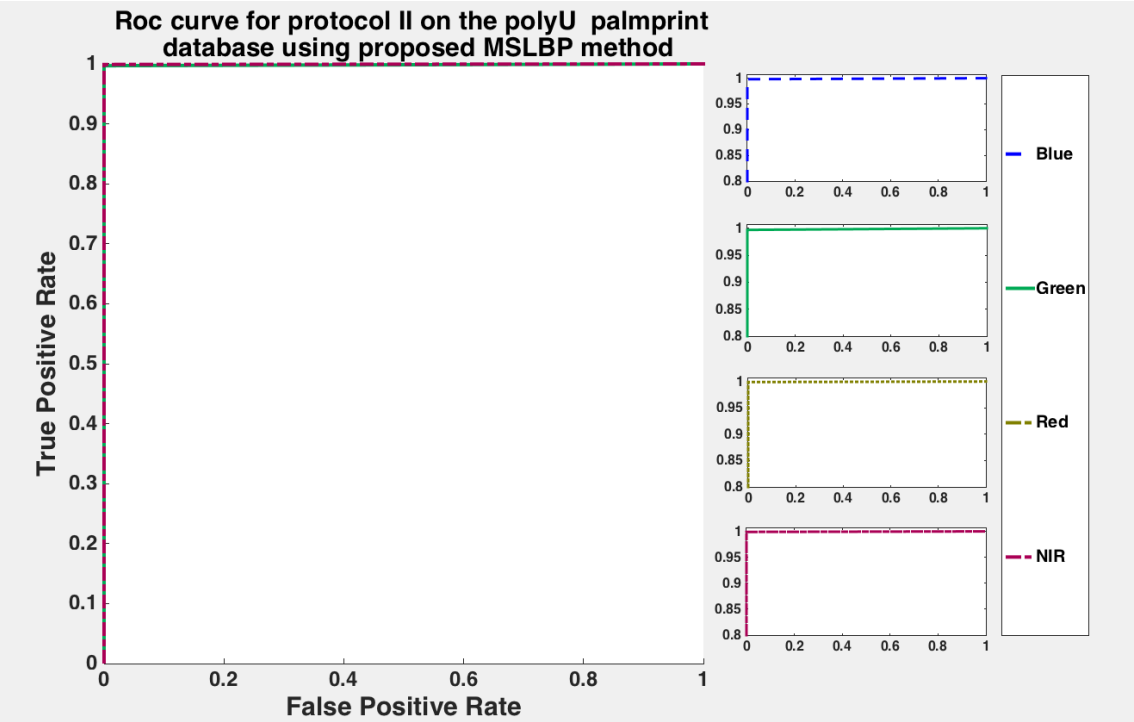

Figure 4.6: ROC curves for the MSLBP descriptor for different spectra (blue, green, red and NIR), computed using the first three images from the two sessions selected as the training set and the latter three images from the two sessions used as the test set.

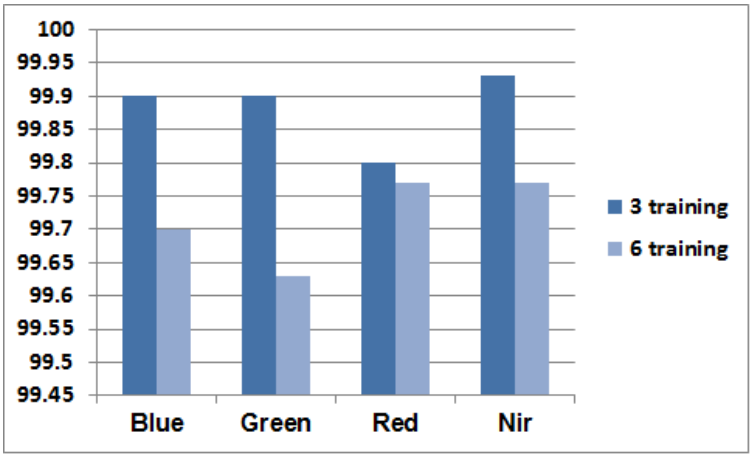

Figure 4.7: A comparison of the MSLBP descriptor with Protocol I and Protocol II for different spectra (blue, green, red and NIR)

From the results, it should be noted that the results of the proposed methodology for Protocol I (6 training and 6 testing sets) outperform those obtained in Protocol II, as shown in Figure 4.7. This confirms that increasing the number of training samples leads to significant improvement in the recognition performance of the multi-spectral palmprint recognition system significantly.

4.4 Computational complexity

The fusion technique can be conducted by means of several different approaches. As mentioned above, the approaches proposed here combine the palm information extracted from the proposed technique to generate a new fused feature vector. However, this tends to give high dimensional feature vectors, which increases the computational cost of the classification process. These proposed approaches will be complex and it is necessary to reduce the computational intensively and difficulty in the classification stage. To solve this problem, the dimensionality issue resulting from the concatenation of palm features in one vector is tackled by projecting our features to the Kernel subspace (see section 4.2.2.3). This is able to improve discriminatory power in the new fused feature vector due to the rich information gained from feature fusion. From the evaluation of the results, it is concluded that the proposed methods yield better result with reduced computational cost. This study, a long with previous research into the merging of features in palmprint images, shows that it higher recognition rates.

4.5 Summary

Information fusion can be carried out at several levels, such as at the level of features, matching score and decision. The richest information is given by feature-level fusion because here integration is performed at an early stage of information fusion. The aim of this chapter is to improve accuracy performance using the fusion of information at feature level for the palm recognition process. Feature-level fusion produces new feature vectors which capture more important information during the fusion process.

In the first part of this chapter, a fusion approach is proposed that combines two feature extraction algorithms, LBP-HF and Gabor filter techniques, for use in feature extraction. The fused features are applied to increase performance in palmprint recognition. However, with the proposed approach there is also the need to resolve the problem of the increased number of features, which can result in an overfitting problem for classification. To overcome this difficulty, SR-KDA is used to reduce dimensionality. When designing the proposed recognition system, the KNN classifier is used for the final decision process. The performance of the proposed methodology was evaluated by employing the publicly available multispectral palmprint PolyU database. Experiments were performed using two different protocols, confirming that the proposed methodology achieves higher recognition rates compared to other existing techniques. Moreover, it has been observed that use of the red spectra band outperforms other spectra bands in terms of the LBP-HF+Gabor features for six training samples, whereas the NIR spectrum performs better with three training samples.

A combination of Gabor filters and LBP-HF is a powerful solution, which considers both the local and global texture information to enhance the quality of the extracted palmprint image. Gabor filters have excellent properties to ensure make some improvements so that the highest frequency bands are covered by narrowly localized oriented filters while the set of filters would cover uniformly the Fourier domain including the highest and lowest frequencies. Furthermore, it is able to capture the discriminative information of the orientations in addition to the scales. LBP-HF introduced here generated a set of features where the histogram bins have a more influential discriminatory ability. The LBP-HF features

are computed from the histograms representing the whole region (i.e. the invariants are constructed globally instead of computing invariant independently at each pixel location). The major advantage of this approach is that the relative distribution of local orientations is not lost.

The objective of the second part of this chapter was to develop algorithm based on moving from the single-scale to a multi-scale approach, since the recognition rate of a single scale system is quite lower as compared to its multi-scale counterpart. A new approach is proposed based on the MSLBP descriptor, to extract palm information in several sub-block windows. The extracted feature vector has high dimensionality, and SR-KDA is used to reduce the size of the dimensions associated with the MSLBP features. All of the experiment results demonstrate that the proposed methodology yields high recognition rates compared to other existing approaches. Moreover, using six training samples yields better results compared to three training samples. Overall, the use of the red spectra band outperforms other spectral bands regarding MSLBP features for both six and three training samples.

The proposed new MSLBP is concatenated into a single vector to effectively extract local feature from the palmprint image.The proposed approach offers significant improvement in the recognition performance.

The next chapter provides a survey of the recent literature concerning research trends relevant to the finger knuckle print (FKP) recognition system.

Part II: Finger knuckle print recognition system

Chapter 5

Finger Knuckle Print Recognition

5.1 Introduction

In recent years, finger knuckle print (FKP) identification has become an increasingly important research topic in biometric applications. The FKP refers to the inherent skin patterns that are formed at the joints on the surface of the backs of the fingers. It has been found that the FKP is highly rich in texture and can be used in the unique recognition of a person. The rich features of the FKP are a key challenge for personal recognition systems, in addition to variations in illumination and orientation and noisy sensors, making the task of identification critical.

It is worth noting that there is a continuously increasing need and demand for security in everyday life, and different approaches are required to address various possible applications. Researchers in the area of FKP recognition are undertaking studies aimed at meeting these needs by developing systems that enable robust recognition while also affording fast computation. The recognition process involves several stages, including the pre-processing of features and their extraction and matching. Thus far, researchers have designed very powerful approaches to extract and match features in FKP recognition. As a key step in this study, this chapter presents a literature review of various techniques essential in obtaining higher recognition rates for FKP.

The remainder of this chapter is organized as follows. Section 5.2 is dedicated to explaining the choice of the FKP as a security biometric. A brief description of the FKP image is presented in section 5.3. Section 5.4 provides an overview of the application and methods of FKP biometric imaging, with conclusions in section 5.5.

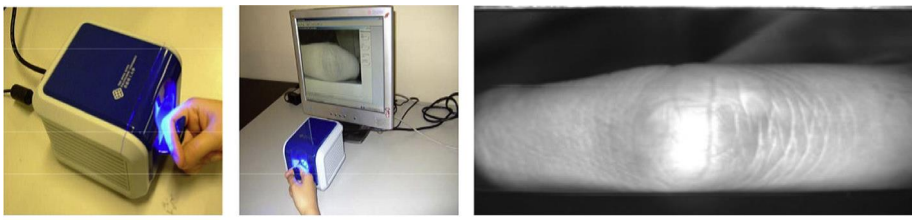

(a) (b)

Figure 5.1: The FKP system: (a) the outlook provided by the FKP image acquisition device; (b) a sample FKP image acquired by the system developed.

5.2 Why finger knuckle print biometrics?

The FKP is one of the most recent physiological biometric modalities to be employed, as it has only recently been observed that the textures on the back surface of the fingers have the potential for use in discriminating among different individuals. Figure 5.1 provides an example of an original FKP image. The FKP's inherent patterns, constituting bending lines on the outer surface of the skin, are very rich and unique among individuals, which provides a novel but promising way to identify a person. Furthermore, FKP biometric systems have the potential for success due their availability, contactless image acquisition, ease of access, stable features and social acceptability. Moreover, they do not vary based on emotions or other factors such as tiredness. However, FKP image patterns are often affected by problems such as noisy sensor data and variations in illumination, so the recognition of a person with high confidence is a critical issue. Thus, one of the principal challenges in enhancing FKP recognition performance is to devise a reliable coding scheme for FKP patterns. Recent studies have shown that researchers in the area of biometric recognition are trying to solve this problem by establishing a system that can be used to recognize a person precisely.

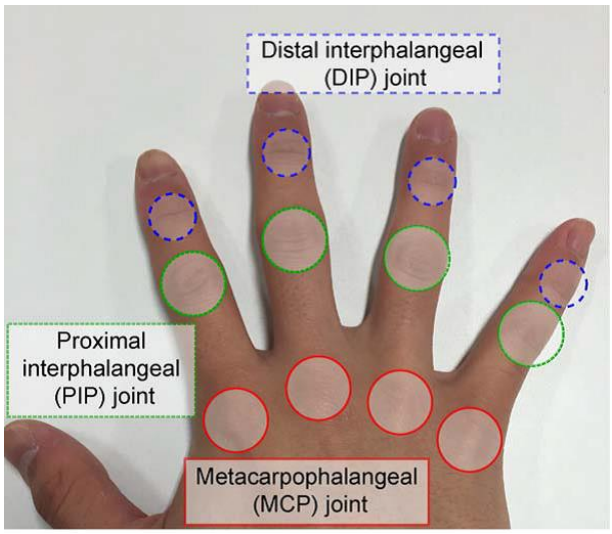

Figure 5.2: Illustration of the back surface of the fingers

5.3 What is finger knuckle print?

FKPs constitute skin patterns that are present on the back surface of the fingers around the phalangeal joints. Each finger of the hand has three phalangeal joints: the one that links the finger to the main part of the hand is the metacarpophalangeal joint; the middle joint of the finger is the proximal inter phalangeal (PIP) joint; and that closest to the tip of the finger is known as the distal joint (see Figure 5.2). At the point of these joints on the dorsum surface, the outer surface of the skin shrinks through flexion, which creates dermal patterns. These consist of lines, wrinkles and contours. The FKP comprises the pattern generated by the PIP joint on the back of the finger, and is used in imaging [127]. The area of FKP capture is very small (see Figure 5.3) when compared to the area captured for palmprint recognition. Furthermore, the FKP also possesses highly unique features which are well suited to a potential biometric system [47].

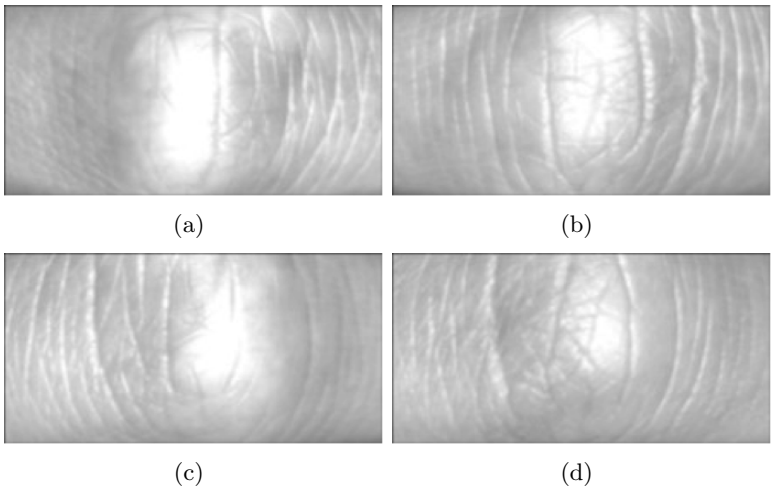

Figure 5.3: Sample ROI images of different fingers from PloyU database [129]: (a) LIF, (b) LMF, (c) RIF, and (d) RMF.

5.4 Approaches to FKP recognition

The FKP is an interesting and challenging problem due to noisy sensor data and variations in illumination. A critical issue in FKP recognition is feature extraction. For this reason, FKP recognition has become an extensively studied area of research where researchers are attempting to establish a system that can be used to accurately recognize a person.

An important issue in FKP biometric recognition relates to feature extraction which has resulted in an increased amount of research in this area. Most research in the literature examines FKP recognition systems for access control uses, and hence the patterns of the readily accessible PIP joint are selected for the study. These feature extraction methods can be classified into subspace analysis, coding approaches, fusion approaches, and other approaches.

5.4.1 Subspace analysis feature extraction method

The development of new subspace algorithms and feature descriptors are major and broad aspects that have attracted the interest of researchers. The subspace approaches reported in the literature have been developed to make finding the discriminatory subspace and constructing classifications an easier task. In terms of subspace approaches for FKP recognition, representative work includes principal component analysis (PCA), linear discriminant analysis (LDA) and independent component analysis (ICA). Subspace methods are employed to extract relevant features from an FKP image and undertake final recognition. Also, they can be used for dimensionality reduction.

Kumar et al [58] used PCA, LDA and ICA subspace techniques for feature extraction from images of the back of the fingers. PCA assesses the basis vectors for spanning an optimal subspace, such that the mean square error among the projections of the training FKP images onto this subspace and the original FKP images is reduced. ICA is employed to find a linear representation of non-Gaussian FKP data, and LDA finds vectors in the underlying space that best discriminate between classes. A PCA subspace method has been proposed which extracts and classifies relevant features from a knuckle image using

the nearest neighbour classifier [79]. The proposed approach for FKP feature extraction and classification has proven quite efficient in obtaining high accuracy in knuckle classification.

Another proposed method referred to as orthogonal linear discriminant analysis (OLDA) has been employed in FKP recognition and is based on applying the PCA subspace to the Gabor feature representation to identify the projection matrix [114]. The nearest neighbour classifier was employed here to classify FKP features.

In another study [45], a complex locality preserving projection (CLPP) approach was developed for FKP recognition. The authors considered distances and angle information between feature vectors to calculate data similarity and used parallel fusion to obtain more information on the data set. The researchers presented two methods: (i) CLPP to extract the low-dimensional features while preserving the manifold of the input data set; (ii) orthogonal CLPP (OCLPP), producing orthogonal-based functions to overcome redundant information. The authors also compared CLPP and OCLPP to manifold preserving learning algorithms.

Elsewhere, weighted linear embedding (WLE) has been used to consider local and non-local FKP features. The local feature is more important than the non-local feature according to manifold learning theory [117]. The Gaussian weighting scheme is used to combine the local and global FKP information. The WLE is used on the right index finger and a recognition rate of 78.2% has been achieved.

5.4.2 Coding-based approaches

Researchers in this field have also developed an assortment of coding algorithms and have achieved exciting results in several studies. The finger knuckle surface has features of rich lines and wrinkles which are bent and are unique to individual humans.

One study has proposed the monogenic coding method [128]. This code is created by applying a monogenic signal to each of the pixels of a finger knuckle image and representing each image pixel as a 3-bit vector obtained by binarizing the monogenic signal at a certain position, which can reflect the local phase and orientation information at this position. Researchers have also applied competitive coding schemes [127], using 2D Gabor filters to extract local orientation information from an image to represent the FKP patterns.

Zhang et al. [127] proposed a novel method for online personal authentication using the FKP. To calculate the matching score, the researchers proposed a band-limited phase-only correlation (BLPOC) function based on texture analysis, which is an effective and efficient means of FKP recognition. The performance of the proposed system is considerably better in terms of the accuracy and speed of recognition.

A recent study [3] has also proposed an FKP recognition method using BLPOC. The phase information is obtained from the 2D discrete Fourier transform (DFT) of FKP images, which comprises the major feature of FKP image representation. This is followed by employing local block matching using BLPOC to handle the nonlinear deformation of FKP images, which is roughly described by the minute translational displacement between local image blocks. Firstly, a BLPOC-based method is used to calculate the similarity between FKP images by correcting the global and local features of FKP images considering the structure of the fingers. Then, BLPOC-based local block matching is used to calculate the correct minute translational displacement between each local FKP image block pair. Finally, the average of a set of BLPOC functions is computed from each local FKP image block pair and the matching process is conducted by means of analysing the peak value of the average attained from the BLPOC function.

A new family of wavelets has also been named Kekre's wavelet [48], which extracts spectral features from the FKP without pre-processing and then compares Kekre's wavelet to the Haar wavelet. Among the current approaches to FKP recognition, Raut et al. [88] have proposed a biometric authentication system using different algorithms for pre-processing with Kekre's wavelet transform (KWT), aiming to develop the transform domain and extract better distinguishing features. KWT was tested on their own database of 500 images.

Another method is based on the Riesz transform to characterize optical FKP patterns for FKP recognition [126]. This coding scheme depends on encoding the local patches of an FKP image by applying a second-order Riesz transform to devise a new 6-bit coding scheme named the RieszCompCode. This method comprises 6-bit planes, of which three are collected by binarizing the image's responses to the three second-order Riesz transforms and the rest are collected from the competitive coding scheme. The normalized Hamming distance is used to compute the similarity between the reference and input of the FKP. Experiments were conducted by implementing the RieszCompCode in the verification system and the results show that the proposed method is efficient in terms of precision. The equal error rate (EER) attained by RieszCompCode is 1.26%. Moreover, the RieszCompCode is fast and thus can be employed for real-time applications.

5.4.3 Fusion approaches

Researchers have paid considerable attention to different fusion techniques for building FKP recognition systems, such as multi-sensor, multi-modal, multi-sample and multiple algorithms. The aim of using fusion is that it improves the accuracy of personal recognition. Several researchers have proposed novel approaches regarding personal recognition based on the fusion of multi-FKPs.

The Uniform Local Binary Pattern (ULBP) has been used to extract features for multiple fingers [2]. Additionally, to produce the most appropriate and best quality classification, an approach is used that is based on fusion at the score level of the extracted ULBP features.

A novel combination of local-local information has been proposed where the local features of the enhanced FKP are extracted using the LBP histogram and speeded up robust features (SURF) [118]. At the recognition stage, the corresponding features of enrolled and query FKP images are matched using the nearest-neighbourhood ratio method. The authors used a weighted sum rule to fuse the derived LBP and SURF matching scores to obtain fused matching scores. Lin [130] suggested applying a feature extraction scheme deriving fusion orientation and magnitude information through Gabor filtering. Moreover, using the fusion of two modalities or more, it is possible to make the final biometric system more robust.

The authors [31] proposed algorithms to extract FKPs features based on 1D Log-Gabor Filter (LGF) to extract the lines features of FKPs and LBP descriptor, is to extract texture features. The extracted FKP features of two the methods are fused at the matching score level in order to improve the recognition accuracy. In another approach, Nathiya [78] proposed the combination of Proximal Interphalangeal (PIP) Joint and Distal Interphalangeal (DIP) Joint for the finger knuckle recognition. They applied LBP and LGF to extract the FKP image pixel information about intensity and textures. The K nearest neighbor classifier (KNN) used to classify the FKP feature for recognition process.

A reconstruction approach has been proposed for finger knuckle print images which possess scaling, rotational and translation variant properties [30]. In this method, the process of reconstruction of the captured finger knuckle image uses a dictionary learning technique

from the template sets in the gallery sample. The same authors have also introduced a new mechanism which integrates multiple orientation coding and texture feature information obtained from finger knuckle print image for personal recognition [29]. For texture feature extraction, the local binary pattern is applied on each Gabor filtering response to obtain LBP maps. The final stage is classification based on the integrated multiple orientation and the fusion of texture features at score level to improve verification performance.

Another study [131] investigated local and global information for FKP recognition. The researchers used Gabor filters to extract local orientation information. By increasing the scale of the Gabor filters to infinity the Fourier transform of the image can be derived. Thus, the Fourier transform coefficients of the FKP image are naturally taken as the global feature. The LGIC approach exploits both local and global information for FKP verification, where global information is also utilized to refine the alignment of FKP images in matching. The final matching distance of two FKPs is a weighted average of local and global matching distances.

Another type of biometric recognition has been proposed based on two types of fusion biometrics: palmprint and Finger Knuckle Print [73, 91]. Different combinations of algorithms have been widely used at the feature level to attain the highest accuracy in identification and verification. The matching process takes places by identifying the linear a phase shift in frequency using phase correlation algorithm. From the identified phase shift, the inverse Fourier transform is taken to define the cross-correlation between phase components. One of the existing studies in this area uses fusion rules at different levels of features and matching scores [91]. The authors propose an algorithm that combines the features of intensity and Gabor images for each FKP in a long vector. The use of images from different combinations of two, three and four fingers result in improved performance compared to each finger separately.

The problem with fusion is the high dimensionality of the feature vectors, which results in computationally expensive algorithms. To address this problem and reduce the feature dimensions, numerous algorithms have been suggested, including kernel PCA (KPCA), which is a dimensionality reduction algorithm inspired by PCA [97, 91]. Gabor filters, PCA and the group collaborative representation based classifier (GCRC) have also been applied for feature identification and extraction, dimensionality reduction and at the classification stage [66]. The GCRC is a novel method that applies group-level constraints in the CRC.

5.4.4 Other approaches

Several other methods for FKP recognition have been investigated in the literature, independently or in combination, to extract texture and local, global or line features.

In 2005, a system was developed to enhance the early recognition of the FKP [104]. The authors proposed the use of a 3D sensor to capture the FKP image. The geometric method is used to extract curvature shape information of the FKP. However, the complexity of 3D data processing means that this is computationally expensive, which is the main disadvantage of this scheme.

An LBP approach has been proposed where the ROI of the captured FKP is divided into multiple blocks [92]. Each block is subjected to a bank of Gabor filters from which LBPs are produced and represented in the form of histograms. The bio hash function is used to perform matching between the fixed-length FKP feature vectors gained from the database image and input image.

A new algorithm, the probabilistic Hough transform (PHT), has also been proposed to

extract line features from the FKP [19]. In this approach, robust features are also derived by means of the speeded up robust features (SURF) algorithm to improve performance. The Euclidean metric is applied in similarity matching between the registered and input FKP images.

Kumar et al. [58] introduced an automated approach and explored a texture analysis method for biometric FKP recognition. In their work, the features of captured FKP images were extracted based on methods for the geometrical analysis of texture and features. The geometrical features were obtained from the finger knuckle surface. In addition, the textural information is obtained by applying PCA, ICA and LDA. The Euclidean distance is used to compute the scores between the reference and input FKP vectors.

A new trend of the research on LBP is to encode the directional information instead of intensity information. Jain [43] proposed a new feature extraction method called Local Direction Pattern (LDP) to encode an FKP image in order to enhance the information as each pixel is represented as a binary LDP code. For classification, Chi-square and SVM classifiers are used as a matching function. In recent research conducted in 2014 [57], the same authors proposed a new approach for verifying personal identities using the FKP. In this approach, minor finger patterns are investigated together with the major FKP to enhance performance. The textural patterns of the back of the finger were extracted using 1D Log Gabor filters, LBP and improved ILBP.

5.5 Finger knuckle print database

The database used to conduct the experiments in the present study was the PolyU FKP database, which contains 7,920 greyscale FKP images. The images are from a total of 165 users (125 male and 40 female) aged 20-50 years, where the majority of participants (143) were aged 20-30 and the other 19 were aged 31-50. The data collection process was undertaken in two separate sessions and the FKP images were collected from the left index finger (LIF), the left middle finger (LMF), the right index finger (RIF) and the right middle finger (RMF). Around 12 images were collected from each finger during the sessions, with each region of interest (ROI) being 110×220 pixels. Figure 5.3 shows the ROI images relating to the four fingers - LIF, LMF, RIF and RMF - for one FKP in the PolyU database. Hence, in total, the database contains 7,920 images collected from 660 different fingers. Figure 5.4 presents the structure of the FKP images database.

5.6 Summary

A brief overview of FKP recognition applications has been provided in this chapter. The overview highlights the important information from relevant existing studies of finger knuckle print recognition. In terms of feature extraction and matching, a number of approaches to FKP recognition have been classified into several different categories in the literature, including subspace-based and code-based approaches. However, there some approaches that cannot be grouped into any one category. Moreover, some fusion methods have been implemented to build finger knuckle print recognition systems with a view to improving the accuracy of the recognition process.

The next chapter comprises two main parts: the first presents the proposed MSLBP descriptor to get a more robust and discriminative representation of FKP features; and the

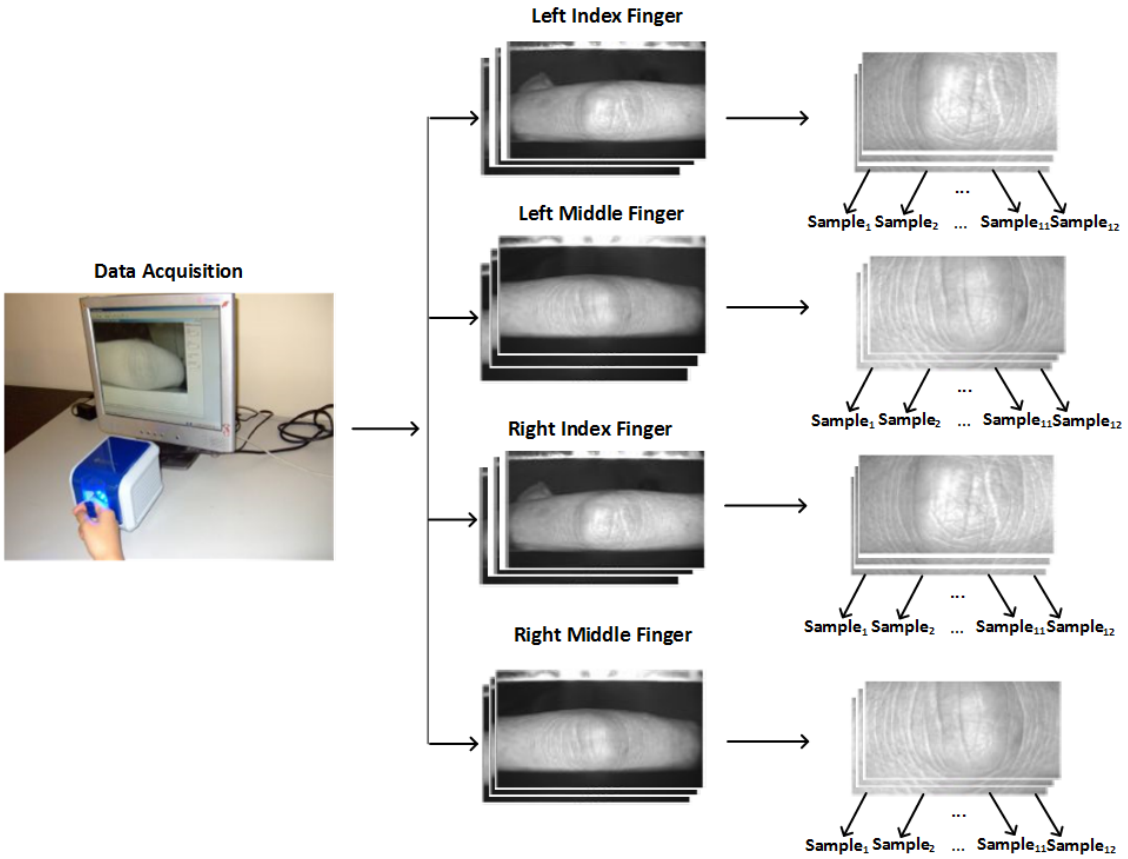

Figure 5.4: Structure of the Hong Kong Polytechnic University (PolyU) Finger Knuckle Print (FKP) Database [121].

subsequent part propose two innovative texture feature approaches for FKP-based person recognition, employing Fibonacci sequence LBP and multi-scale Fibonacci sequence LBP feature descriptors.

Chapter 6

Variants of the Local Binary Pattern Based on Modifying and Encoding Thresholding Schemes for Finger Knuckle Print Recognition

6.1 Introduction

FKP recognition has challenging problems relating to noisy data and variations in lighting when images are captured from sensors. The success of an FKP recognition system depends on a robust generation of powerful discriminative patterns.

Researchers have proposed several extensions of LBP-based texture descriptors, which have focused on improving robustness to noise using various encoding and thresholding schemes. As mentioned earlier, LBP is among the most computationally efficient high-performance textural feature discriminators. In terms of discriminative power, a number of variants of LBP descriptors have been proposed in recent years to improve robustness to noise. For example, Hafiane et al. [37] suggested the median binary pattern (MBP), which provides robustness to noise because the texture primitives are obtained by thresholding a 3×3 neighbourhood on the local median. Also, Guo et al proposed LBP variance (LBPV) to discriminate the local contrast data into the one-dimensional LBP histogram [35].

The aim of this chapter is to propose efficient methods which provide robust and discriminative representation for FKP features. The shift LBP descriptor [24, 62] has motivated the proposal Fibonacci sequence LBP (FSLBP) descriptor of texture features. One of the key challenges of FKP is to improve the robustness against lighting variations and the noise of images using different encoding or thresholding of the patterns. In the proposed FSLBP descriptor, the threshold is adjusted using Fibonacci numbers of order n to generate a distribution of binary codes at every pixel position and thus create descriptors that are more robust against variations of the lighting as shown in Figure 5.4. In addition, the proposed technique extends the FSLBP approach by using a multi-scale FSLBP to analyse the effect of multi-scale data. Although discriminative features play a very important role in FKP recognition success, the classifier performance also holds the key to further improve

the recognition accuracy. When designing the proposed recognition system, the k-nearest neighbour (KNN) classifier has been used.

This chapter is structured into several sections. This study is based on LBP and section 6.2 is concerned with the first proposal of the MSLBP descriptor, which provides the main steps of the methodology. Subsection 6.2.2 introduces the concept of the MSLBP descriptor. The proposed approach adopts a multiple-scale perspective for the FKP data, and subsection 6.2.3 describes the classification method. Subsection 6.2.4 reports on the results of experiments, followed by a discussion in Subsection 6.2.5.

The second main section 6.3 is concerned with the proposed FSLBP and FSMLBP descriptors. Here the threshold is adjusted using sequence Fibonacci values to compute the image descriptor, enabling optimal performance in terms of classification. This section is organized as follows. Subsection 6.3.2 introduces the framework for the FKP recognition system. The proposed FSLBP method is explained in subsection 6.3.2.1, while subsection 6.3.2.2 is concerned with the proposed FSMLBP descriptor. Subsection 6.3.2.3 provides a brief review of the FKP recognition stage. Subsection 6.3.3 then describes the results of experiments using the public PolyU database and provides a discussion of the results, including a comparison of the proposed approaches against other methods in subsection 6.3.4. Finally, section 6.4 gives the conclusions of the chapter.

6.2 Multi-scale shift local Binary Pattern-Based descriptor for finger knuckle print recognition

6.2.1 Introduction

Researchers have designed rich, dominant feature descriptors in biometric recognition, such as LBP [56, 64, 87] , Gabor [80, 81], and a concatenate of LBP and Gabor [29] among others. In contrast to global features, similar to LDA and PCA, these local features possess certain advantages due to their stable performance against noise and variations in illumination. Gabor features describe the local structure of the images in terms of their scale and orientation, while LBP features provide invariance against monotone transformation and confer robustness to some extent to changes in image capture conditions.

As previously mentioned, LBP is a method that is widely used to analyse an image's local textural features. The proposed method is based on SLBP, which was originally based on the concept of LBP histograms. The SLBP operator is extended to multi-scale by using radii of different sizes. The classification of this new proposed feature is performed by using PCA and RLDA . The results show clearly that the proposed methodology provides good results in FKP recognition. However, in FKP recognition systems, LBP-based descriptors have rarely been employed. In particular, there has been a lack of studies of using SLBP-based descriptors.

6.2.2 Proposed Multi-scale Shift Local Binary Pattern (MSLBP)

The concepts of SLBP and MSLBP were described and defined in sections 4.3.2.1 and 4.3.2.2. Multiscale SLBP is the generalised version of SLBP which offers a powerful and attractive texture descriptor showing improvements in terms of performance accuracy. In the SLBP method, a pattern code is computed using a varying number of interval to generate a distribution of binary codes at every pixel position, in order to create more robust descriptors against variations in the environment. As mentioned earlier, in this variant the

main difference is that the threshold uses different values k but within the limits $-l$ and l. For example, if $l = 3$, the differences between neighbouring values and the central pixel value are encoded using four thresholds which are $-3, -2, -1, 0, 1, 2, 3$, as shown in Equations 4.16 and 4.17. However, the MSLBP is based on a very simple principle of varying the radius R of the LBP label and combining the resulting histograms. The neighbourhood of the MSLBP operator is described with the parameters (P, R), where $R = r_1, r_2, .., r_n$, where n is the number of radii used in the process of MSLBP calculation. MSLBP histograms for different values of R can be determined according to Equation 4.18. The set of histograms computed at different radii provides regional information about the observation vector (e.g, 2^8 yields 2048 bins for 8 scales, where R is from 1 to 8). However, there is an issue pertaining to the high level of dimensionality in multi-resolution analysis and this problem can be reduced using the technique of feature selection to reduce unnecessary information.

Equation 4.18 defines the FKP descriptor for multi-resolution, and it is developed by applying the shift LBP operators at r scales to an image. MSLBP histograms for different values of R could be calculated by summing these vectors as defined in Equation 4.19. Here is the equation referred to:

$$F_{Q,r} = [H_{Q,1}, H_{Q,2}, \ldots, H_{Q,R}]$$

The combination of features brings with it the problem of overfitting due to the high dimensionality of data. To address this problem, the reduction of the dimensionality of the resulting descriptors is carried out.

6.2.3 FKP recognition process

This section highlights the steps in the classification which consist of the following: random sampling, PCA and LDA (explained in detail in Chapter 2). LDA is a powerful technique for predicting observed data; however, it cannot predict unobserved data. Furthermore, LDA may not work for non-linearly separable datasets. In particular, when the dataset is highly dimensional, its performance degrades. As described in section 4.3.2.2 (MSLBP), SLBP histograms are calculated for radius from 1 to R before concatenating the extracted features from all radii features. This results in one high-dimensional feature vector. This leads to the dimensionality problem in the proposed method and further increases computational complexity. To overcome this problem, the random subspace method and PCA are used in this chapter, providing an effective solution to the problem of concatenating multi-scale FKP histograms. This in turn improves the performance of LDA-based FKP recognition. Random subspaces and sub-sampling are employed to construct ensembles of LDA classifiers which are then fused into a decision process.

The random subspace method works by employing sufficient training data in each subspace by performing a dual principal subspace method for learning. As mentioned earlier in subsection 2.4.1, when applying PCA, the high-dimensional FKP feature is projected to a low-dimensional feature space and then LDA is performed in this PCA subspace. Usually, eigenvectors with zero eigenvalues are removed from the PCA subspace, since as the training samples have some inherent zero elements with no discriminative information. To construct a stable RLDA classifier, the PCA subspace dimension is dependent on the training set size. Then, these new features will be used for the training and testing of the LDA classifier as discussed in detail in subsection 2.5.1. The flowchart in Figure 6.1 describes the main steps of the FKP recognition process.

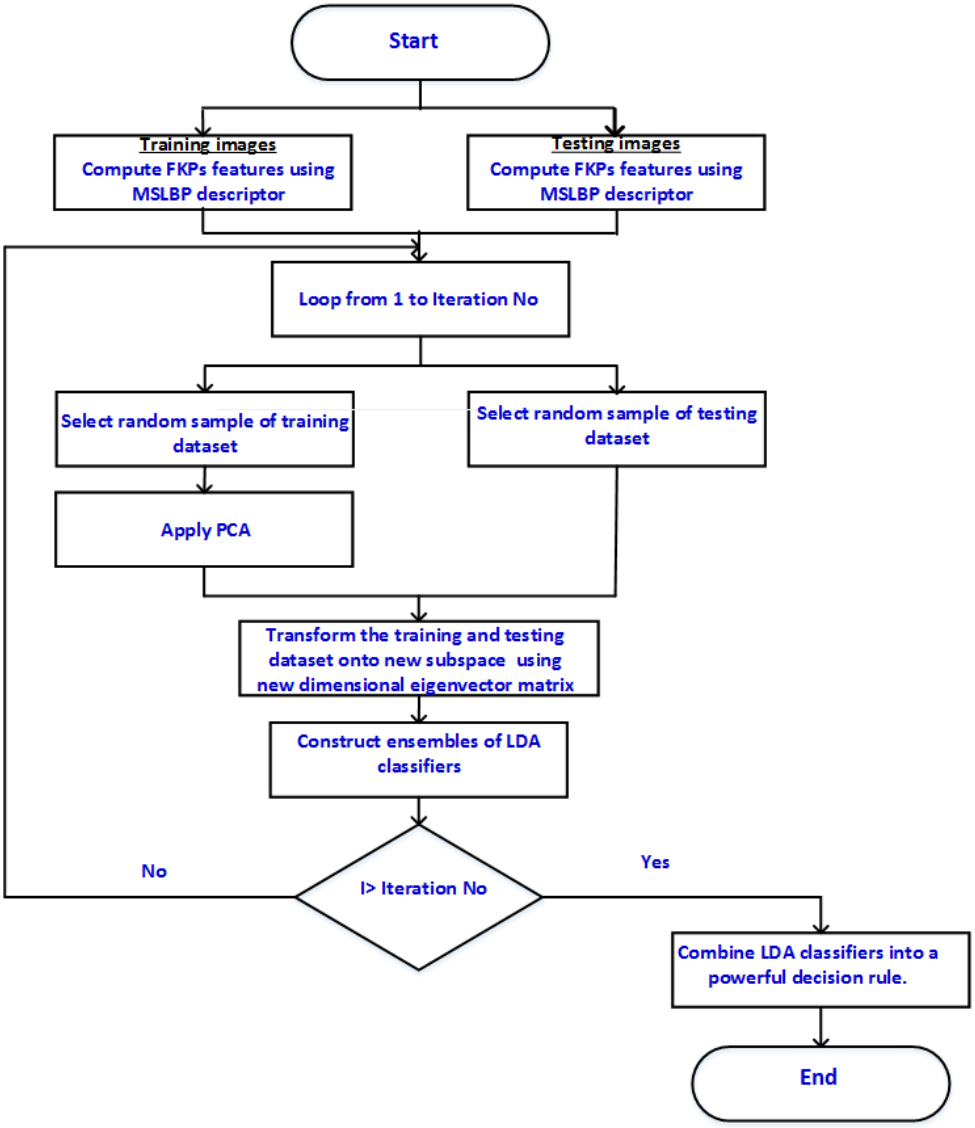

Figure 6.1: Flowchart of the main steps of the FKP recognition process.

6.2.4 Experiments and results

6.2.4.1 protocol I

The aim of this experiment is to evaluate the performance of the proposed methodology. To achieve this the same evaluation protocol set up is adopted as in a previous study [73], where 3 images for each type of FKPs (LIF, LMF, RIF, and RMF) are selected randomly as training images and the rest of the images are used for the test images. Therefore, for each FKP (LIF, LMF, RIF and RMF) there are 495 (165x3) training samples and 1485 (165x9) test samples. For FKP features, a MSLBP descriptor was generated with different radii for 8 scales (from 1 to 8) and eight neighbours. The final dimension of the MSLBP is 2048 (8x256). It should be noted that the experimentation process was repeated 5 times to obtain the different training datasets. The MSLBP has been compared to the Log-Gabor method [73], where the FKP trait was filtered using a 1D Log-Gabor filter and the real and

imaginary parts of each filtered image were used to form the feature vector.

Methods	Recognition Rate (%)			
	LIF	LMF	RIF	RMF
Log-Gabor [73]	88.15	87.70	88.96	88.62
SLBP	63.22	69.19	71.11	74.55
Proposed MSLBP	**91.58**	**92.19**	**92.05**	**91.04**

Table 6.1: Recognition rate for FKP feature descriptors MSLBP compared with the previous work in experiment 1.

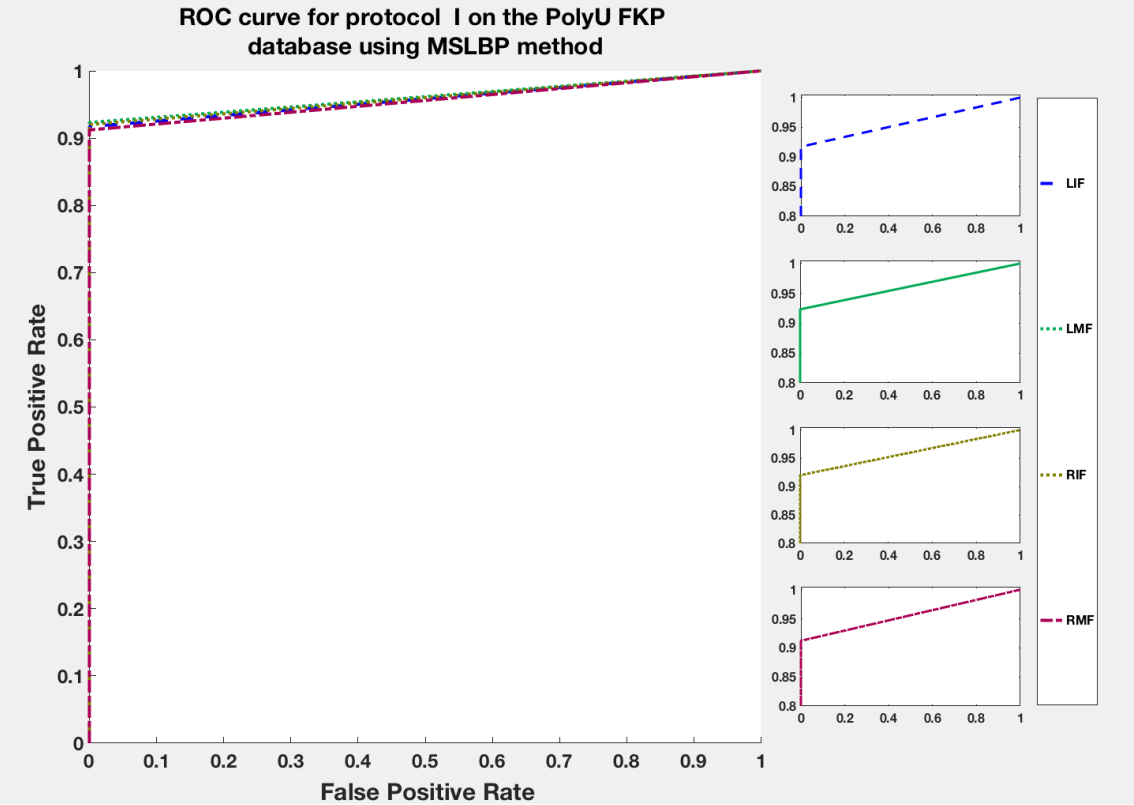

Figure 6.2: LDA ROC curves for the MSLBP descriptor for different modalities (LIF, LMF, RIF and RMF), using 3 images selected randomly for training and the rest of the images are used for the testing.

The results of the experiments are listed and compared in Table 6.1. It can be seen that the MSLBP provides increased performance under a variation of illumination conditions with 92.19% accuracy obtained for LMF. For the left index finger (LIF), MSLBP obtains a performance of 91.58% which is 28.36% higher and 3.43% higher than SLBP and Log-Gabor methods, respectively. The recognition rate for the right index finger (RIF) results clearly show that the proposed approach yields 92.05% accuracy, which is a significant increase when compared to the SLBP and Log-Gabor methods. In the case of the right middle finger (RMF), it is clear from the results that there are increases in performance over the 16.49% and 2.42% for SLBP and Log-Gabor methods respectively. Figure 6.2 illustrate the ROC curves resulting from plotting the FAR versus GAR rates for the different FKP data

sets. It is evident from this that the recognition rate of the LMF in the MSLBP approach outperforms other modalities (LIF, RIF and RMF).

6.2.4.2 Protocol II

The effectiveness of the proposed methodology is evaluated using the FKP datset described previously which is publicly available. Evaluation of the same state-of-the-art approaches was used, specifically the CLPP [45], Gabor+PCA+LDA [91] and Gabor+KPCA+LDA [97]. OCLPP is an orthogonal complex locality preserving projection (OCLPP), which uses distance and angle information between feature vectors to evaluate data similarity. The combines the extracted features of intensity and the Gabor images of each FKP are combined in a long vector [91]. Elsewhere, a bank of Gabor filter was applied to a pre-processed FKP image [97]. Then, kernel principal component analysis (KPCA) and linear discriminant analysis (LDA) were used for dimension reduction and the classification stage.

In the experiment in the present study, six samples were selected at random for the LIF, LMF, RIF and RMF modalities for the training set while the rest of the samples were the testing set. Therefore, for each modality there were 990 (165x6) training samples and 990 (165x6) test samples. It is worth mentioning that the same parameters of the MSLBP were utilised as detailed in Protocol I.

Methods	Recognition Rate (%)			
	LIF	LMF	RIF	RMF
Intensity+Gabor [91]	89.90	88.59	89.49	88.48
OCLPP[45]	87.87	87.49	86.94	87.38
Gabor+KPCA+LDA[97]	-	-	-	91.67
Proposed MSLBP	**93.80**	**94.70**	**92.20**	**94.80**

Table 6.2: Recognition rate for FKP feature descriptors MSLBP compared with the previous work in experiment 2.

When the FKP features were applied using the MSLBP approach an increase in performance of 3.13% and 7.42% resulted when compared to the existing techniques. In the case of the right middle finger, the proposed method clearly outperforms MSLBP by achieving a 94.80% recognition rate as shown in Table 6.2. For the right index finger, the proposed MSLBP outperforms the SLBP and other methods achieving 92.20% accuracy which is 2.71% higher than Intensity+Gabor and 5.26% higher than OCLPP. In relation to the left index finger, the recognition rate of the proposed method is 93.80% and thus it outperforms the Intensity+Gabor and OCLPP methods. For the left middle finger, the proposed histogram-based features yield higher results when compared to existing techniques. A accuracy of 94.70% is obtained, which is improvement of approximaately 6.11-7.21%. The results for the effectiveness of the MSLBP approach are presented in Figure 6.3, which reflects the ROC curves showing the best recognition rates for all fingers.

6.2.5 Discussion

Multi-scale SLBP histogram features were employed and applied to FKP images using different radii. The proposed technique has been able to extract more discriminative information from FKP image data. This has led to significant improvements in performance

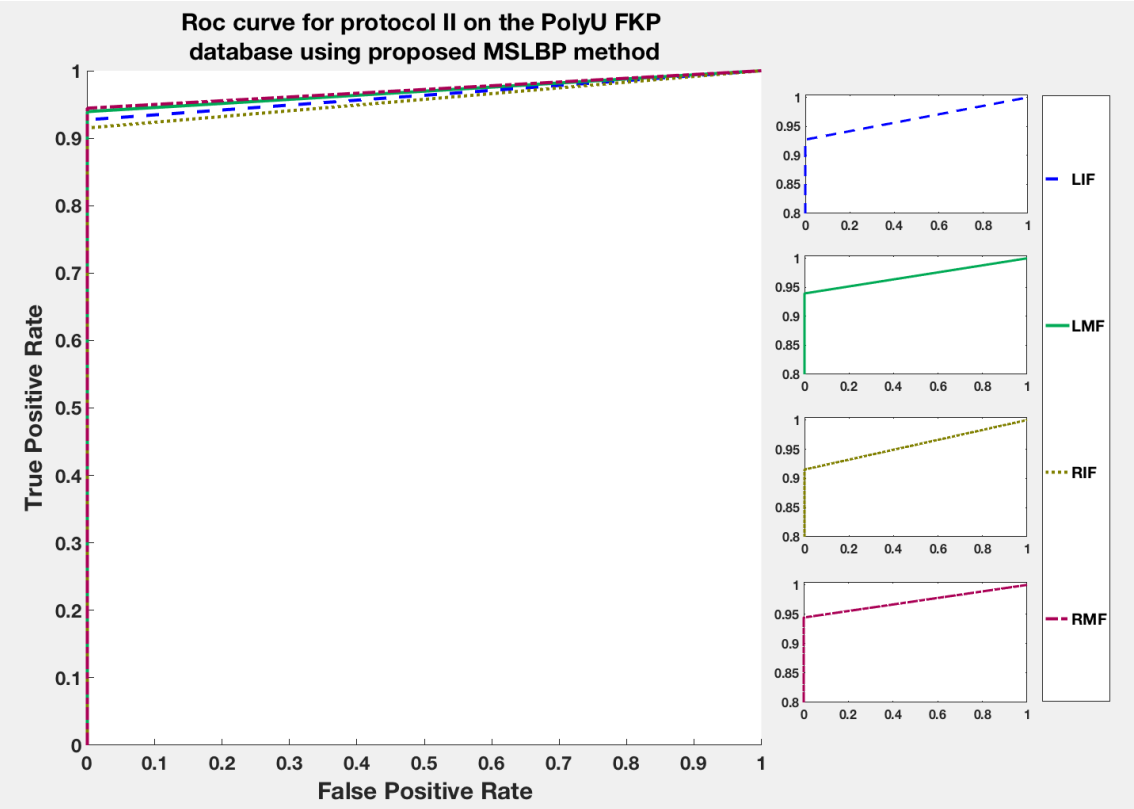

Figure 6.3: LDA ROC curves for the MSLBP descriptor, using the six samples selected random to LIF, LMF, RIF and RMF for the training set while the rest of the samples to the testing set.

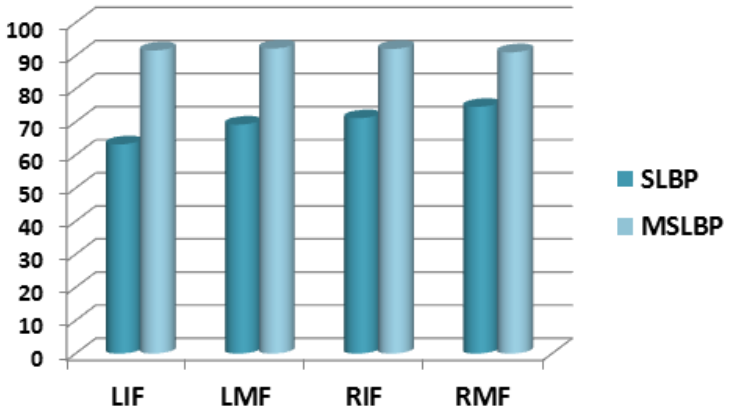

Figure 6.4: Comparison of SLBP and MSLBP approaches where 3 images for each type of FKP (LRF, LMF, RIF, and RMF) were selected randomly for training and the rest of the images are used as the test images.

when compared to methods for both experimental protocols which are similar to those usually used by researchers. The use of different radii in MSLBP suggest a significant effect on recognition rates. Figure 6.4 and Table 6.1 show the results for the proposed method

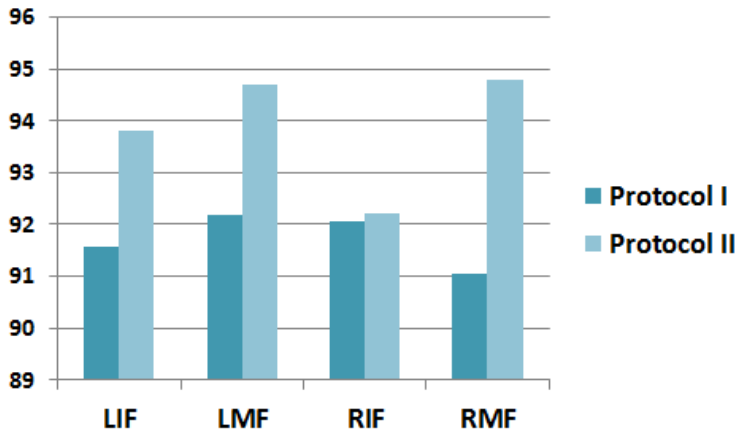

Figure 6.5: Comparison of MSLBP method for different modalities (LIF, LMF, RIF and RMF), in Protocols I and II.

with three training sets, where it can be seen that the recognition rate for the single scale is considerably lower compared to the multi-scale counterpart. Experiments were performed using the FKP database, which contains 7,920 images of 165 different people (125 male and 40 female). For FKP features, the SLBP descriptor was generated with radius = 1 and 8 neighbours, yielding a final dimension of the SLBP of 256. The multi-scale descriptor was created with different radii for 8 scales (from 1 to 8) and 8 neighbours, in which all FKP features from previous radii were concatenated to construct the final feature vector with a dimension of 2048.

The results presented clearly demonstrate the robustness of the MSLBP and its superiority over other reported methods. However, the advantage of higher recognition accuracy from multi-scale methods comes at the cost of high dimensionality and computational complexity. One of the solutions to high dimensionality is to determine the optimal FKP feature subspace in a lower dimension that can precisely describe the FKP features. The results obtained show that our methodology achieves outstanding results, comparable with those of all reported approaches in both protocols. It is also be noted that the results for our proposed method for Protocol II are slightly better in comparison to those of Protocol I, as shown in Figure 6.5. This is because three training and six testing samples were employed for the experiments in Protocol I, which does not provide results as good as those for the 6 training and 6 test datasets in Protocol II.

6.3 Finger knuckle print recognition using a Fibonacci sequence local binary pattern descriptor

6.3.1 Introduction

A flurry of research conducted to improve the accuracy of personal recognition has brought some interesting state-of-the-art methods. The shift LBP descriptor [62, 24] motivated the proposal of the FSLBP descriptor for texture features in present study. Here, Fibonacci numbers of n order are used to generate a distribution of binary codes at every pixel position and thus descriptors are created that are more robust against variations in the lighting of images as shown in Figure 5.3. To achieve more accurate recognition, the proposed method

extends the FSLBP approach by employing a multi scale FSLBP. This provides interesting information about the merging of features at the scale that gives the highest recognition rate.

6.3.2 Finger knuckle print recognition

In this section, the proposed FKP recognition system is described. The framework for FKP recognition should be based on the best finger type with the highest recognition rate. The general scheme of the proposed unimodal FKP recognition system is shown in Figure **??**. The first stage for a given loaded image comprises pre-processing, feature extraction, dimensionality reduction and classification. The main novelty lies in the introduction of FSLBP and FSMLBP descriptors for feature extraction followed by SR-KDA to reduce the size of the dimension of the extracted FKP feature vectors. Then, the KNN classifier is applied for the recognition task.

6.3.2.1 FSLBP-based feature extraction

The wide use of and extensive research into LBP descriptors have led to the development of various algorithms for finding the optimal threshold, providing robust performance. We propose modifying the thresholding scheme for the pixel values of the operator to make LBP more robust against these negligible changes in pixel values. This technique is considered to be a simple yet effective tool which labels the pixels of an image with a binary number. First, the value of the current pixel g_c is applied as a threshold for each of its neighbours g_p $\{0, 1, \ldots, Q-1\}$, considering the result as a binary number. However, in the Fibonacci sequence, a local binary pattern (FSLBP) code is generated for every pixel position. Mathematically, the FSLBP for a position (x, y) and a value k, can be represented as shown in Equation 3.1. Here, k varies within the set of Fibonacci numbers and for every change in k a new binary code is generated and added to the histogram of patterns.

$$\mathrm{FSLBP}_{\mathrm{Q,r}}(x, y, k) = \sum_{p=0}^{Q-1} S\left(g_p - g_c - k\right)^{2^p} \tag{6.1}$$

where Q represents the evenly distributed sample points on a circle with radius r whereas S can be represented as:

$$S(x) = \begin{cases} 1 & \text{if } x \geq 0 \\ 0 & \text{otherwise} \end{cases} \quad \text{and } k\epsilon\,[t_0, t_n] \cap Z \tag{6.2}$$

k=n+1, and for every different value k assumes a new binary code is created within the limits t_0 and t_n. In the present cases, k is the Fibonacci numbers of order n, which represents a threshold value. k is defined by Equation 6.3 with the starting conditions $t_0 = 1$ and $t_1 = 1$:

$$t_l = t_{l-1} + t_{l-2}, \quad \mathrm{l} = 2, 3, .., n \tag{6.3}$$

If n is assigned to be equal equal to 5, for example, the Fibonacci sequence (k) will be 1,1,2,3,5 and 8. Figure 6.6 shows an example of Fibonacci numbers. Then, each pixel position will contribute to the histogram with six binary codes. The values in the final histogram are divided by $n + 1$, giving the histogram the sum equal to the number of pixel positions considered, as in the rest of the LBP-family [62].

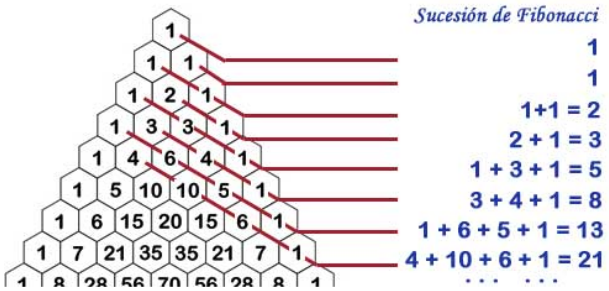

Figure 6.6: Construction of Pascal coefficients. The Fibonacci numbers are the sums of the "shallow" diagonals (shown in red) in Pascal's triangle.

6.3.2.2 FSMLBP-based feature extraction

The proposed algorithm, the Fibonacci sequence multi-scale local binary pattern (FSMLBP), has been verified as an efficient and effective descriptor for FKP recognition. As mentioned in section 3.3, a multi-scale approach has been employed and used successfully to capture structures which exist at different scales [12]. In its multi-scale version, the FSLBP has been used for prediction and shows improvement in terms of classification over the former version of the FSLBP. The code extracted for all overlapping neighbourhoods is added to a histogram. In the multi-scale version, the radius of the FSLBP is changed and the outcomes are concatenated. However, the problem of high dimensionality is associated with multi-resolution analysis and this can be minimized using a feature selection technique to eliminate redundant information. A selection of radii of different sizes, according to the neighbouring pixel's location in relation to the centre pixel, leads to the creation of a multi-scale presentation through the concatenation of FSLBP histograms from every scale with the value of a specific radius [83]; this 2^8 yields 1024 bins for 4 scales ($R = 1, 3, 5, 7$). This histogram contains information concerning the distribution of the multi-scale features over the whole FKP image. The different values of multi-scale FSLBP are considered to be more accurate than the use of a single-scale representation of FSLBP with significantly variation illuminations. The histogram of FSMLBP is calculated as follows:

$$H_{Q,r}(p) = \sum_{i=0}^{M-1} \sum_{j=0}^{N-1} g\left(\text{FSLBP}_{Q,r}(i,j), p\right), \; p \in [1, n+1] \tag{6.4}$$

where n is the maximum bin value of FSMLBP and R is the maximum radius used to the multi-scale case.

The set of histograms calculated for different sizes of radii gives regional information regarding the observation vector. The outcome of the multi-scale FKP descriptor is defined in Equation (3.6) as follows:

$$F_{Q,r} = [H_{Q,1}, H_{Q,2}, \ldots, H_{Q,R}] \tag{6.5}$$

The main problem in both approaches is the extremely large number of features, which can result in an overfitting problem for classification. To overcome this difficulty, spectral regression kernel discriminant analysis (SR-KDA) is applied as a dimensionality reduction technique.

6.3.2.3 FKP recognition stage

Before going into the classification step, dimension reduction is first performed on stored histogram FKP feature vectors in order to handle the problems associated with the dimensionality problem. This results in high dimensional feature vectors that increase the computational cost of the proposed approach. In this proposed approach, the overfitting of the FKP features due to high dimensionality is addressed using SR-KDA (see section 2.4.2), which provides an efficient solution to the problem of the merging of features. After dimension reduction, the KNN approach is adopted to identify FKP in the testing phase by comparing its features to one of a training set of classes. As mentioned earlier in section 2.5.2, the nearest neighbour classifier is well known as a nonparametric decision method. Each an unknown FKP image in the testing phase is classified based on the distance of its features from the FKP features of the training images. The nearest neighbour is the FKP image which has the minimum distance from the training FKP image in the feature space. In this work, the distance between two FKP features can be measured based on Euclidean distance.

6.3.3 Experiments on the poly-U database

The proposed methods were implemented and tested using the 165 subjects (125 males and 40 females) from the PolyU FKP database [121]. Two experiments were designed to test the validity of the methods proposed for feature extraction. The proposed approaches were compared with the existing techniques in the FKP literature.

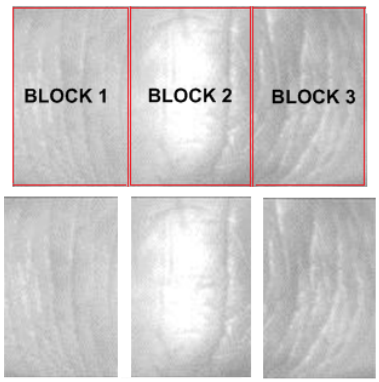

Figure 6.7: FKP ROI image divided into three blocks of 110x74 pixels

6.3.3.1 Protocol I

The experiment followed the same protocol set up as for Intensity+Gabor [91], OCLPP [45], GCRC [66] and MSLBP [24] to evaluate the performance of the FSLBP and FSMLBP methods. The methods proposed in two previous studies [45, 91] have been introduced in section 6.2.4. GCRC [66] is a group collaborative representation-based classifier, applied to group-level constraints in the CRC at the classification stage. MSLBP is the multi-scale shift local binary pattern which is computed as a set of a histograms at different radii provides regional information about the FKP images and further concatenates the histograms into a long observation vector.

Methods	Recognition Rate (%)			
	LIF	LMF	RIF	RMF
Intensity+Gabor [91]	89.90	88.59	89.49	88.48
OCLPP[45]	87.87	87.49	86.94	87.38
GCRC[66]	90.51	90.40	91.01	91.01
MSLBP[24]	93.80	94.70	92.20	94.80
Proposed FSLBP	**96.67**	**97.17**	**96.16**	**96.06**
Proposed FSMLBP	**96.77**	**97.68**	**97.27**	**97.37**

Table 6.3: Comparison of recognition rates using proposed approach with state-of-the-art methods using 6 training and 6 testing samples

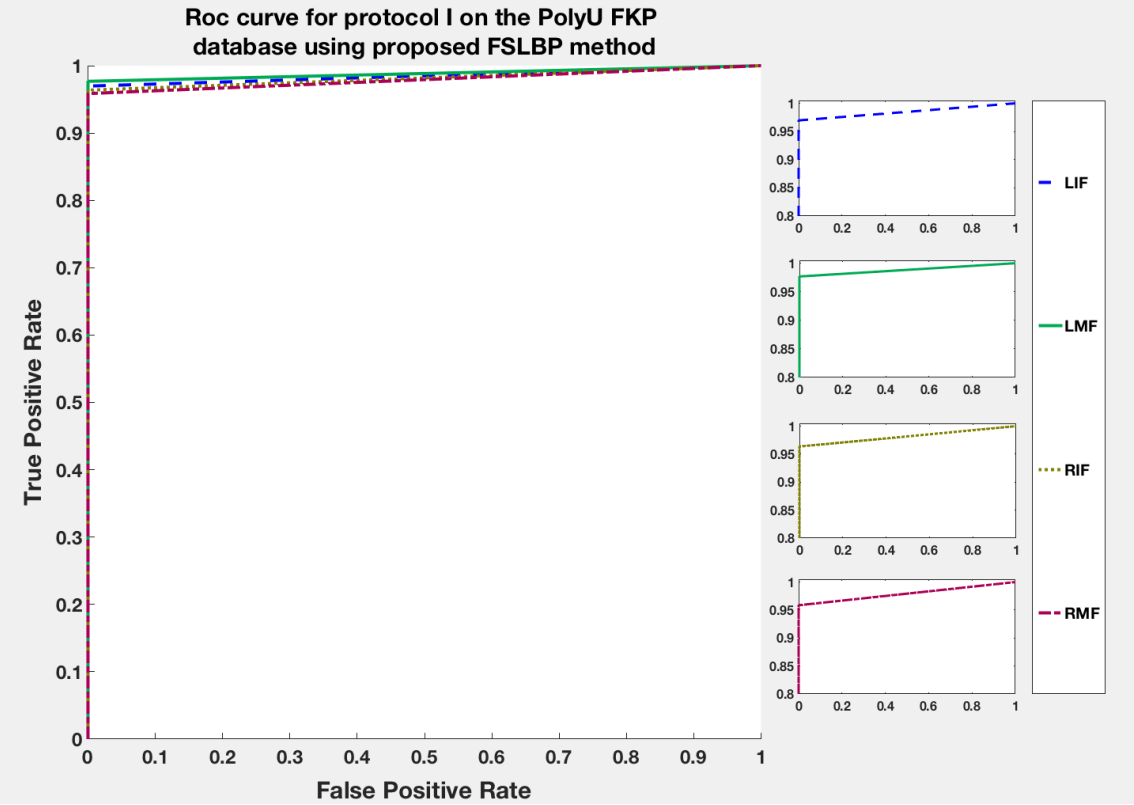

Figure 6.8: ROC curves for the FSLBP descriptor for different modalities (LIF, LMF, RIF and RMF), computed using six images captured in the first session for the training set and six images captured in the second session for the testing set.

The present experiments used 6 images in the training phase and the remaining images in the testing phase. Therefore, for each modality (LIF, LMF, RIF and RMF) there were 990 (165x6) training samples and 990 (165x6) test samples. The FSLBP descriptor was generated with radius sizes of 6 and 8 neighbours. In the FSLBP feature extraction, the original FKP image was divided into three blocks of 110x74 pixels as shown in Figure 6.7. The final dimension of the FSLBP was 768 (3x256) for a single scale. As for the FSMLBP descriptor, the parameters were set to R=1,3,5 and 7, comprising different radii for 4 scales, with 8 neighbour values. The final dimension of the FMLBP was 3072 (3x4x256)

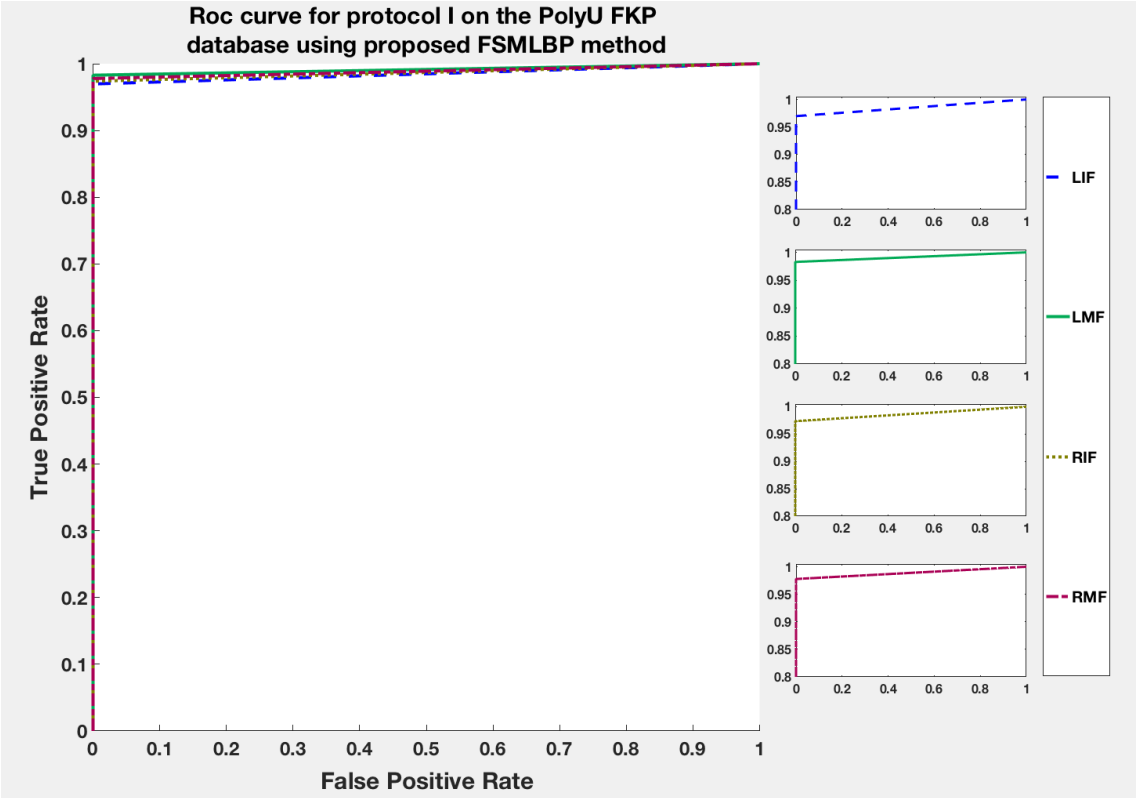

Figure 6.9: ROC curves for the FSMLBP descriptor for different modalities (LIF, LMF, RIF and RMF), computed using six images captured in the first session for the training set and six images captured in the second session for the testing set.

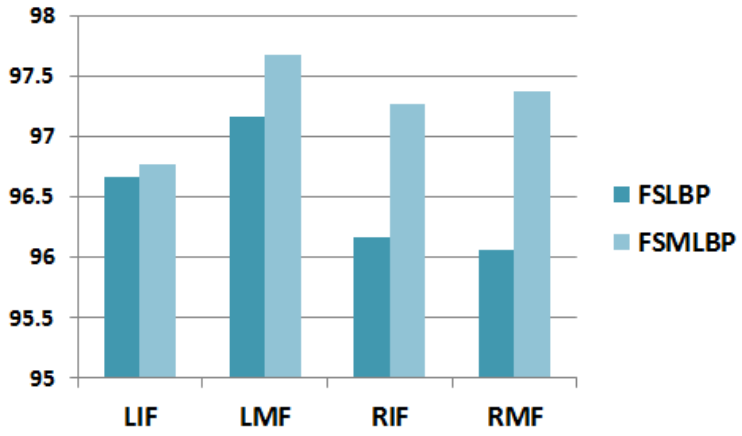

Figure 6.10: Comparison of FSLBP and FSMLBP methods for different modalities (LIF, LMF, RIF and RMF) in Protocol I.

for four scales. The results of the two methods are listed and compared in Table 6.3. The FSMLBP approach yields the highest rate of 96.77%, while the FSLBP comes second at 96.67% for the LIF. Moreover, it can be seen that, in the case of the LMF, the FSMLBP achieves the best result of 97.68%, which is 0.51% higher than the FSLBP compared to

other existing methods, resulting in increased performance rates of 9.09%, 10.19%, 7.28% and 2.98% compared to Intensity+Gabor, OCLPP, GCRC and MSLBP respectively. In relation to the RIF, the results obtained show that the FSMLBP achieves the best result, with a performance accuracy of 97.27%, followed by the FSLBP with a rate of 96.16%. In addition, for the RMF, the experiments show that the FSMLBP technique achieves an accuracy of 97.37%, outperforming the FSLBP approach, but the FSLBP in turn shows improved performance of 7.58%, 8.68%, 5.05% and 1.26% over Intensity+Gabor, OCLPP, GCRC and MSLBP respectively.

6.3.3.2 Protocol II

For validation purposes, the same protocol set up was adopted as in GCRC [66]. This method has been introduced in section 6.2.4. The images from the two sessions of data collection were divided in half, with the first 3 images from the two sessions selected as a training set and the latter 3 as the test images.

Methods	Recognition Rate (%)			
	LIF	LMF	RIF	RMF
GCRC[66]	98.99	98.48	99.56	99.29
Proposed FSLBP	**99.09**	**99.39**	**99.70**	**99.70**
Proposed FSMLBP	**99.39**	**99.60**	**99.80**	**99.80**

Table 6.4: Comparison of recognition rates using proposed approach with state-of-the-art methods using the first three images from the two sessions selected as the training set and the latter three images from the two sessions used as the test.

All parameters of the proposed methods were initialized as described in Protocol I. The comparison of the results using the KNN classifier is summarized in Table 6.4. This table clearly demonstrates the advantage of the proposed approaches in terms of the robustness of the histogram features in addition to effectiveness compared over the other reported methods. The FSMLBP offers attractive recognition performance rates of 99.39%, 99.60%, 99.80% and 99.80% for the LIF, LMF, RIF and RMF respectively. The results highlighted in bold indicate that the FSLBP approach outperforms the GCRC. With regard to the LIF, the FSLBP method achieves an accuracy of 99.09%, which is better than the GCRC. In relation to the LMF, the recognition rate of the FSLBP of the FSLBP is 99.39% and it thus outperforms the GCRC method. Moreover, it can be seen that, in the case of the RIF and RMF, the FSLBP method achieves the best results with a rate of 99.70%. The ROC curves for the FSLBP method are shown in Figure 6.11. The effectiveness of the proposed FSMLBP method is presented in Figure 6.12, reflected in the ROC curves showing the best recognition rates for all fingers.

6.3.4 Discussion

From the results summarized in Tables 6.3 and 6.4, it is shown that the FSLBP and FSMLBP approaches achieved recognition rates of more than 96.0% for all fingers (LIF, LMF, RIF and RMF). The ROCs in Figures 6.8, 6.9, 6.11 and 6.12 plot the false acceptance rate versus the genuine acceptance rate for different FKP databases, represented by the LIF, LMF, RIF and RMF.

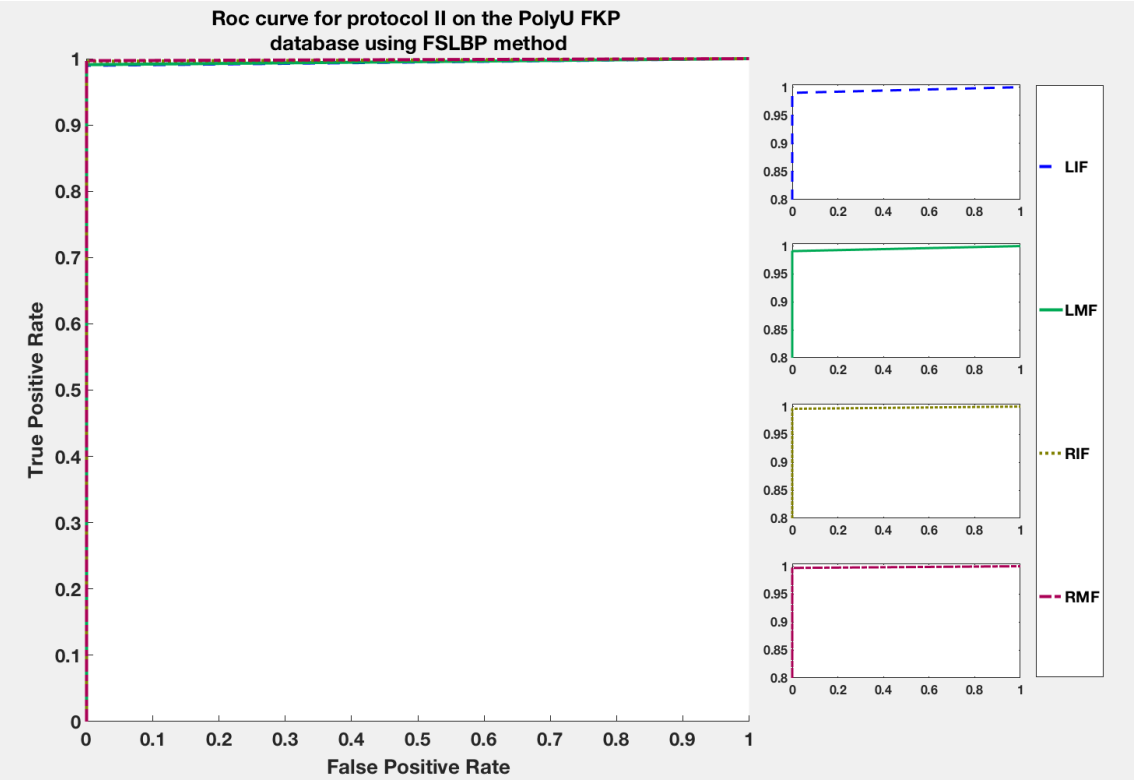

Figure 6.11: ROC curves for the FSLBP descriptor for different modalities (LIF, LMF, RIF and RMF), computed using the first three images from the two sessions selected as the training set and the latter three images from the two sessions used as the test set.

As shown in Figures 6.14 and 6.15, greater accuracy is achieved by dividing the sessions in half to provide training and testing samples in the FSLBP and FSMLBP approaches. Moreover, the findings indicate that the FSMLBP performs well and can obtain greater accuracy than the FSLBP, as shown in Figures 6.10 and 6.13. It can also be observed from the tables and graphs that the performance for the LMF is better compared to other fingers. However, in Protocol II the right fingers demonstrate better performance compared to left fingers.

6.4 Computational complexity

The proposed methods are simple and effective to implement. The multi-feature approach has resulted in improved performance, but the fusion process brings dimensionality problems which increase the computational cost of the proposed approaches. A solution needs to be found for the problem of the increased computational complexity due to the of merging FKP features, which could involve finding the optimal feature subspace in a lower dimension that can still accurately represent the data. The dimensions of the FKP feature vector can be reduced by using feature selection or extraction methods such as PCA and SR-KDA as explained above (see section 6.2.3 and 6.3.2.3). The results clearly show that the proposed approaches yield high recognition accuracy with an attempt to simplify the process involved and thus speeding up the task. A great deal of attention has been focussed to reducing computational complexity while enhancing the performance of the FKP recognition system.

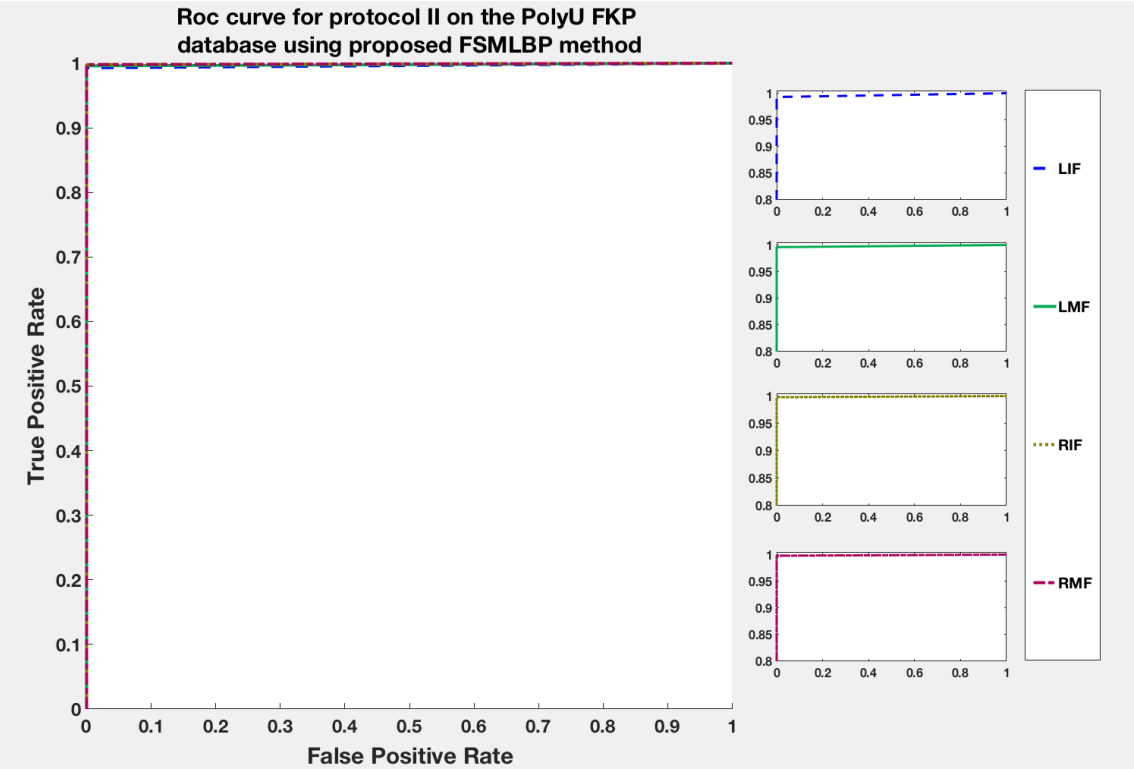

Figure 6.12: ROC curves for the FSMLBP descriptor for different modalities (LIF, LMF, RIF and RMF), computed using the first three images from the two sessions selected as the training set and the latter three images from the two sessions used as the test set.

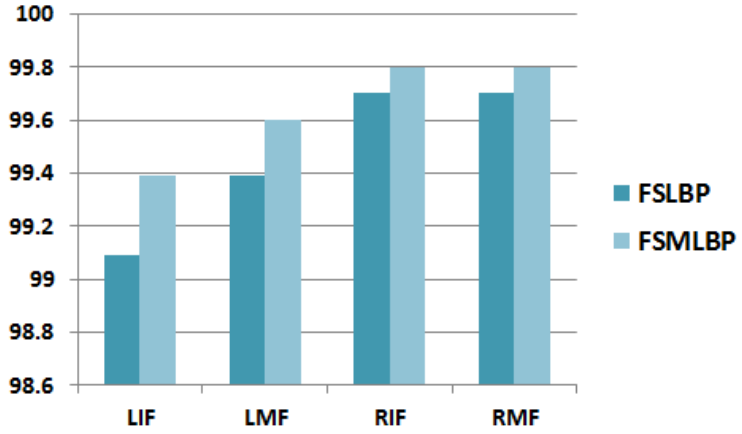

Figure 6.13: Comparison of FSLBP and FSMLBP methods for different modalities (LIF, LMF, RIF and RMF) in Protocol II.

6.5 Summary

The LBP histogram has gained a reputation as a powerful and attractive texture descriptor showing excellent results in the event of extreme variations in illumination. A number of variants of LBP have also proven successful in biometric recognition. The multi-scale

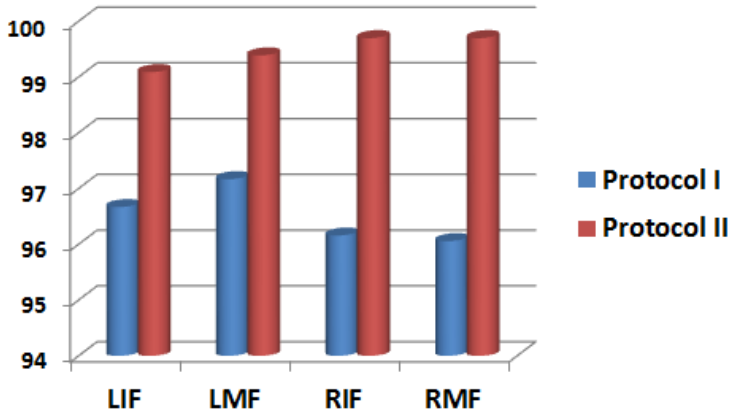

Figure 6.14: Comparison of Protocol I and Protocol II for FSLBP method in different modalities (LIF, LMF, RIF and RMF).

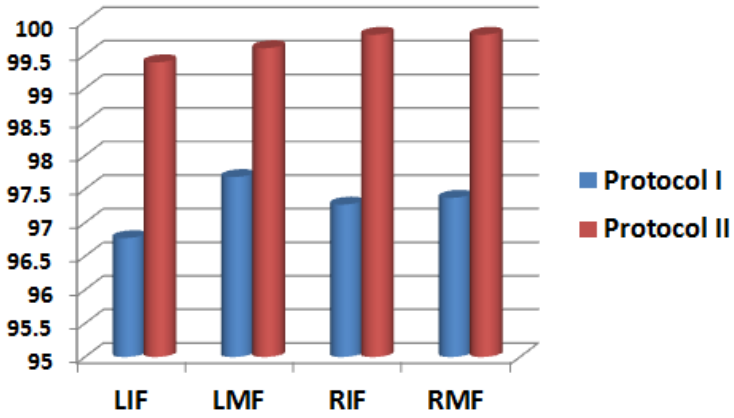

Figure 6.15: Comparison of Protocol I and Protocol II for the FSMLBP method in different modalities (LIF, LMF, RIF and RMF).

LBP has resulted in improved performance as compared to single-scale LBP, but the former involves high dimensional feature vectors which leads to computationally expensive algorithms.

The first part of this chapter was concerned with the development of a more accurate method for the extraction of FKP features. The proposed multi-scale SLBP feature descriptor has improved performance over other state-of-the-art techniques. Another contribution relates to the concatenation of the LBP histograms generated, and a solution was also given to address the issue of overfitting and dimensionality reduction in order to reduce computational complexity. This has been achieved by integrating and merging the features of the multi-scale LBP of individual scales, which produces the highest recognition rates when compared with single-scale. The proposed framework has been tested on different protocols and the results are quite similar despite using a lower number of training samples in experiment 1. Further, it has been observed that MSLBP for RMF outperforms other finger modalities with six training samples and that LMF performs better with three training samples.

The second part of this chapter has proposed two innovative texture feature approaches for FKP-based person recognition, employing FSLBP and FSMLBP feature descriptors. These are novel algorithms for extracting robust FKP patterns and their use leads to more accurate performance in FKP recognition. The SR-KDA is applied as a dimensionality reduction method to overcome overfitting and a KNN classifier is used to assess FKP recognition performance. The proposed approaches have been evaluated using challenging datasets and yield significantly improved results compared to existing techniques. The results also indicate that the recognition rate of the single-scale approach is lower compared to the FSMLBP method for all fingers (LIF, LMF, RIF and RMF).

The advantage behind using Fibonacci numbers of order n is to generate a distribution of binary codes at every pixel position having a normal distribution to extract most of the FKP information . This technique is simple yet effective which labels the pixels of an image with a binary number, which is robust to distortions that may occur during the scanning process (noise, blurring, change in contrast, etc.). The FSLBP is also able to extract the weak lines and reduce the false recognition rates. In its multi-scale version, the technique has been used for prediction and shows improvement in terms of classification over the former version of the FSLBP. However, the benefit of higher recognition accuracies from multi-scale methods comes at the expense of high dimensionality problem and computational cost. One of the solution to high dimensionality is to find the optimal feature subspace to reduce its dimension to accurately represent the data.

The next chapter provides a description of the proposed new feature set inspired by the completed local binary pattern, known as the dynamic threshold CLBP for FKP recognition.

Chapter 7

Feature Description Based on Dynamic Thresholds Completed Local Binary Pattern for Finger Knuckle Print Recognition

7.1 Introduction

Several new extensions of LBP-based texture descriptors have been proposed, focusing on improving the robustness to noise by using different encoding or thresholding schemes. In this chapter, the CLBP descriptor [34] has motivated the proposal of the dynamic threshold CLBP (dTCLBP) descriptor to analyse the performance of the FKP recognition system. The dTCLBP descriptor was applied as a basic feature in the initial recognition phase. The dTCLBP feature is the combination of two components, sign and magnitude, where the sign component is the same as in the original LBP, while the magnitude feature is encoded using a dynamic thresholding method. The magnitude component is computed by taking the absolute value of difference divided radius, and compares a neighbouring pixels with the median of the dynamic thresholds. To address noise and make the feature more robust, the dynamic threshold values are set as the $1 - \frac{min\,of\,megnitude}{max\,of\,megnitude}$ of the magnitude metrics of the differences between a pixel and one neighbour. Then median of the dynamic threshold values used as the threshold instead of using the mean of all magnitude matrices in CLBP. Two codes are then concatenated to form the TCLBP feature vector for each image.

The main body of this chapter is composed of two main sections. Section 7.2 describes the different steps in the proposed FKP recognition approach. Subsection 7.2.2 presents a brief overview of the CLBP, followed by descriptions of the main steps of the methodology in subsection 7.2.3. The proposed dTCLBP is introduced in subsection 7.2.3.1. As the proposed methodology uses feature reduction, subsection 7.2.3.2 provides a brief description of the PCA technique, while subsection 7.2.3.3 provides a summary of the LDA method. Subsection 7.2.4 addresses the experimental results and discusses the results.

The second main section 7.3 is concerned with the proposed the combination of the sign and magnitude features descriptor. Subsection 7.3.1 introduce the framework for the FKP recognition system, and subsection 7.3.2.1 reviews the dTCLBP descriptor. Subsection 7.3.2.2 describes the classification method, while subsection 7.3.3 provides the results of experiments on the proposed method, which are discussed in subsection 7.3.4. The chapter

ends with conclusions in section 7.4.

7.2 Finger knuckle print recognition using dynamic thresholds completed local binary pattern descriptor

7.2.1 Introduction

Feature extraction is a fundamental process in biometric recognition and is a critical step towards the understanding and analysis of image content. These features are the main elements used in the matching phase. The success of a matching process depends on the accuracy of the extracted features.

This section proposes a new method for FKP recognition, which is a modification of the CLBP method. The dTCLBP feature is the combination of two components, sign and magnitude, where the sign component is the same as the original LBP while the magnitude feature is encoded by the dynamic threshold. The performance of the proposed approach has been compared to some state-of-the-art approaches.

7.2.2 A brief review of the completed local binary pattern CLBP

With its numerous properties, LBP has become a powerful discriminator. Among these properties are the fact that its computational complexity is low and it is less sensitive to changes in illumination, unlike many other descriptors [77]. Guo et al [34] used a CLBP descriptor by splitting local image differences into two complementary components, sign s_p and magnitude m_p. Given a centre pixel g_p and its neighbour g_c, $p = 0, 1, \ldots, 7$, the local difference between g_p and g_c is defined as in Equation 7.1 [34, 76]:

$$\mathrm{s_p} = \mathrm{g_p} - \mathrm{g_c}, \quad \mathrm{m_p} = |\mathrm{g_p} - \mathrm{g_c}| \tag{7.1}$$

Two operators, known as CLBP_S and CLBP_M respectively, are proposed for coding, where the CLBP_S is equivalent to the conventional LBP and the CLBP_M measures the local variance of magnitude. The CLBP_M can be expressed as follows [34, 76]:

$$\mathrm{CLBP\_M_{P,R}} = \sum_{p=0}^{P-1} t\left(m_p - c\right)^{2^p} \tag{7.2}$$

$$t(x, c) = \begin{cases} 1 & \text{if } x \geq c \\ 0 & \text{if } x < c \end{cases} \tag{7.3}$$

where the threshold c is set as the mean value of m_p for the whole image. Guo et al [34] observed that the centre pixel, which expresses the local grey level of the image, also contains discriminative information. Thus, they defined an operator known as the CLBP_C to extract the local central information as follows [34, 76]:

$$\mathrm{CLBP\_C_{P,R}} = \ t\left(g_p, c_l\right) \tag{7.4}$$

where the threshold c_l is set as the average grey level of the whole image. By combining the three operators, CLBP_S, CLBP_M, and CLBP_C, it was shown that there is a significant improvement in relation to rotation-invariant texture classification.

7.2.3 Proposed methodology: FKP recognition

A schematic diagram of the proposed FKP recognition system is shown in Figure 7.1. As mentioned previously, the system comprises the following steps: FKP image acquisition, feature extraction, reduction of features and classification. The FKP features are extracted using the dTCLBP descriptor in the first phase of recognition. The PCA is presented as a dimensionality reduction algorithm to reduce the amount of unnecessary information. Classification is performed using a LDA classifier for FKP recognition. The major components of the proposed FKP system are explained below.

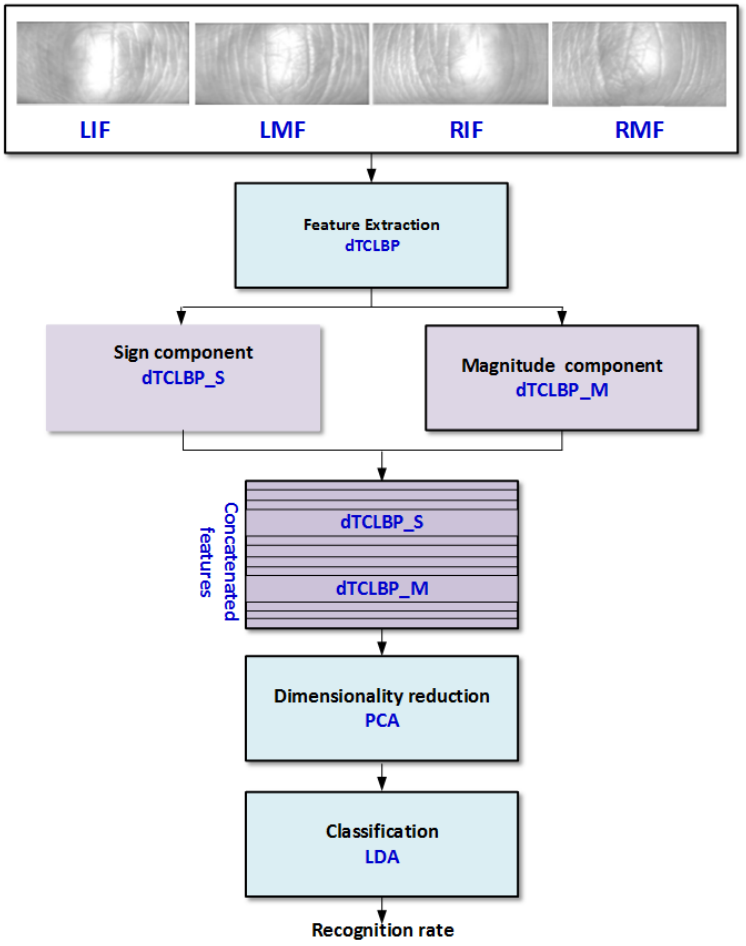

Figure 7.1: The general scheme of the FKP recognition system.

.

7.2.3.1 dTCLBP-based feature extraction

dTCLBP is proposed based on the customized LBP texture feature for the classification of FKP images. The dTCLBP descriptor has two components which are used to encode the local texture property of an image. The first signifies the sign feature, whereas the second is the magnitude feature vector which corresponds to gradient information achieved according to the magnitude of local differences [21]. If g_c is the centre pixel and g_p is one of neighbours and $p = 0, 1, \ldots, 7$, the g_c and g_p can be computed by $d_p = g_p - g_c$. This is divided into

two components, specifically sign *sp* and magnitude *mp* as defined in Equation 7.5. The local difference sign-magnitude transform is used to compute dTCLBP_S and dTCLBP_M, which represent texture features. dTCLBP_S is the same as the original LBP descriptor. In order to encode magnitude features the threshold value λ is set to the median of the dynamic thresholds T_P instead of comparing the neighbours with the mean of the absolute value of the differences between the centre pixel and one neighbour as used in CLBP [34]. The dynamic thresholds $[T_0, T_1, \ldots, T_7]$ are calculated as defined in Equation 7.6 to increase the robustness of the magnitude features. As dTCLBP_M is not a binary code as defined in Equation 7.7, local pattern operator is created by comparing the magnitude matrices with the median of the set of the dynamic threshold as defined in (7.8); all magnitude values greater than or equal to median threshold λ are quantized to 1, otherwise to 0 as follows:

$$\mathrm{s_p} = \mathrm{d_p}, \quad \mathrm{m_p} = \frac{|\mathrm{d_p}|}{\mathrm{Radius(R)}} \tag{7.5}$$

$$\mathrm{T_P} = 1 - \frac{\min(m_p)}{\max(m_p)} \tag{7.6}$$

Radius R defines the distance of the neighbours to the centre, while $p = 0, 1, \ldots, 7$ provides the number of samples for that distance (these are employed as neighbours). In addition, $\min(m_p)$ is the minimum value of magnitude m_p from the whole image, while $\max(m_p)$ relates to the maximum value of magnitude of m_p from the whole image, in order to calculate the dynamic thresholds T_P for each neighbour as follows:

$$\mathrm{dTCLBP\_M_{(P,R)}} = \sum_{p=0}^{P-1} t\left(m_p, \lambda\right) 2^p \tag{7.7}$$

$$t(x, \lambda) = \begin{cases} 1 & \text{if } x \geq \lambda \\ 0 & \text{if } x < \lambda \end{cases} \tag{7.8}$$

Finally, the two different histograms, for dTCLBP_S, and dTCLBP_M, are concatenated to form the feature vector for pattern classification.

7.2.3.2 Feature reduction

To reduce the size of the dimension of the feature vectors of the training dataset, a multivariate statistical technique known as PCA is used. The basic concept of PCA was described and defined in section 2.4.1. Here, the 6 training images linked to each subject modality were employed to create the training FKP vector. As mentioned before, the training images each have a vector of FKP modality in a $D \times N$ matrix format, where D is the dTCLBP of the feature dimension and N is the total number for each modality. The covariance matrix is created using FKP training images. The principal components are obtained from an analysis that consists of finding the eigenvectors from a covariance matrix derived from a set of training images. A adequate dimensions were retained in the training FKP data to estimate 99% of the energy. Using this new d-dimensional eigenvector matrix, the training and testing FKP datasets are projected onto the new subspace.

The proposed system, the PCA stage is only used to generate the low-dimensional feature vector of the training and testing datasets separately for each type of finger modality.

7.2.3.3 Recognition stage

After reducing the size of the FKP features, the next stage is to match the features of the FKP in the testing phase with the FKP features in the training set which have the same identity. The LDA is designed to classify an FKP (unknown class) into one of the training sets (known class). The LDA approach has been employed in the considerably wider area of object recognition (such as the face, iris, or speech.). A linear border between the different classes is established for separate classes using a linear classifier. The approach adopted by Fisher [26] locates a linear combination in connection with the variables so as to separate two classes as much as possible. The most suitable possible direction is sought regarding the separation of the two classes. As discussed earlier in section 2.5.1, LDA can be achieved by maximizing the ratio of the determinant of the within-class variance and the determinant of the between-class variance. If the kth class has a Gaussian distribution with mean μ_k and covariance, then the maximum conditional probability is chosen, which is equivalent to classifying as follows:

$$\arg\max_{k}(g_k)$$

where g_k is the discriminant function. Just as a reminder, the definition of the discriminant, as evaluated in equation 2.9, is as follows.

$$g_k\left(x_i\right) = \ x^T\Sigma_k^{-1}\mu_k - \frac{1}{2}\mu_k\Sigma_k^{-1}\mu_k + log\pi_k$$

More details on LDA classification for FKP recognition is provided in section 2.5.1.

7.2.4 Experimental results and discussion

Experiments were undertaken using the PolyU FKP database, which is publicly available. To test the performance of the proposed methodology, comparisons were made with other existing methods described in the literature (Intensity+Gabor [91], OCLPP [45] and GCRC [66]). As mentioned in section 6.3.3.1, the intensity+Gabor approach combines the extracted features of intensity and Gabor the images of each FKP in a long vector [91]. Orthogonal complex locality preserving projections (OCLPP) consider distance and angle information between feature vectors to evaluate data similarity. The group collaborative representation based classifier GCRC [66] applies group-level constraints in the CRC at the classification stage.

For the results to be comparable to the reported methods, experiments were implemented adopting the same protocol set up, training all FKP images in the first session and testing all images in the second session (6 training sets and 6 test sets). Therefore, for each modality (LIF, LMF, RIF and RMF) there were 990 (165x6) training samples and 990 (165x6) test samples.

The results are summarized in Table 7.1. The dTCLBP offers an attractive recognition performance rate of 92.12% in relation to LIF. Moreover, it can be seen that in the case of LMF, the dTCLBP method achieves the best result with a rate of 93.03% as shown in Figures 7.2 and 7.3. Furthermore, if compared against other existing methods, it results in increased performance of 4.44%, 5.54% and 2.63% in contrast to 'Intensity+Gabor', OCLPP and GCRC respectively. With regards to RIF, the results displayed in the table

Table 7.1: Recognition rate precentages for the proposed method with similar state-of-the-art methods using PolyU FKP database with 6 samples of training and 6 samples of testing.

Method	Recognition Rate (%)			
	LIF	LMF	RIF	RMF
Intensity+Gabor [91]	89.90	88.59	89.49	88.48
OCLPP [45]	87.87	87.49	86.94	87.38
GCRC [66]	90.51	90.40	91.01	91.01
Proposed method (dTCLBP)	**92.12**	**93.03**	**91.51**	**92.02**

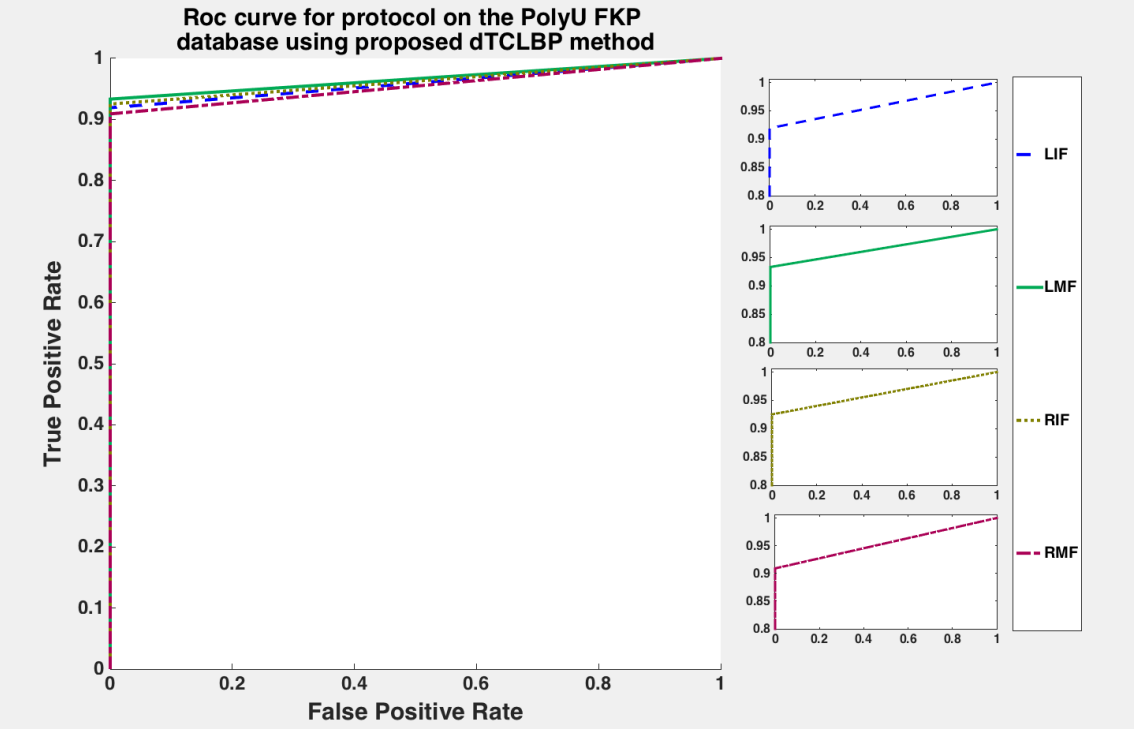

Figure 7.2: Comparison of proposed dTCLBP approach where 6 images for each type of FKPs (LIF, LMF, RIF, and RMF) were selected for training and the rest of the images used as test images

.

demonstrate that the dTCLBP method achieves an accuracy of 91.51%, which is higher than the 'Intensity+Gabor', OCLPP and GCRC methods. In the case of of RMF, dTCLBP achieves the best result with a performance accuracy of 92.02%, which is also higher than the existing 'Intensity+Gabor', OCLPP and GCRC methods.

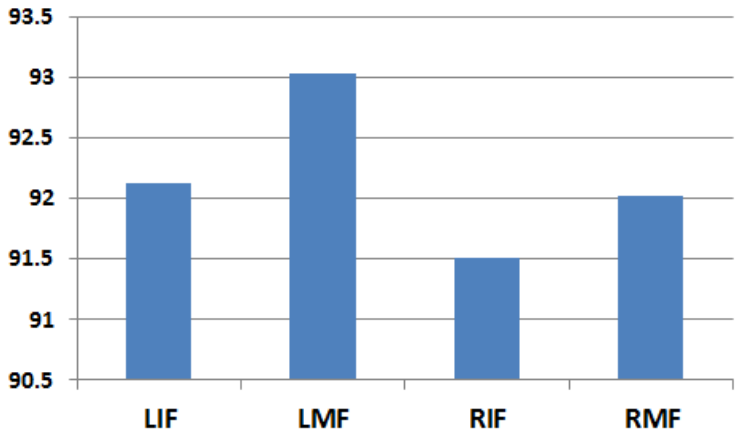

Figure 7.3: Comparison of proposed dTCLBP method for different modalities (LIF, LMF, RIF and RMF)

.

7.3 Finger knuckle print recognition based on combining the sign and magnitude features.

7.3.1 Introduction

Section 7.2.3.1 introduces the proposed dTCLBP descriptor, which has been successfully applied in the FKP recognition task. In addition, it constitutes a simplification in the implementation of the approach to extracting FKP features. The aim of this part of chapter is to focus on the improvement in the performance of the dTCLBP descriptor. The work was extended (see section 7.2) by partitioning an image of FKP into three blocks, as shown in Figure 7.4. The dTCLBP descriptor was employed to extract the FKP features from 3 blocks in the initial recognition phase. Then, SR-KDA was applied to reduce the size of the dimension of the resulting FKP feature vectors of the dTCLBP descriptor. The final step is a classification process based on the extracted FKP features, using the KNN classifier. The method was evaluated using two protocols, tested on the PolyU FKP database.

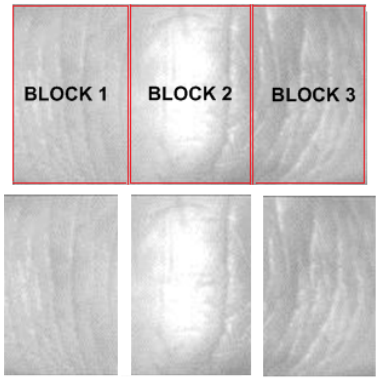

Figure 7.4: FKP ROI image divided into three blocks of 110x74 pixels

7.3.2 Proposed FKP recognition system using dTCLBP and SR-KDA methods

This section discusses the proposed FKP recognition system. Calculating dTCLBP histogram on each block of FKP image and concatenating all block features results in one long high-dimensional feature vector. This brings the problem of dimensionality to the proposed method and further more increases the computational cost. The solution to this problem is to apply SR-KDA to reduce the dimensionality of the extracted FKP feature vectors and the use of the KNN classifier for recognition. The next sections discuss the proposed FKP recognition system.

7.3.2.1 A brief review dynamic thresholds completed local binary pattern (dTCLBP)

As mentioned in section 7.2.3.1, the idea of the dTCLBP descriptor is based on two different histograms for the sign and magnitude components. The dTCLBP descriptor offers a powerful and attractive method, showing improvements in terms of the accuracy of results, as reported in section 7.2. As a brief overview, the dTCLBP feature is the combination of two features, namely $dTCLBP\_S$ and $dTCLBP\_M$. The $dTCLBP\_S$ is the same as the original LBP and is used to code the sign information of local difference, as defined in Equation 7.1. The $dTCLBP\_M$ descriptor is used to code the magnitude features by means of the λ of the dynamic thresholds that are set as $1 - \frac{min\ of\ magnitude}{max\ of\ magnitude}$ of the magnitude metrics (m_p) for the whole image. Then, the final threshold value (λ) is set to the median of the dynamic thresholds (T_P), instead of comparing the neighbours with the mean of the absolute value of the differences between a pixel and a single neighbour as used in CLBP, and compares neighbouring pixels are compared with the median of dynamic thresholds. As a reminder, here the $dTCLBP\_M$ is defined as in Equations 7.7 and 7.8.

$$dTCLBP\_M_{(P,R)} = \sum_{p=0}^{P-1} t\left(m_p, \lambda\right) 2^p$$

$$t(x, \lambda) = \begin{cases} 1 & \text{if } x \geq \lambda \\ 0 & \text{if } x < \lambda \end{cases}$$

The $dTCLBP\_S$ and $dTCLBP\_M$ histograms of the local differences are combined to create the FKP feature vector for the pattern classification process. SR-KDA is applied to reduce the size of the dimensions of the FKP feature vectors to reduce the amount of unnecessary information, thus improving the recognition performance and also speeding up the recognition process.

7.3.2.2 Recognition stage

Calculating the dTCLBP histogram on each block of FKPs and concatenating all FKP features results in one long high-dimensional feature vector; this results in a dimensionality problem for the proposed method and furthermore increases the computational cost. The solution to this problem is to apply SR-KDA to create low-dimensional feature vectors for the training and test datasets separately for each type of finger, i.e. LIF, LMF, etc. More details on the SR-KDA method are provided in section 2.4.2. This section also highlights the classification step, for which KNN technique is used to classify FKPs based on the closest trained FKP datasets created from SR-KDA (explained in detail in section 2.5.2).

7.3.3 Experiments and Results

7.3.3.1 Protocol I

The proposed approach has been assessed using the PolyU FKP database. To test the validity of the methodology, it was compared to three existing approaches. The results of the experiments are shown for the same set of training images and the same set of testing images as used for Intensity+Gabor [91], OCLPP [45], and GCRC [66]. The methods proposed for the those methods are described in section 7.2.4.

In this protocol, 6 images selected from the first session were used for the training set and 6 images from the second session were used in the testing phase. Thus, for each modality (LIF, LMF, RIF and RMF) there were 990 (165x6) training samples and 990 (165x6) test sets. In dTCLBP feature extraction, the original FKP image was divided into 3 patches of 110x74 pixels, as shown in Figure 7.4. The final dimension of the dTCLBP was 1536 (3x512). As shown in Table 7.2, the proposed approach produces outstanding results, clearly indicating that the dTCLBP method offers an attractive recognition performance rate of 96.16% in relation to the LIF. Compared to Intensity+Gabor, OCLPP and GCRC, it can be observed from Table 7.2 that in the case of the LMF, the results clearly show that the dTCLBP method obtains the best result with a rate of 97.47%. In relation to the RIF, it results in significant increases in performance of 6.57%, 9.12% and 5.05% over Intensity+Gabor, OCLPP and GCRC respectively. In addition, the experiments reveal that the dTCLBP technique achieves an accuracy of 96.77%, an improvement of 5.76-9.39% over the other methods for the RMF.

Table 7.2: Evaluation of performance of the proposed dTCLBP with state-of-the-art methods using the PolyU FKP database with 6 training samples and 6 testing samples.

Method	Recognition Rate (%)			
	LIF	LMF	RIF	RMF
Intensity+Gabor [91]	89.90	88.59	89.49	88.48
OCLPP [45]	87.87	87.49	86.94	87.38
GCRC [66]	90.51	90.40	91.01	91.01
Proposed method (dTCLBP)	**96.16**	**97.47**	**96.06**	**96.77**

7.3.3.2 Protocol II

In evaluating the accuracy of the proposed methodology, the same protocol set up was used as for Log-Gabor [73] and MSLBP [24] with 3 training and 9 testing samples for the LIF, LMF, RIF and RMF. As mentioned in sections 6.2.4.1 and 6.3.3.1 the FKP trait is filtered using the 1D Log-Gabor filter and the real and imaginary parts of each filtered image are used to form the feature vector [73]. MSLBP is the multi-scale shift local binary pattern, which is a computed set of histograms at different radii providing regional information about the FKP image and these histograms are further concatenated into a long observation vector.

The results using the KNN classifier are provided in Table 7.3. The results highlighted in bold indicate that the dTCLBP method yields improved and outstanding results compared to the other reported approaches, clearly demonstrating the advantage of the proposed method in terms of the robustness of the histogram features. With regard to the LIF,

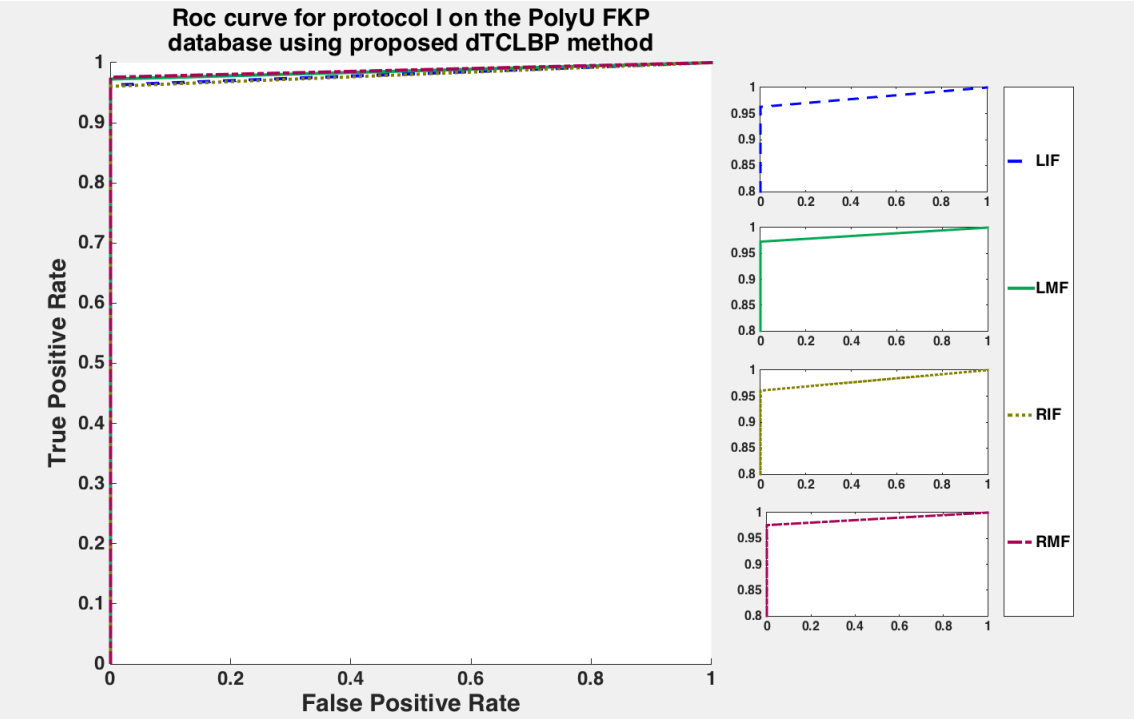

Figure 7.5: ROC curves for the proposed dTCLBP descriptor for different modalities (LIF, LMF, RIF and RMF), computed using the PolyU FKP database with 6 samples of training and 6 samples of testing.

the dTCLBP method achieves an accuracy of 93.74%, which is higher than the Log-Gabor and MSLBP methods. Compared to Log-Gabor and MSLBP, the recognition rate of the dTCLBP in relation to the LMF is promising at 96.46%. Moreover, it can be seen that in the case of the RIF and RMF, the dTCLBP method achieves the best result with rates of 95.05% and 95.25% respectively.

Table 7.3: Evaluation of performance of the proposed dTCLBP with state-of-the-art methods using the PolyU FKP database with 3 training samples and 9 testing samples.

Method	Recognition Rate (%)			
	LIF	LMF	RIF	RMF
Log-Gabor[73]	88.15	87.70	88.96	88.62
MSLBP [24]	91.58	92.19	92.05	91.04
Proposed method (dTCLBP)	**93.74**	**96.46**	**95.05**	**95.25**

7.3.4 Discussion

The proposed technique has been shown to be successful in capturing discriminative information from FKP images. This leads to significant improvements in performance compared to all other reported methods in both protocols. Tables 7.2 and 7.3 provide the results for the proposed technique with three and six training sets, clearly demonstrating the effi-

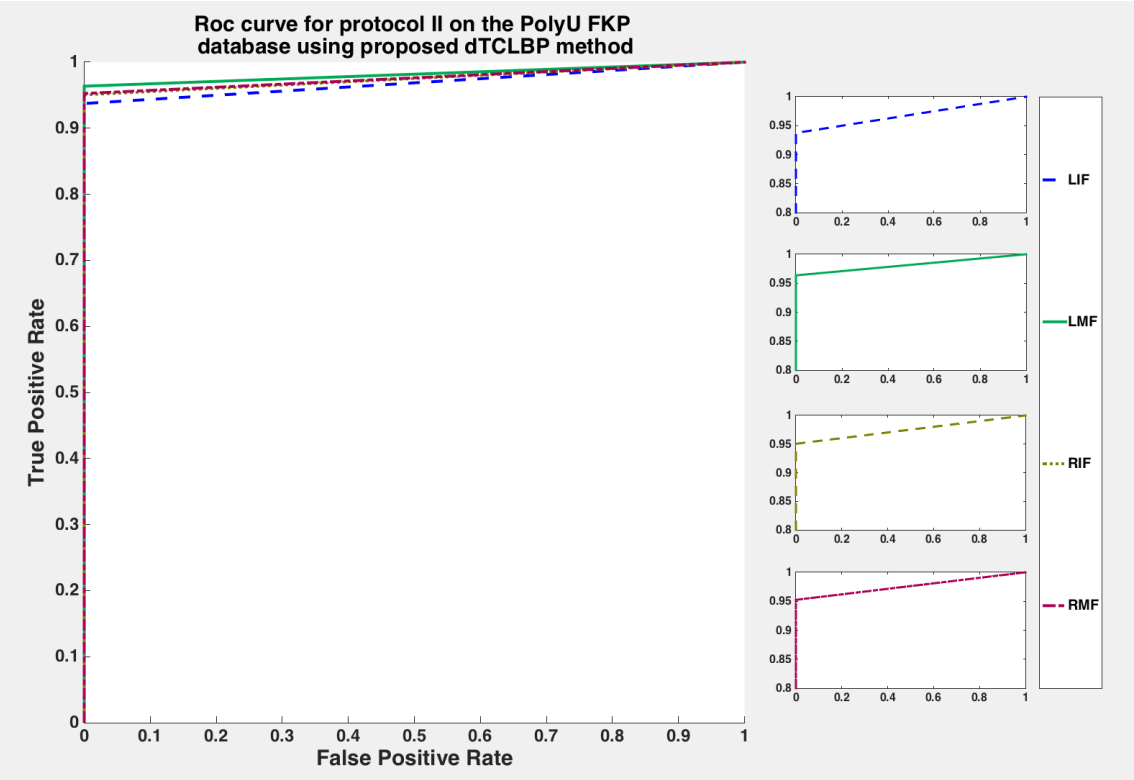

Figure 7.6: ROC curves for the proposed dTCLBP descriptor for different modalities (LIF, LMF, RIF and RMF), computed using PolyU FKP database with 3 samples of training and 9 samples of testing.

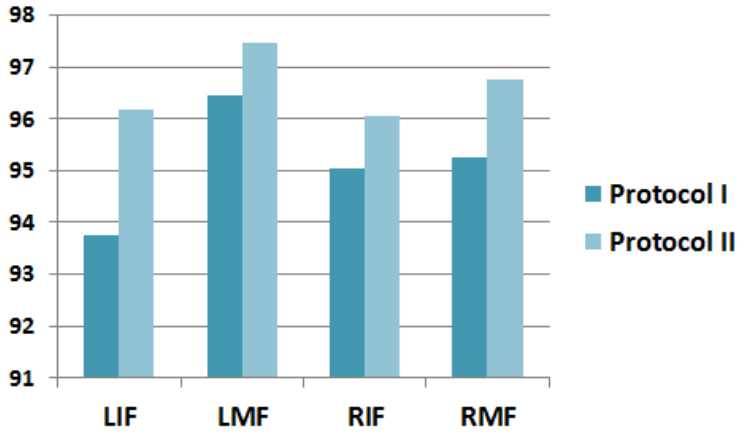

Figure 7.7: Comparison of proposed dTCLBP method for different modalities (LIF, LMF, RIF and RMF), Protocols I and II

.

ciency of the dTCLBP descriptor for FKP recognition. Experiments were performed using the FKP database, which contains 7,920 images collected from 660 different fingers. For the FKP features, the dTCLBP descriptor was generated with radius = 6 and 8 neighbours, yielding a final dimension of the dTCLBP of 512D for each patch.

The results obtained show that the proposed methodology achieves excellent performance higher than 93%, compared to existing FKP methods. It should be noted that the results of the methodology for Protocol I are slightly higher in comparison to those of Protocol II, as shown in Figure 7.7. This is because 3 training and 9 testing samples were employed for the experimentation in Protocol II, which does not provide results as good as those for the 6 training and 6 testing samples in Protocol I. The ROCs in Figures 7.5 and 7.6 plot the FAR versus the GAR rate for different FKP dataset, represented by the LIF, LMF, RIF and RMF. As can be observed from the tables and figures, the recognition rate for the LMF is better than for the other fingers.

7.4 Summary

In this chapter, the dTCLBP approach is proposed for extracting FKP features in the initial recognition phase. The dTCLBP feature is a combination of two components, sign and magnitude, where the sign component is the same as in the original LBP while the magnitude feature is encoded by the dynamic threshold.

In the first part of this chapter, PCA was used as the dimension reduction technique. The classification process is performed by applying LDA. Furthermore, the dTCLBP descriptor was evaluated on the PolyU FKP database, yielding improved results when compared to the existing methods. Experiments indicated that the most outstanding results were achieved when classification was performed for LMF.

In the second part, improvements in recognition rates were sought. To achieve this, the FKP image is partitioned into three patches. The dTCLBP approach is proposed for extracting FKP features, while SR-KDA is used to address the problem of high dimensionality associated with the dTCLBP features. The evaluation of the accuracy of the approach has shown that it achieves attractive results reaching an accuracy rates above 93% compared to other existing FKP methods. Furthermore, it has been observed that the use of six training sets in the experimentation in Protocol I yields slightly higher performance in comparison to Protocol II. The experiments indicate that the LMF outperforms other finger modalities in terms of dTCLBP features.

The proposed method has some advantages, such as the simplification of implementation and its robustness in changing image conditions. The system offered considerable improvement in the recognition performance because it benefits to keep the patterns which provide a vast majority of Local texture information. In CLBP, three operators which are CLBP_S, CLBP_M, and CLBP_C are combined in order to improve discriminative power of the original LBP operator. While in the proposed approach only two different histograms, for dTCLBP_S, and dTCLBP_M, are concatenated to form the feature vector which contains robust information for FKP biometric. This brings interesting facts of dTCLBP over CLBP that is its smaller size thus making it faster to process in a pattern classification.

Chapter 8 closes this thesis with the conclusions of the research and suggestions for future work.

Chapter 8

Conclusion and Future Work

This chapter aims to review the main contributions of this research in relation to the design of the proposed finger knuckle print and palmprint recognition system. The study has discussed developments carried out in the implementation of FKP and palmprint recognition systems and proposed solutions in the field of recognition systems.

In general, FKP and palmprint recognition is a difficult task due to inherent difficulties in pattern recognition. This is coupled with specific problems in terms of adverse conditions, such as noisy sensor data and variations in illumination and so the identification of a person with high confidence is a critical issue. Thus, one of the key challenges in improving the performance of FKP and palmprint recognition is to devise a sound coding scheme for FKP and palmprint patterns. The identification system for palmprint and FKP recognition consists of four steps: image acquisition, pre-processing, feature extraction and classification. The main contribution of this study for the development of the proposed FKP and palmprint recognition system essentially concerns the feature extraction stage. A new algorithm is proposed for this process. The study has addressed the challenges and difficulties encountered, together with experiments conducted to substantiate the theoretical concepts. This work contributes to knowledge in the area of FKP and palmprint recognition by conducting a thorough review and comparison of existing methods. New algorithms have been developed to allow the stated aims and objectives to be achieved. The research adds knowledge and techniques that are summarized below.

8.1 Summary of main contributions

Firstly, two techniques were proposed in Chapter 3 in an attempt to improve the accuracy of palmprint images recognition. The contributions of this chapter are as follows:

- The first proposed method is an extension of LBP and is based on the conventional threshold using Pascal's coefficients of order n. The main concept is to use a varying number of intervals to generate a distribution of binary codes for every pixel position, creating robust descriptors against changing image conditions. Furthermore, this method is also extended to modified the MLBP in this research, referred to as the PCMLBP descriptor, where the PCMLBP features of the different scales are first extracted and their histograms subsequently concatenated into a large feature. The evaluation of the results of the proposed PCMLBP shows that the blue spectral band outperforms the other spectral bands obtained with 3 and 6 training samples.

- This research proposes a novel scheme to determine a new set of features based on the combination of the PHOG descriptor with the PCLBP descriptor so that the histogram bins have a more powerful discriminatory capability. The evaluation of the performance of our proposed approach was conducted using the PolyU multispectral palmprint database. The results of the experiments performed demonstrate that the proposed methods achieve a high recognition rate. Evaluation of the results has shown that the PCLBP-PHOG attains a higher recognition rate and outperforms the PCMLBP and other state-of-art methods; and in particular, that the red spectral band performs better compared to other spectral palmprints.

Secondly, Chapter 4 consists of two contributions based on an information fusion technique at feature level for the palm recognition process, which can be summarized as follows:

- The first contribution introduces a novel fusion approach that combines two algorithms, LBP-HF and Gabor filter technique, to create a new palmprint feature extraction algorithm. The proposed technique is evaluated using the multispectral palmprint data available from the PolyU database, which includes the red, green, blue and NIR spectra. In addition, the proposed approach exhibits better results compared to a number of existing methods.

- In the second contribution of chapter 4 a new technique, the MSLBP approach is proposed. This involves extending the original SLBP to a multi-scale a process to obtain discriminating palmprint features. The MSLBP approach entails extracting histograms and concatenating them in a single vector. However, this approach results in an extremely high number of palmprint features and this can result in an overfitting problem for classification. In this study, the performance of the proposed approach is evaluated by employing the public multispectral palmprint database available from the PolyU. Extensive experiments clearly demonstrate the superiority of the proposed approach compared to state-of-the-art methods.

Thirdly, Chapter 6 proposed novel techniques which are modified versions of the LBP method for FKP-based person recognition. These contributions are summarized below:

- The first part of chapter 6 discusses the use of the MSLBP descriptor-based method in FKP recognition to analyse its performance. Experiments were conducted using an FKP database consisting of 7,920 images from 660 different fingers. The results obtained show that the proposed FKP recognition method achieves an excellent recognition rate of up to 94%. Furthermore, it has been observed that MSLBP for the right middle finger (RMF) outperforms other finger modalities for six training samples and the left middle finger (LMF) performs better for three training samples.

- Two new techniques were proposed in the first part of chapter 6 in an attempt to improve the accuracy of the FKP recognition system. These two proposed techniques are modified versions of the LBP method: one employs a thresholding scheme based on sequence Fibonacci values to compute the image descriptor, enabling optimal performance in terms of classification, while the second uses a multi-scale FSLBP. The use of Fibonacci numbers of n order is considered to generate a distribution of binary codes at every pixel position, thus creating descriptors that are robust against variations in the lighting of FKP images. Both methods were evaluated on the publicly available

PolyU FKP database, yielding improved - indeed outstanding - recognition performance compared to other existing techniques. The results show that the recognition rate is quite high with FSMLBP compared to FSLBP for all fingers.

Finally, Chapter 7 is concerned with a modification to the CLBP method to be used as a powerful discriminatory texture descriptor in biometric trait analysis. It is composed of two parts, which are summarized below:

- In the first part of chapter 7, a new feature set inspired by the CLBP, known as the dTCLBP, is proposed for FKP recognition. First, the dTCLBP descriptor is applied as a basic feature in the initial recognition phase. The dTCLBP feature is the combination of two components, sign and magnitude, where the sign component is the same as the original LBP, while the magnitude feature is encoded by the dynamic threshold. To evaluate the recognition performance of the proposed approach, analysis was conducted using the FKP database available from the PolyU. A significant improvement in recognition performance was achieved compared to existing FKP recognition methods.

- The proposed method in the first part of Chapter 7 was again applied, focusing on improving the performance of the dTCLBP descriptor. The dTCLBP descriptor was applied to extract the FKP features from 3 blocks in the initial recognition phase. The evaluation of the results with segmented images (3 blocks) has shown that the proposed approach yields slightly higher performance in comparison to state-of-the-art methods.

8.2 Future work

1. The fusion of multi-modal biometric approaches has attracted increasing attention and interest among researchers. It is easy to implement and can be integrated to enhance the performance of biometric recognition systems. Many fusion schemes have been studied to achieve this aim. These methods have been evaluated for separate features of palmprint and FKP image. Fusion can be performed using different methods and there are various possible areas for future work in validating the performance of the proposed approach, such as the following:

    - combining the left and right FKP images, or combining palmprint spectra, where the idea of image fusion refers to the concept of combining information from several images to obtain better computational perspectives;
    - investigating the fusion of two kinds of biometrics: one comprises biometric features that are representations of contactless biometrics such as face, gait, or ear; another consists of image features typical of contact biometrics like fingerprints, FKPs, or palmprints.

2. The proposed multi-feature descriptors that result in the problem of dimensionality are a major barrier to multi-scale approaches. This feature selection study is the first step towards identifying a subset of the most representative features for the correct and accurate representation of an image. The initial results support the notion that even the first few runs of feature concatenation result in the reduction of variance among recognition rates on different scales. However, in the future, other feature

selection strategies may be employed, for example heuristic or greedy approaches, to investigate the effect of feature selection at different scales or radii of multi-scale approaches.

3. Ensemble learning is based on the fusion of a set of weak classifiers to build up a strong classifier. These weak classifiers do not always make the same levels of error, so the overall error of the fused classifier is lower than that of each individual weak classifier. In Chapters 3 and 6, an ensemble learning framework was applied which combines multiple LDA classifiers, each using different random sets of features. The results indicate that this leads to a significant increase in recognition rates compared to the individual LDA classifier. In this technique, there are a number of possible areas for future work:

    - using an ensemble framework which combines different types of classifier;
    - creating a stronger ensemble by combining different methods in a single framework in the classification process in the image pre-processing, feature extraction or matching stages.

4. Statistical probability measures defined by latent variable analysis (LVA) lead to greater accuracy in recognition systems and have been used successfully for different classification and pattern recognition applications such as face detection. In this study, the implementation of LVA is recommended as it might yield optimal performance in identifying FKPs and palmprints

5. The biometric system depends on partial-to-full palmprint image matching in some fields, for example in forensics, in which it is more usual to detect partial and noisy palmprint images. An important problem is that, when the full palmprint is not captured, there is an extreme reduction in precision. For this reason, it is recommended that future work investigates the methods proposed in this research as being highly effective in noisy partial-to-full palmprint recognition.

6. Machine learning systems are used to recognize objects in images, match news items, posts or products with users interests, and select relevant results of search. Increasingly, these applications make use of a class of techniques called deep learning. Deep learning methods are representation learning methods with multiple levels of representation, obtained by composing simple but non-linear modules that each transform the representation at one level (starting with the raw input) into a representation at a higher, slightly more abstract level. With the composition of a number of transformations, very complex functions can be learned. For classification tasks, higher layers of representation amplify aspects of the input that are important for discrimination and suppress irrelevant variations. The deep learning dramatically improved the state-of-the-art in biometric recognition, visual object recognition, object detection and many other domains such as drug discovery and genomics. The challenge is to enhance accuracy and maintain the classification speed simultaneously. We expect much of the future progress using deep learning in palmprint or FKP in classification tasks in order to produce impressive results.

References

[1] Mir AH, Rubab S, and Jhat ZA. Biometrics verification: a literature survey. *International Journal of Computing and ICT Research*, 5(2):67–80, 2011.

[2] Mounir Amraoui, Mohamed El Aroussi, Rachid Saadane, and MOHAMMED WAHBI. Finger-knuckle-print recognition based on local and global feature sets. *Journal of Theoretical & Applied Information Technology*, 46(1), 2012.

[3] Shoichiro Aoyama, Koichi Ito, and Takafumi Aoki. A finger-knuckle-print recognition algorithm using phase-based local block matching. *Information Sciences*, 268:53–64, 2014.

[4] GS Badrinath, Naresh K Kachhi, and Phalguni Gupta. Verification system robust to occlusion using low-order zernike moments of palmprint sub-images. *Telecommunication Systems*, 47(3-4):275–290, 2011.

[5] GS Badrinath, Kamlesh Tiwari, and Phalguni Gupta. An efficient palmprint based recognition system using 1d-dct features. In *International Conference on Intelligent Computing*, pages 594–601. Springer, 2012.

[6] WW Boles and SYT Chu. Personal identification using images of the human palm. In *TENCON'97. IEEE Region 10 Annual Conference. Speech and Image Technologies for Computing and Telecommunications., Proceedings of IEEE*, volume 1, pages 295–298. IEEE, 1997.

[7] Anna Bosch, Andrew Zisserman, and Xavier Munoz. Representing shape with a spatial pyramid kernel. In *Proceedings of the 6th ACM international conference on Image and video retrieval*, pages 401–408. ACM, 2007.

[8] Meriem Dorsaf Bounneche, Larbi Boubchir, Ahmed Bouridane, Bachir Nekhoul, and Arab Ali-Chérif. Multi-spectral palmprint recognition based on oriented multiscale log-gabor filters. *Neurocomputing*, 205:274–286, 2016.

[9] Ioan Buciu and Alexandru Gacsadi. Biometrics systems and technologies: A survey. *International Journal of Computers Communications & Control*, 11(3):315–330, 2016.

[10] Deng Cai, Xiaofei He, and Jiawei Han. Efficient kernel discriminant analysis via spectral regression. In *Seventh IEEE International Conference on Data Mining (ICDM 2007)*, pages 427–432. IEEE, 2007.

[11] Mary Cannon, Majella Byrne, David Cotter, Pak Sham, Conall Larkin, and Eadbhard O'Callaghan. Further evidence for anomalies in the hand-prints of patients with

schizophrenia: a study of secondary creases. *Schizophrenia Research*, 13(2):179–184, 1994.

[12] Chi-Ho Chan, Josef Kittler, and Kieron Messer. Multi-scale local binary pattern histograms for face recognition. In *International Conference on Biometrics*, pages 809–818. Springer, 2007.

[13] Atul S Chaudhari, Girish K Patnaik, and Sandip S Patil. Implementation of minutiae based fingerprint identification system using crossing number concept. *Informatica Economica*, 18(1):17, 2014.

[14] GY Chen, Tien D Bui, and Adam Krzyzak. Palmprint classification using dual-tree complex wavelets. In *Image Processing, 2006 IEEE International Conference on*, pages 2645–2648. IEEE, 2006.

[15] GY Chen and Balázs Kégl. Palmprint classification using contourlets. In *Systems, Man and Cybernetics, 2007. ISIC. IEEE International Conference on*, pages 1003–1007. IEEE, 2007.

[16] GY Chen and Balázs Kégl. Invariant pattern recognition using contourlets and adaboost. *Pattern Recognition*, 43(3):579–583, 2010.

[17] Jiansheng Chen, Yiu-Sang Moon, Ming-Fai Wong, and Guangda Su. Palmprint authentication using a symbolic representation of images. *Image and Vision Computing*, 28(3):343–351, 2010.

[18] Yong Jian Chin, Thian Song Ong, Michael KO Goh, and Bee Yan Hiew. Integrating palmprint and fingerprint for identity verification. In *Network and System Security, 2009. NSS'09. Third International Conference on*, pages 437–442. IEEE, 2009.

[19] Michał Choras and Rafał Kozik. Knuckle biometrics based on texture features. In *2010 International Workshop on Emerging Techniques and Challenges for Hand-Based Biometrics*, 2010.

[20] John G Daugman. Biometric personal identification system based on iris analysis, March 1 1994. US Patent 5,291,560.

[21] Reza Davarzani, S Mozaffari, and Kh Yaghmaie. Image authentication using lbp-based perceptual image hashing. *Journal of AI and Data Mining*, 3(1):20–29, 2015.

[22] Rafael M Diaz, Carlos M Travieso, Jestis B Alonso, and Miguel A Ferrer. Biometric system based in the feature of hand palm. In *Security Technology, 2004. 38th Annual 2004 International Carnahan Conference on*, pages 136–139. IEEE, 2004.

[23] Feng Du, Pengfei Yu, Hongsong Li, and Liqing Zhu. Palmprint recognition using gabor feature-based bidirectional 2dlda. In *Computer Science for Environmental Engineering and EcoInformatics*, pages 230–235. Springer, 2011.

[24] Wafa El-Tarhouni, Muhammad K Shaikh, Larbi Boubchir, and Ahmed Bouridane. Multi-scale shift local binary pattern based-descriptor for finger-knuckle-print recognition. In *Microelectronics (ICM), 2014 26th International Conference on*, pages 184–187. IEEE, 2014.

[25] Ricardo J Ferrari, Rangaraj M. Rangayyan, JE Leo Desautels, and Annie France Frère. Analysis of asymmetry in mammograms via directional filtering with gabor wavelets. *Medical Imaging, IEEE Transactions on*, 20(9):953–964, 2001.

[26] Keinosuke Fukunaga. *Introduction to statistical pattern recognition*. Academic press, 2013.

[27] Dennis Gabor. Theory of communication. part 1: The analysis of information. *Journal of the Institution of Electrical Engineers-Part III: Radio and Communication Engineering*, 93(26):429–441, 1946.

[28] Jun-ying Gan and Dang-pei Zhou. A novel method for palmprint recognition based on wavelet transform. In *Signal Processing, 2006 8th International Conference on*, volume 3. IEEE, 2006.

[29] Guangwei Gao, Jian Yang, Jianjun Qian, and Lin Zhang. Integration of multiple orientation and texture information for finger-knuckle-print verification. *Neurocomputing*, 135:180–191, 2014.

[30] Guangwei Gao, Lei Zhang, Jian Yang, Lin Zhang, and David Zhang. Reconstruction based finger-knuckle-print verification with score level adaptive binary fusion. *IEEE transactions on image processing*, 22(12):5050–5062, 2013.

[31] Abdellah Guebla, Abdallah Meraoumia, Hakim Bendjenna, and Salim Chitroub. Using of finger-knuckle-print in biometric security systems. In *Information Technology for Organizations Development (IT4OD), 2016 International Conference on*, pages 1–5. IEEE, 2016.

[32] Xiumei Guo, Weidong Zhou, and Yanli Zhang. Collaborative representation with hm-lbp features for palmprint recognition. *Machine Vision and Applications*, 28(3-4):283–291, 2017.

[33] Zhenhua Guo, David Zhang, Lei Zhang, and Wangmeng Zuo. Palmprint verification using binary orientation co-occurrence vector. *Pattern Recognition Letters*, 30(13):1219–1227, 2009.

[34] Zhenhua Guo, Lei Zhang, and David Zhang. A completed modeling of local binary pattern operator for texture classification. *Image Processing, IEEE Transactions on*, 19(6):1657–1663, 2010.

[35] Zhenhua Guo, Lei Zhang, and David Zhang. Rotation invariant texture classification using lbp variance (lbpv) with global matching. *Pattern recognition*, 43(3):706–719, 2010.

[36] Zhenhua Guo, Lei Zhang, David Zhang, and Xuanqin Mou. Hierarchical multiscale lbp for face and palmprint recognition. In *2010 IEEE International Conference on Image Processing*, pages 4521–4524. IEEE, 2010.

[37] Adel Hafiane, Guna Seetharaman, Kannappan Palaniappan, and Bertrand Zavidovique. Rotationally invariant hashing of median binary patterns for texture classification. In *International Conference Image Analysis and Recognition*, pages 619–629. Springer, 2008.

[38] Chin-Chuan Han, Hsu-Liang Cheng, Chih-Lung Lin, and Kuo-Chin Fan. Personal authentication using palm-print features. *Pattern recognition*, 36(2):371–381, 2003.

[39] Dewen Hu, Guiyu Feng, and Zongtan Zhou. Two-dimensional locality preserving projections (2dlpp) with its application to palmprint recognition. *Pattern recognition*, 40(1):339–342, 2007.

[40] De-Shuang Huang, Wei Jia, and David Zhang. Palmprint verification based on principal lines. *Pattern Recognition*, 41(4):1316–1328, 2008.

[41] Koichi Ito, Takafumi Aoki, Hiroshi Nakajima, Koji Kobayashi, and Tatsuo Higuchi. A phase-based palmprint recognition algorithm and its experimental evaluation. In *Intelligent Signal Processing and Communications, 2006. ISPACS'06. International Symposium on*, pages 215–218. IEEE, 2006.

[42] Anil K Jain and Jianjiang Feng. Latent palmprint matching. *Pattern Analysis and Machine Intelligence, IEEE Transactions on*, 31(6):1032–1047, 2009.

[43] Ankur Jain, Richa Gupta, and Madasu Hanmandlu. Finger knuckle print based authentication. In *Proceedings of the International Conference on Image Processing, Computer Vision, and Pattern Recognition (IPCV)*, page 1. The Steering Committee of The World Congress in Computer Science, Computer Engineering and Applied Computing (WorldComp), 2012.

[44] Wei Jia, De-Shuang Huang, and David Zhang. Palmprint verification based on robust line orientation code. *Pattern Recognition*, 41(5):1504–1513, 2008.

[45] Xiaoyuan Jing, Wenqian Li, Chao Lan, Yongfang Yao, Xi Cheng, and Lu Han. Orthogonal complex locality preserving projections based on image space metric for finger-knuckle-print recognition. In *Hand-Based Biometrics (ICHB), 2011 International Conference on*, pages 1–6. IEEE, 2011.

[46] Sincy John and Kumudha Raimond. A survey on feature extraction techniques for palmprint identification. *Editorial Committees*, page 20.

[47] Usha K and Ezhilarasan M. Personal recognition using finger knuckle shape oriented features and texture analysis. *Journal of King Saud University-Computer and Information Sciences*, 2015.

[48] HB Kekre and VA Bharadi. Finger-knuckle-print verification using kekre's wavelet transform. In *Proceedings of the International Conference & Workshop on Emerging Trends in Technology*, pages 32–37. ACM, 2011.

[49] Emad Khalifa, Somaya Al-Maadeed, Muhammad Atif Tahir, Ahmed Bouridane, and A Jamshed. Off-line writer identification using an ensemble of grapheme codebook features. *Pattern Recognition Letters*, 59:18–25, 2015.

[50] Rizwan Ahmed Khan, Alexandre Meyer, Hubert Konik, and Saida Bouakaz. Human vision inspired framework for facial expressions recognition. In *2012 19th IEEE International Conference on Image Processing (ICIP)*, pages 2593–2596. IEEE, 2012.

[51] Choge H Kipsang, Tadahiro Oyama, Stephen Karungaru, Satoru Tsuge, and Minoru Fukumi. Palmprint recognition based on local dct feature extraction. In *Neural Information Processing*, pages 639–648. Springer, 2009.

[52] Adams Kong, David Zhang, and Mohamed Kamel. Palmprint identification using feature-level fusion. *Pattern Recognition*, 39(3):478–487, 2006.

[53] Adams Kong, David Zhang, and Mohamed Kamel. A survey of palmprint recognition. *pattern recognition*, 42(7):1408–1418, 2009.

[54] Adams Wai-Kin Kong and David Zhang. Competitive coding scheme for palmprint verification. In *Pattern Recognition, 2004. ICPR 2004. Proceedings of the 17th International Conference on*, volume 1, pages 520–523. IEEE, 2004.

[55] Wai Kin Kong and David Zhang. Palmprint texture analysis based on low-resolution images for personal authentication. In *Pattern Recognition, 2002. Proceedings. 16th International Conference on*, volume 3, pages 807–810. IEEE, 2002.

[56] Ajay Kumar. Can we use minor finger knuckle images to identify humans? In *Biometrics: Theory, Applications and Systems (BTAS), 2012 IEEE Fifth International Conference on*, pages 55–60. IEEE, 2012.

[57] Ajay Kumar. Importance of being unique from finger dorsal patterns: Exploring minor finger knuckle patterns in verifying human identities. *IEEE Transactions on Information Forensics and Security*, 9(8):1288–1298, 2014.

[58] Ajay Kumar and Ch Ravikanth. Personal authentication using finger knuckle surface. *Information Forensics and Security, IEEE Transactions on*, 4(1):98–110, 2009.

[59] Ludmila I Kuncheva, James C Bezdek, and Robert PW Duin. Decision templates for multiple classifier fusion: an experimental comparison. *Pattern recognition*, 34(2):299–314, 2001.

[60] Ludmila I Kuncheva and Christopher J Whitaker. Measures of diversity in classifier ensembles and their relationship with the ensemble accuracy. *Machine learning*, 51(2):181–207, 2003.

[61] SY Kung, Shang-IIung Lin, and Ming Fang. A neural network approach to face/palm recognition. In *Neural Networks for Signal Processing [1995] V. Proceedings of the 1995 IEEE Workshop*, pages 323–332. IEEE, 1995.

[62] Gustaf Kylberg and Ida-Maria Sintorn. Evaluation of noise robustness for local binary pattern descriptors in texture classification. *EURASIP Journal on Image and Video Processing*, 2013(1):1–20, 2013.

[63] Lovasz L, Pelikan J, and Vesztergombi K. Binomial coefficients and pascals triangle. In *Discrete Mathematics*, pages 43–64. Springer, 2003.

[64] Eui Chul Lee, Hyunwoo Jung, and Daeyeoul Kim. New finger biometric method using near infrared imaging. *Sensors*, 11(3):2319–2333, 2011.

[65] Maylor KH Leung, Alvis Cheuk M Fong, and Siu Cheung Hui. Palmprint verification for controlling access to shared computing resources. *Pervasive Computing, IEEE*, 6(4):40–47, 2007.

[66] Fei Li, Mingyan Jiang, Xianye Ben, Tingting Pan, and Menglei Sun. Group collaborative representation with l2 norm regularization in finger-knuckle-print recognition. *Journal of Computational Information Systems*, 11(3):1053–1062, 2015.

[67] Jing Li, Jian Cao, and Kaixuan Lu. Improve the two-phase test samples representation method for palmprint recognition. *Optik-International Journal for Light and Electron Optics*, 124(24):6651–6656, 2013.

[68] Peng Li and Simon JD Prince. Probabilistic methods for face registration and recognition. *Advances in Face Image Analysis: Techniques and Technologies: Techniques and Technologies*, page 178, 2010.

[69] Wenxin Li, David Zhang, and Zhuoqun Xu. Palmprint identification by fourier transform. *International Journal of Pattern Recognition and Artificial Intelligence*, 16(04):417–432, 2002.

[70] Laura Liu and David Zhang. Palm-line detection. In *Image Processing, 2005. ICIP 2005. IEEE International Conference on*, volume 3, pages III269–III272. IEEE, 2005.

[71] Guangming Lu, David Zhang, and Kuanquan Wang. Palmprint recognition using eigenpalms features. *Pattern Recognition Letters*, 24(9):1463–1467, 2003.

[72] Abdallah Meraoumia, Salim Chitroub, and Ahmed Bouridane. Fusion of multispectral palmprint images for automatic person identification. In *Electronics, Communications and Photonics Conference (SIECPC), 2011 Saudi International*, pages 1–6. IEEE, 2011.

[73] Abdallah Meraoumia, Salim Chitroub, and Ahmed Bouridane. Palmprint and finger-knuckle-print for efficient person recognition based on log-gabor filter response. *Analog Integrated Circuits and Signal Processing*, 69(1):17–27, 2011.

[74] Abdallah Meraoumia, Salim Chitroub, and Ahmed Bouridane. An efficient multispectral palmprint identification system using radial basis function. In *New Circuits and Systems Conference (NEWCAS), 2013 IEEE 11th International*, pages 1–4. IEEE, 2013.

[75] Goh Kah Ong Michael, Tee Connie, and Andrew Beng Jin Teoh. Touch-less palm print biometrics: Novel design and implementation. *Image and Vision Computing*, 26(12):1551–1560, 2008.

[76] S Nagaraja, CJ Prabhakar, and PU Praveen Kumar. Complete local binary pattern for representation of facial expression based on curvelet transform. In *International Conference on Multimedia Processing, Communication and Information Technology (MPCIT)*, pages 48–56, 2013.

[77] Loris Nanni, Sheryl Brahnam, and Alessandra Lumini. A simple method for improving local binary patterns by considering non-uniform patterns. *Pattern Recognition*, 45(10):3844–3852, 2012.

[78] R Nathiya, B Shanmugapriya, G Sivaseema, and J Priyadharshini. Dorsal fingerprint patterns using lbp and gabor for identifying human identities. 2015.

[79] Shubhangi Neware, Kamal Mehta, and AS Zadgaonkar. Finger knuckle identification using principal component analysis and nearest mean classifier. *International Journal of Computer Applications*, 70(9), 2013.

[80] Shubhangi Neware, Kamal Mehta, and AS Zadgaonkar. Finger knuckle print identification using gabor features. *International Journal of Computer Applications*, 98(18), 2014.

[81] Aditya Nigam and Phalguni Gupta. Finger knuckleprint based recognition system using feature tracking. In *Chinese Conference on Biometric Recognition*, pages 125–132. Springer, 2011.

[82] Jin Soo Noh and Kang Hyeon Rhee. Palmprint identification algorithm using hu invariant moments and otsu binarization. In *Computer and Information Science, 2005. Fourth Annual ACIS International Conference on*, pages 94–99. IEEE, 2005.

[83] Timo Ojala, Matti Pietikainen, and Topi Maenpaa. Multiresolution gray-scale and rotation invariant texture classification with local binary patterns. *IEEE Transactions on pattern analysis and machine intelligence*, 24(7):971–987, 2002.

[84] Tunkpien P, Panduwadeethorn S, and Phimoltares S. Compact extraction of principle lines in palmprint using consecutive filtering operations. *Proc of the Second International Conference on Knowledge and Smart Technologies*, pages 39–44, 2010.

[85] Xin Pan and Qiu-Qi Ruan. Palmprint recognition using gabor feature-based (2d) 2 pca. *Neurocomputing*, 71(13):3032–3036, 2008.

[86] Ying-Hun Pang, Tee Connie, Andrew Teoh Beng Jin, and David Ngo Chek Ling. Palmprint authentication with zernike moment invariants. In *Signal Processing and Information Technology, 2003. ISSPIT 2003. Proceedings of the 3rd IEEE International Symposium on*, pages 199–202. IEEE, 2003.

[87] Young Ho Park, Dat Nguyen Tien, Hyeon Chang Lee, Kang Ryoung Park, Eui Chul Lee, Sung Min Kim, and Ho Chul Kim. A multimodal biometric recognition of touched fingerprint and finger-vein. In *Multimedia and Signal Processing (CMSP), 2011 International Conference on*, volume 1, pages 247–250. IEEE, 2011.

[88] RD Raut, Santosh Kulkarni, and Neha N Gharat. Biometric authentication using kekre's wavelet transform. In *Electronic Systems, Signal Processing and Computing Technologies (ICESC), 2014 International Conference on*, pages 99–104. IEEE, 2014.

[89] Alessandro Riera, Aureli Soria-Frisch, Mario Caparrini, Ivan Cester, and Giulio Ruffini. Multimodal physiological biometrics authentication. *Biometrics: Theory, Methods, and Applications*, pages 461–482, 2009.

[90] Haifeng Sang, Weiqi Yuan, and Zhijia Zhang. Research of palmprint recognition based on 2dpca. In *Advances in Neural Networks–ISNN 2009*, pages 831–838. Springer, 2009.

[91] Zahra S Shariatmadar and Karim Faez. An efficient method for finger-knuckle-print recognition by using the information fusion at different levels. In *Hand-Based Biometrics (ICHB), 2011 International Conference on*, pages 1–6. IEEE, 2011.

[92] Zahra S Shariatmadar and Karim Faez. Finger-knuckle-print recognition via encoding local-binary-pattern. *Journal of Circuits, Systems, and Computers*, 22(06):1350050, 2013.

[93] Hongbin Shen and Kuo-Chen Chou. Using optimized evidence-theoretic k-nearest neighbor classifier and pseudo-amino acid composition to predict membrane protein types. *Biochemical and biophysical research communications*, 334(1):288–292, 2005.

[94] Suprosanna Shit, Subhadeep Datta, Srijata Chakravorti, Soumi Bandopadhyay, and Amitava Chatterjee. Palmprint authentication technique using fuzzy embedded radon transform and collaborative representation based classifier. In *Communications and Signal Processing (ICCSP), 2015 International Conference on*, pages 0545–0549. IEEE, 2015.

[95] Wei Shu and David Zhang. Palmprint verification: an implementation of biometric technology. In *Pattern Recognition, 1998. Proceedings. Fourteenth International Conference on*, volume 1, pages 219–221. IEEE, 1998.

[96] Zhao Song, Xu Yan, and Liu YuanPeng. Palmprint verification based on orthogonal code. In *Information and Computing (ICIC), 2010 Third International Conference on*, volume 3, pages 221–224. IEEE, 2010.

[97] MR Swati and M Ravishankar. Finger knuckle print recognition based on gabor feature and kpca+ lda. In *Emerging Trends in Communication, Control, Signal Processing & Computing Applications (C2SPCA), 2013 International Conference on*, pages 1–5. IEEE, 2013.

[98] Deepti Tamrakar and Pritee Khanna. Occlusion invariant palmprint recognition with ulbp histograms. *Procedia Computer Science*, 54:491–500, 2015.

[99] Deepti Tamrakar and Pritee Khanna. Palmprint verification with xor-sum code. *Signal, image and video processing*, 9(3):535–542, 2015.

[100] Wu W, Mallet Y, Walczak B, Penninckx W, Massart DL, Heuerding S, and Erni F. Comparison of regularized discriminant analysis linear discriminant analysis and quadratic discriminant analysis applied to nir data. *Analytica Chimica Acta*, 329(3):257–265, 1996.

[101] Xiaogang Wang and Xiaoou Tang. Random sampling for subspace face recognition. *International Journal of Computer Vision*, 70(1):91–104, 2006.

[102] Yanxia Wang and Qiuqi Ruan. Kernel fisher discriminant analysis for palmprint recognition. In *Pattern Recognition, 2006. ICPR 2006. 18th International Conference on*, volume 4, pages 457–460. IEEE, 2006.

[103] Yanxia Wang and Qiuqi Ruan. Palm-line extraction using steerable filters. In *Signal Processing, 2006 8th International Conference on*, volume 3. IEEE, 2006.

[104] Damon L Woodard and Patrick J Flynn. Finger surface as a biometric identifier. *Computer Vision and Image Understanding*, 100(3):357–384, 2005.

[105] Xiang-Qian Wu, Kuan-Quan Wang, and David Zhang. Approach to line feature representation and matching for palmprint recognition. *Ruan Jian Xue Bao/Journal of Software*, 2004.

[106] Xiangqian Wu, Kuanquan Wang, and David Zhang. Hmms based palmprint identification. In *Biometric Authentication*, pages 775–781. Springer, 2004.

[107] Xiangqian Wu, Kuanquan Wang, and David Zhang. Palmprint texture analysis using derivative of gaussian filters. In *Computational Intelligence and Security, 2006 International Conference on*, volume 1, pages 751–754. IEEE, 2006.

[108] Xiangqian Wu, David Zhang, and Kuanquan Wang. Fisherpalms based palmprint recognition. *Pattern recognition letters*, 24(15):2829–2838, 2003.

[109] Xiangqian Wu, David Zhang, and Kuanquan Wang. Palm line extraction and matching for personal authentication. *Systems, Man and Cybernetics, Part A: Systems and Humans, IEEE Transactions on*, 36(5):978–987, 2006.

[110] Niyogi X. Locality preserving projections. In *Neural information processing systems*, volume 16, page 153. MIT, 2004.

[111] Xingpeng Xu, Zhenhua Guo, Changjiang Song, and Yafeng Li. Multispectral palmprint recognition using a quaternion matrix. *Sensors*, 12(4):4633–4647, 2012.

[112] Xuebin Xu, Longbin Lu, Xinman Zhang, Huimin Lu, and Wanyu Deng. Multispectral palmprint recognition using multiclass projection extreme learning machine and digital shearlet transform. *Neural Computing and Applications*, 27(1):143–153, 2016.

[113] Yong Xu, Qi Zhu, Zizhu Fan, Minna Qiu, Yan Chen, and Hong Liu. Coarse to fine k nearest neighbor classifier. *Pattern recognition letters*, 34(9):980–986, 2013.

[114] Wankou Y., Changyin S., and Zhongxi S. Finger-knuckle-print recognition using gabor feature and olda. In *2011 30th Chinese Control Conference (CCC)*, pages 2975–2978, 2011.

[115] Masaaki Yamanaka et al. Personal authentication using feature points on finger and palmar creases. In *Applied Imagery Pattern Recognition Workshop, 2003. Proceedings. 32nd*, pages 282–287. IEEE, 2003.

[116] Wang-li Yang and Li-li Wang. Research of palmprint identification method using zernike moment and neural network. In *Natural Computation (ICNC), 2010 Sixth International Conference on*, volume 3, pages 1310–1313. IEEE, 2010.

[117] Jun Yin, Jingbo Zhou, Zhong Jin, and Jian Yang. Weighted linear embedding and its applications to finger-knuckle-print and palmprint recognition. In *Emerging Techniques and Challenges for Hand-Based Biometrics (ETCHB), 2010 International Workshop on*, pages 1–4. IEEE, 2010.

[118] Peng Fei Yu, Hao Zhou, and Hai Yan Li. Personal identification using finger-knuckle-print based on local binary pattern. In *Applied Mechanics and Materials*, volume 441, pages 703–706. Trans Tech Publ, 2014.

[119] Yibin Yu, Yaofang Tang, Jinguo Cao, and JunYing Gan. Multispectral palmprint recognition using score-level fusion. In *Green Computing and Communications (GreenCom), 2013 IEEE and Internet of Things (iThings/CPSCom), IEEE International Conference on and IEEE Cyber, Physical and Social Computing*, pages 1450–1453. IEEE, 2013.

[120] Feng Yue, Wangmeng Zuo, David Zhang, and Kuanquan Wang. Orientation selection using modified fcm for competitive code-based palmprint recognition. *Pattern recognition*, 42(11):2841–2849, 2009.

[121] David Zhang, Zhenhua Guo, Guangming Lu, and Wangmeng Zuo. An online system of multispectral palmprint verification. *IEEE Transactions on Instrumentation and Measurement*, 59(2):480–490, 2010.

[122] David Zhang, Wai-Kin Kong, Jane You, and Michael Wong. Online palmprint identification. *Pattern Analysis and Machine Intelligence, IEEE Transactions on*, 25(9):1041–1050, 2003.

[123] David D Zhang. *Automated biometrics: Technologies and systems*, volume 7. Springer Science & Business Media, 2013.

[124] Huan Zhang. A fast palmprint verification system based on fractal coding. *International Journal of Information Acquisition*, 9(01):1250003, 2013.

[125] Lei Zhang and Lei Zhang. Characterization of palmprints by wavelet signatures via directional context modeling. *Systems, Man, and Cybernetics, Part B: Cybernetics, IEEE Transactions on*, 34(3):1335–1347, 2004.

[126] Lin Zhang, Hongyu Li, and Ying Shen. A novel riesz transforms based coding scheme for finger-knuckle-print recognition. In *Hand-Based Biometrics (ICHB), 2011 International Conference on*, pages 1–6. IEEE, 2011.

[127] Lin Zhang, Lei Zhang, and David Zhang. Finger-knuckle-print: a new biometric identifier. In *2009 16th IEEE International Conference on Image Processing (ICIP)*, pages 1981–1984. IEEE, 2009.

[128] Lin Zhang, Lei Zhang, and David Zhang. Monogeniccode: A novel fast feature coding algorithm with applications to finger-knuckle-print recognition. In *Emerging Techniques and Challenges for Hand-Based Biometrics (ETCHB), 2010 International Workshop on*, pages 1–4. IEEE, 2010.

[129] Lin Zhang, Lei Zhang, David Zhang, and Hailong Zhu. Online finger-knuckle-print verification for personal authentication. *Pattern recognition*, 43(7):2560–2571, 2010.

[130] Lin Zhang, Lei Zhang, David Zhang, and Hailong Zhu. Online finger-knuckle-print verification for personal authentication. *Pattern recognition*, 43(7):2560–2571, 2010.

[131] Lin Zhang, Lei Zhang, David Zhang, and Hailong Zhu. Ensemble of local and global information for finger–knuckle-print recognition. *Pattern Recognition*, 44(9):1990–1998, 2011.

[132] Shuwen Zhang and Xuxin Gu. Palmprint recognition based on the representation in the feature space. *Optik-International Journal for Light and Electron Optics*, 124(22):5434–5439, 2013.

[133] Guoying Zhao, Timo Ahonen, Jiří Matas, and Matti Pietikäinen. Rotation-invariant image and video description with local binary pattern features. *Image Processing, IEEE Transactions on*, 21(4):1465–1477, 2012.

[134] Yang Zhao, Wei Jia, RongXiang Hu, and Jie Gui. Palmprint identification using lbp and different representations. In *Hand-Based Biometrics (ICHB), 2011 International Conference on*, pages 1–5. IEEE, 2011.

[135] Leqing Zhu and Rui Xing. Hierarchical palmprint recognition based on major line feature and dual tree complex wavelet texture feature. In *Fuzzy Systems and Knowledge Discovery, 2009. FSKD'09. Sixth International Conference on*, volume 4, pages 15–19. IEEE, 2009.

[136] Wangmeng Zuo, David Zhang, and Kuanquan Wang. Bidirectional pca with assembled matrix distance metric for image recognition. *Systems, Man, and Cybernetics, Part B: Cybernetics, IEEE Transactions on*, 36(4):863–872, 2006.